University of Venda
Creating Future Leaders

# IMPACTS OF CLIMATE CHANGE ON WATER RESOURCES AVAILABILITY FOR AGRICULTURE IN NZHELELE AREA, LIMPOPO PROVINCE

BY

NDOU NALEDZANI

STUDENT NO: 15012020

A dissertation submitted to the Faculty of Science, Engineering, and Agriculture in fulfilment of the award of Master of Earth Science's degree in Hydrology Water Resources

SUPERVISOR: Dr R. MAKUNGO

CO SUPERVISOR: Mr T.R. NKUNA

## ABSTRACT

Many countries worldwide are experiencing climate change associated impacts on their most valuable sectors such as water resources and agriculture, and South Africa is no exception. The impacts of climate change on water resources availability are projected to increase in almost all regions. This will have a devastating impact on agriculture, especially in a semi-arid and water scarce area of South Africa. This study investigated the impacts if climate change on the availability of water resources for agriculture in Nzhelele area, Limpopo Province. The Soil and Water Assessment Tool (SWAT) was used to evaluate the impacts of climate change on future water resources availability. The SWAT model was calibrated and validated using data for the periods 1991-2000 and 2001-2009 using the SWATCUP-SUFI-2 technique. SWAT model was then fed with projected rainfall and temperature data from Conformal Cubic Atmospheric model (CCAM) for the periods 2023-2053 (near future) and 2053–2082 (far future) to simulate future inflows. Crop water requirements (CWR) for selected crops (maize, tomato, groundnuts, and sweet potato) were estimated using the crop coefficient approach for wet season (summer) and dry season (winter) in near future and far future. The CWRs were compared with inflows to evaluate the availability of water to meet future CWRs. The SWAT model performance was evaluated based on evaluation criteria Coefficient of determination ($R^2$), Nash-Sutcliffe efficiency (NSE), percent bias (PBIAS) and ratio of the root mean square error to the standard deviation of measured data (RSR). The model showed good performance statistics of $R^2$ of 0.71, NSE of 0.56, PBIAS of +0.6% and RSR of 0.66. The study findings revealed that simulated inflows will decrease by 28.67% and 48.22% in the near future and far future, respectively, relative to the baseline period 1987-2009. A comparison of inflows and CWR showed that in near future, water requirements for maize, tomato, groundnuts, and sweet potato in wet season will exceeds inflows by 49.54, 10.05, 9.43, and 9.14%, respectively. In the dry season, water requirements for tomato and sweet potato will be higher than inflows by 29.87 and 71.12%, respectively. However, estimated water requirements for maize were 62% lower than inflows in dry season. In far future, water requirements for maize, tomato, groundnuts, and sweet potato in wet season will be higher than inflows by 66.08, 26.9, 27.15, and 37.22%, respectively, and in dry season water requirements for tomato and sweet potato and maize will be higher than inflows by 62.30, 89.42 and 25.87%, respectively. The study concluded that projected inflows will not be able to meet the simulated future crop water requirements in Raliphaswa irrigation scheme under changing climatic conditions.

**Keywords**: Agriculture, Climate change, Conformal-Cubic Atmospheric Model (CCAM), SWAT, water resources.

## DECLARATION

I, Naledzani Ndou hereby declare that this dissertation for Master of Earth Sciences in Hydrology and Water Resources titled: "**Impacts of climate change on water resources availability for agriculture in Nzhelele area, Limpopo province**," submitted at the University of Venda is my own original work and has not been submitted at this or any other University and all sources used in this study have been cited and acknowledged.

Student's signature Date……05/04/2024……………..

## ACKNOWLEDGEMENTS

I would like to acknowledge the following people for their assistance that led to the success of this study, this work would not have been possible without their help.

- Special thanks to my supervisors, Dr. R. Makungo and Mr. T.R. Nkuna for their advice, direction, patience, and guidance throughout this study
- The National Research Fund (NRF) for funding this research.
- The Council for Scientific and Industrial Research (CSIR) and South African Weather Service (SAWS) for providing me with the data used in this research work.
- Ms. V. Mbaimbai for her assistance with data collection and running SWAT model.
- I am grateful to my family for their love, motivation, encouragement, and support throughout this study.
- I want to especially thank and honor my late father, who laid the groundwork for my continuous intellectual growth, by dedicating this dissertation to him.

# TABLE OF CONTENTS

# LIST OF FIGURES

# LIST OF TABLES

## LIST OF ACRONYMS

| | |
|---|---|
| CCAM | Conformal Cubic Atmospheric Model |
| CMIP5 | Coupled Model Inter-comparison Project 5 |
| CORDEX | Co-ordinated Regional Downscaling Experiment |
| CWR | Crop Water Requirements |
| DAFF | Department of Agriculture, Forestry and Fisheries |
| DEA | Department of Environmental Affairs |
| DEM | Digital Elevation Model |
| ET | Evapotranspiration |
| $ET_0$ | Reference Evapotranspiration |
| ENSO | El Niño Southern Oscillation |
| GCMs | Global Circulation Model |
| GHGES | Greenhouse Gas Emission Scenarios |
| GHGs | Greenhouse gases |
| HBV | Hydrologiska Byrans Vattenbalansavdelning |
| HRUs | Hydrologic response units |
| IWR | Irrigation Water Requirements |
| NSE | Nash-Sutcliffe Efficiency |
| PBIAS | Percent bias |
| $R^2$ | Coefficient of determination |
| RCMs | Regional Climate Models |
| RCPs | Representative Concentration Pathway |
| RSR | Ratio of the root mean square error to the standard deviation of measured data |
| SADC | Southern African Development Community |
| SRTM | Shuttle Radar Terrain Model |
| SWAT | Soil and Water Assessment Tool |
| WEAP | Water Evaluation and Planning |

# CHAPTER 1: INTRODUCTION

## 1.1. Background

Existing evidence has indicated that climate change is currently in progress (Zhu and Ringler, 2012). Africa has been highlighted as one of the continents adversely affected by the impacts of climate change since the region has low adaptive capacity and high vulnerability (Kusangaya et al., 2014; Serdeczny et al., 2015). However, increasing evidence have regarded the Southern African region as one the most regions in Africa that are vulnerable to many and different impacts of climate change with water resources projected to be the most highly affected sector by these impacts (Kusangaya et al., 2014). Driven by alterations in the energy balance caused by an increase in the atmospheric greenhouse gases which affect the absorption, scattering and emission of radiation within the atmosphere and the earth's surface (Coulibaly et al., 2018; Dennis and Dennis, 2012), the United Nations Framework Convention on Climate Change (UNFCCC) have defined climate change as a change observed in the climate itself, typically over an extended period of time and causes configuration of the global atmosphere (van der BanK and Karsten, 2019).

Changes in the rates of evapotranspiration, temperature and rainfall attributed to climate change have a great influence in the water balance (Coulibaly et al., 2018). However, changes in the amount, frequency and intensity of rainfall are associated with a direct impact on the magnitude and timing of runoff as well as the intensity of floods and droughts (Mimi and Jamous, 2010). Low and irregular rainfall coupled with an increase in the frequency and intensity of rainfall extremes such as drought has been identified by the climate change projections for Southern Africa with the 2015/16 drought being the worst experienced in many parts of this region (Mabhaudhi et al., 2018). Over the past century, climate change have greatly affected the global and regional hydrological cycles resulting in a large-scale impacts on water resources affecting both ground and surface water availability for domestic, industrial and agricultural supply (Hagemann et al., 2013; Mimi and Jamous, 2010).

According to Afshar and Suhaimi (2018), the Intergovernmental Panel on Climate Change stated that it has been expected that water resources and freshwater ecosystems in nearly all regions of the world are to be negatively affected by climate change. Moreover, future projections have shown a deterioration in the global freshwater availability as a result of climate change (Juana et al., 2012). While climate in Southern Africa have a large spatial and temporal variability, expected impacts of climate change on water resources are likely to intensify in magnitude, diversity and severity (Kusangaya et al., 2014).

Given that agricultural sector is highly dependent on climatic variables such as temperature, humidity and rainfall, this sector will be adversely affected by decline in water resources availability attributed to climate change (Maponya and Mpandeli, 2012a; Mizyed, 2009). Warmer temperatures leading to high rates of crop evapotranspiration and decreased water availability from effective rainfall influenced by climate change will result in accelerated water shortages which will have adverse impacts on food production (Zhang and Cai, 2013).

Zwane (2019) stated that water availability is a most important factor that restricts agricultural production mostly in South Africa. The country's agricultural sector is the most consumer of water using about 60% of the total water resources in the country (Blignaut et al., 2009). According to Benhin (2008), agriculture in South Africa is highly affected by climate change due to its high dependence on climatic variables (temperatures and precipitation) and also due to the combined effects of the following: (i) South Africa is semi-arid and many farming activities are practiced on marginal lands, (ii) droughts occurs frequently and (iii) the country's water resources are scarce because of its high rainfall spatial variability.

## 1.2. Research problem

Great effects of climate change are being experienced in different parts of the world with predictions showing that some regions in Southern Africa will have decreased rainfall and more wind, while other regions will have increased rainfall associated with hotter and humid conditions (Maluleke and Mokwena, 2017). In South Africa, climate change has become the greatest concern and is currently putting the country's freshwater resources under extreme pressure due to its associated impacts (Dallas and Rivers-Moore, 2014; Ziervogel et al., 2014). Already declared as a water-scarce country, South Africa is typically the 30$^{th}$ driest nation in the world (Adom et al., 2022; Mutamba, 2019). The country was currently faced with one of the worst droughts recorded in 2014/2015 with Limpopo, Kwazulu-Natal, Mpumalanga, North West and Free State being the provinces in South Africa experiencing the devastating impacts of this drought (Maponya and Mpandeli, 2016). Additionally, the impacts of climate change have also been felt through developmental stresses such as unemployment, poverty and food insecurity (Maponya and Mpandeli, 2012a).

Over the past five decades, South Africa has experienced an increase in annual temperatures by at least 1.5 times the global observed of 0.56 degree Celsius coupled with enhanced frequency of extreme rainfall events (Ziervogel et al., 2014). According to Schulze (2016), this increase in average temperatures accompanied by changes in rainfall patterns will have a drastic impact on farming and food production of the already vulnerable agricultural sector of the country by causing a shift in the optimum growing areas for crops as well as by generating frequent and severe extreme weather events.

Agriculture in South Africa is a major source of food in accounting for approximately 50% of maize which is regarded as the region main staple food (Benhin, 2008). However, the current extreme conditions associated with the changing climate have led to an extreme depletion of ground and surface water resources which have caused a decline in the country's agricultural production, since the availability of water is the most factor that limit the success of this sector (El Chami and El Moujabber, 2016; Zwane, 2019). Although agricultural sector is extremely vulnerable to climate change, there is an expectation that increased temperatures, exacerbating rainfall patterns and water shortages will adversely affect all the sectors of the economy with a possibility of a fallout of 1.5% in the gross domestic product (GDP) of the country by 2050 (Benhin, 2008). Blignaut et al. (2009) stated that a fall out in rainfall is likely to have a negative impact on the net agricultural income of the South African provinces which contribute to approximately 10% of the total production of both field crops and horticulture. Added to this, a decline in rainfall by 1% is likely to result in a 1.1% decline in maize production and a 0.5% decline in winter wheat.

Amongst other provinces currently exposed to drought in South Africa, Drought in the Limpopo Province has become the biggest challenge facing famers due to the semi-arid conditions of the area associated with low and unreliable rainfall (Maponya and Mpandeli, 2016). According to Gbetibouo et al. (2010), the Limpopo Province is characterised by a large number of small- scale farmers which are highly dependent on rain-fed agriculture. However, the drought conditions in the province will have an impact of the production, access and distribution of food therefore posing a major threat on food security (Maponya and Mpandeli, 2016). Adverse conditions of the climate will also hinder the production of Maize and vegetables which are the main common crops grown in the rural communities of the Limpopo province (Maponya and Mpandeli, 2012a).

This study therefore focuses on the assessment of possible impacts of climate change on the availability of water resources for agriculture in Nzhelele area which is in the Limpopo province. According to a study by Saruchera et al. (2010), Nzhelele area is characterised by active farming irrigation, the irrigation schemes in Nzhelele consists of 13 villages lying along Nzhelele river valley. Saruchera et al. (2010), further stated that, farmers in these irrigation schemes have identified water scarcity as a major restriction to a successful farm productivity (accounts for approximately 81% of all restrictions).

### 1.3. Justification of the study

Statistical evidence and future projections on changes in rainfall patterns and increased temperatures coupled with extreme events such as floods and droughts attributed to climate change in South Africa have provided adequate reason to assess the impacts of climate change and variability on the availability of water resources for agriculture in Nzhelele area of the Limpopo Province. According to Maponya and Mpandeli (2016), agriculture in the Limpopo Province is regarded as the engine of South Africa, contributing nearly 60% of all fruit, vegetables, maize, wheat and cotton in the country. However, since the province is dominated by small scale-famers, they tend to suffer the most impacts of climate change due to their reliability on rain-fed agriculture, lack of financial capacity, less adaptive capacity, high reliability on natural resources, and lack of resources, skills and illiteracy to enable them to detect the occurrence of extreme hydrological and meteorological events (Maponya et al., 2013). The results obtained after conducting this study will probably provide information that can be used as input for development certain strategies on how to mitigate and cope with the impacts of climate change to improve agricultural productivity.

There are tens of millions of subsistence farmers in Africa who depend on rainfed agriculture in a climate system that exhibits a great deal of natural variability (Engelbrecht et al., 2015). However, only few studies have been conducted to analyse the impacts of climate change on agriculture, especially in South Africa (Mqadi, 2007). Ndhleve et al. (2017) further stated that the poor and farming communities with limited adaptive capacity are most likely to be affected by changes in climate. But, only few studies prove that rural communities are aware of these changes in climatic conditions (Chikosi et al., 2019). For this reason, it is important to study how climate change will affect water availability for agriculture in Nzhelele area in order to aid in bridging the gap of on studies similar to this one. Kom et al. (2020) also highlighted that it is important for smallholder farmers to have a basic understanding of the state of their local climate and participate in adaptation activities since they depend on rain-fed farming for their livelihood.

### 1.4. Research Objectives

#### 1.4.1. Main objective

The main aim of this study was to investigate the impacts of climate change on the availability of water resources for agriculture in Nzhelele area.

#### 1.4.2. Specific objectives

a) To predict future climate change impacts on water resource availability

b) To project future irrigation crop water requirements under climate change conditions
c) To determine the adequacy of inflows to meet the crop water requirements.

### 1.5. Research questions

a) What are the expected changes to climate in the study area?
b) What is the impact of climate change on available water resources in Nzhelele area?
c) What are current and future water requirements in the study area?

### 1.6. Study area

#### 1.6.1. Location

The study area covers two quaternary catchments (A80A and A80B) of the Nzhelele catchment. It is located within the Soutpansberg area in the northeast of the Makhado Local Municipal within the Vhembe District in the eastern part of the Limpopo Province, South Africa. The study area lies at $23^0$ S latitude and $30^0$ E longitude with an average altitude of 903 m (Stroebel, 2004). It is situated near the borders of Botswana and Zimbabwe, and was part of the former Venda homeland (Stroebel, 2004). The study area consists of three irrigation schemes which are Mamuhohi, Mandiwana and Raliphaswa. Mamuhohi and Mandiwana irrigation schemes are government owned schemes with area under irrigation measuring 67.0 and 77.0 hectares, respectively. The total area under irrigation in Raliphaswa irrigation scheme measures 15.0 hectares and it is a non-government-owned irrigation scheme. The irrigation schemes receive water from Raliphaswa irrigation weir.

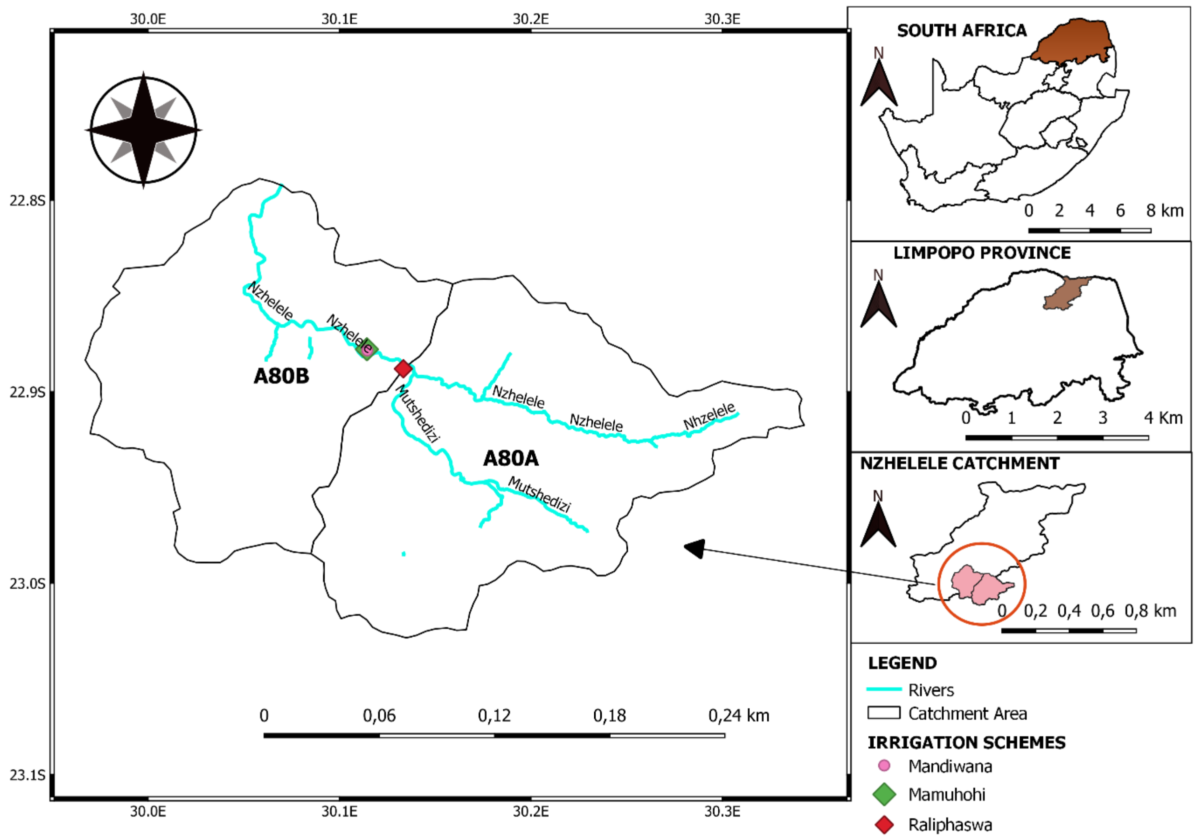


Figure 1.1: Map of study area

### 1.6.2. Climate

Nzhelele is a semi-arid area characterised by average annual rainfall ranging from 300 mm to 820 mm. The amount of rainfall received in the area is highest in summer season and lowest in winter season (Ramarumo et al., 2019). Average daily maximum temperature ranges from $28^0$ C to $22^0$ C in summer and winter respectively, while average daily minimum temperatures ranges from $19^0$ C to $11^0$ C in summer and winter respectively (Meteoblue, 2014).

### 1.6.3. Hydrology

The study area is drained by Nzhelele River which is a major watercourse characterised by low and variable flow pattern because of unreliable rainfall within the river's catchment (Amposah-dacosta and Mathada, 2017; Edokpayi et al., 2018; Odiyo and Makungo, 2018). The river originates high in the Soutpansberg (Earle et al., 2006). It leaves the mountains areas and meanders in a north-eastward direction across the lowveld where it joins the Limpopo River 33 km east of Musina (Amposah-dacosta and Mathada, 2017; Edokpayi et al., 2018). It has a catchment area of 4236 $km^2$. According to Busari (2008), Mutshedzi, Mutshundudi, Tshiruru, Mutamba and Wyllie Rivers are main tributaries of Nzhelele River

#### 1.6.4. Vegetation and land use

The biodiversity within the study area is rich in flora and fauna (Ramarumo, 2017). Meanwhile, the Savannah Biome vegetation dominated by three vegetation types which includes, the Soutpansberg Sandy Bushveld, Musina Mopane Bushveld and Makuleke Sandy Bushveld covers the largest portion of the district (Magwede et al., 2019). These biomes are associated with a distinctive and favourable ecological niches that encourage both flora and fauna diversity within the district (Ramarumo, 2017). The area is dominated by agricultural activities such as, livestock and crop faring, as well as communal cattle farming enterprises which make up about 50% of farming activities commencing in the area (Stroebel, 2004).

#### 1.6.5. Topography

The topographical setting of Nzhelele area is closely associated to its geology and structural history. The area is characterised by high mountainous terrain formed by the Soutpansberg and are divided by narrow east-west trending valley. The bedrock faults and fracture zones influence low altitudes areas between ridges and hilltops. According to Mukheli (2018), the elevation and hills within Nzhelele area ranges between 700 to 1400 m above sea level.

### 1.7. Limitations of the study

Nzhelele area consists of a cluster of 13 small-scale irrigation schemes. This study focused only on Raliphaswa irrigation scheme which limits the applicability of the study's conclusions to other small-scale farmers in the area as well as in other areas with ongoing active small-scale irrigation schemes.

### 1.8. Organisation of the study

This study consists of 6 chapters. Chapter 1 provides the introduction which covers the background, research problem, justification of the study, study objectives and the study area. Chapter 2 reviews literature on climate change and its impacts on water resources availability, agriculture, and crop water requirements, as well as climate change models and hydrological models. Chapter 3 gives details of the methodologies used to achieve the study objectives, data collection and data analysis. Chapter 4 and 5 are research results chapters; chapter 4 presents the results of climate change impacts on future water resources availability for agriculture in the study area and chapter 5 draws the results summary, conclusions, and recommendations.

# CHAPTER 2: LITERATURE REVIEW

## 2.1. Introduction

This chapter provides an overview of climate change impacts on water resources availability, agriculture, and future crop water requirements. A review of greenhouse gas emission scenarios, climate change projection models and hydrological models is also provided in this chapter. It also reviews the factors that cause climate change and the potential impacts associated with it.

## 2.2. Climate change and its impact on water resources

According to Botai et al. (2018), the existence of climate change and variability has been globally agreed to be a reality. Omotayo (2018) further argued that this phenomenon is radially becoming one of the most threats posing a lot of pressure to several critical sectors of civilization and remains fiercely argued, contested, and debated worldwide. This chapter highlights the concept and a better view of climate change as a long-term changes in global and regional climatic patterns such as temperatures, precipitation and wind patterns, or as a change in the properties of the climate that prevails for a prolonged period of time, usually decade or longer as a result of natural causes or human activities (Zhuang et al., 2019). The changing climate has been observed through changes in rainfall patterns, increased temperatures and rising of sea levels, water shortages causing high prevalence of vector-borne diseases and increased weather extremes such as floods and droughts (Karim et al., 2017). It threatens various sectors of the economic development including natural resources, agriculture and food security, forestry, tourism, manufacturing and human well-being (Ubisi et al., 2017).

Safwan et al. (2019) affirmed that climate change has emerged one of the biggest challenges faced by humanity nowadays. It has been scientifically agreed that global climate change is caused by the emissions of greenhouse gases (GHGs) into the atmosphere due to human activities (du Plessis et al., 2003; Grossman, 2018). An increase in GHGs such as methane, carbon dioxide and nitrous oxide due to anthropogenic activities such as deforestation, burning of fossil fuels and industrial production alters the composition of the atmosphere by trapping the atmospheric heat which will in turn facilities changes in the climatic variables (Karim et al., 2017). According to Sejian et al. (2015) the emission of GHGs have increased by approximately 75% with the agricultural sector being the potential source of these gases and it accounts for about 24% of the total emissions due to anthropogenic activities.

Atmospheric temperature is used on a wide range as an indicator of changes in the climate both on a global and regional scale (Mimi and Jamous, 2010). Sejian et al. (2015) stated that, a 0.6 +/- 0.2 of an increase in average global surface temperature had been observed over the 20th century with projections showing a possible rise by 0.3 °C -2.5 °C in the next 50 years and 1.4 °C -5.8 °C in the next century. Added to this, an increment in the average world temperature of just 0.7 °C has been a current evidence of a changing global climate since 1900 (Ngaira, 2007). However, it has been widely accepted that the local climates are to be affected by future increases in global temperatures accompanied by rainfall variability worldwide (Cullis et al., 2019). A warming in the climatic system will intensify the hydrological cycle which will accelerate the evaporation rates and increase liquid precipitation; this will later affect the distribution of runoff, soil moisture and groundwater storages on a spatial and temporal scale, including an increase in droughts and floods frequency (Pathak et al., 2014).

Since the 20th century, it has been without doubt that climate change has become the most notable environmental issue (Rahman, 2013). According to Pathak et al. (2014), climate change is a very critical determiner of the availability of water in a region. Moreover, water resource sector is adversely affected by the changing climate through the impact on rainfall, and temperature which are the main drivers of the hydrological cycle controlling the availability of water (Sharma and Gosain, 2010). Though the impacts of climate change may differ in intensity and characteristics from region to region, it is expected that almost all regions worldwide are to face a net negative impact attributed to climate change on their water resources and freshwater ecosystems (Abbaspour et al., 2009). Increased temperatures attributed to climate change lead to high evaporation rates causing drying out of many areas which enhance the possibility of droughts (Dias et al., 2015). Beran et al. (2016 ), further stated that, streams are likely to dry out due to their high sensitivity to dry periods, and this will have a negative impact on the ecology of water stream along with user's water availability.

Climate change poses a great negative impact on both natural and human systems by exacerbating their vulnerability at diverse scales and with different intensity (Madhusoodhanan et al., 2016). According to Arnell et al. (2015), water is currently faced with increasing challenges across many parts word-wide. The expected alterations in the components essential for water balance (precipitation and evapotranspiration) consequent to climate change will probably affect both surface and groundwater resources (Kumar et al., 2017), However, the impacts of climate change accompanied by increased water demand is likely to result water shortages which will enhance the risk of water scarcity to a large number of people (Abbaspour et al., 2009). For example, Asia is accepted as one of the planet's regions with high vulnerability to climate change (Akram, 2012). Gao et al. (2018) reported that, Asia is home to approximately 60% of the entire population globally, which makes it the most densely populated continent on earth (Mendelsohn, 2014) . Gao et al. (2018) further stated that, the continent is recognised as the world's most hot spot for water uncertainty. According to Chellaney (2012), Asia is the driest continent in the world, with the amount of freshwater available less than half the global annual average of 6380 $m^3$ per resident. Though the changing climate may additionally increase water scarcity by causing changes in the hydrological cycle (Gao et al., 2018), such as altering rainfall pattern, exacerbating climate variability and the occurrence of weather extremes (Prudhomme et al., 2013). The availability of water per capita in Asia is actually decreasing by 1.6% per year as a result of hasty population and economic growth, irrigation expansion, increased household intake and industries that consume large water quantities (Chellaney, 2012).

Considering that Asia is a very large and diverse region, climate change and the associated impacts on freshwater availability will be determined by the location (Hijioka et al., 2014). Guo et al. (2016) stated that, central Asia is amongst the regions that are extremely suffering from trans-boundary water and energy problems. Moreover, large parts of central Asia are characterised by arid to semi-arid conditions, with low precipitation and less water availability dominating these parts (Malsy et al., 2012).

In Europe, Leipprand et al. (2008) stated that, the changing global climate have posed a great impact on precipitation, temperature and radiation budgets, and have altered the regional water balance in many parts of this region. Estrela et al. (2012), further reported that many European countries have been affected by water scarcity. The droughts events experienced in the early 21st century increased due to all components of the hydrological cycle, including low runoff and long periods of soil moisture shortages and have been broadly considered as unusually severe in Europe (Hanel et al., 2018). Researchers agreed that lower rainfall and high evapotranspiration rates will intensify droughts events in some European areas, with a great impact in Spain.

It is anticipated that the most vulnerable region in Europe will experience a direct negative impact attributed to climate change on their available water resources (Estrela and Sancho, 2016). According to Alcamo et al. (2007), central and southern Europe will experience an increase in water stress, and a 19% and 35% increment on the percentage area under high water stress is expected from today to by 2070s respectively. Furthermore, a study conducted by Prudhomme et al. (2013) have indicated that by the end of the 21st century, the severity of drought is likely to increase by a frequency of more than 20% globally, with regional hotspots including central and western Europe.

In North America, global climate change impacts will remain to be a key interest in areas prone to water scarcity, such as along the US-Mexico border (Duran-Encalada et al., 2017). According to Lankao (2010), droughts episodes have been recorded in Mexico city in the past years, 136 droughts occurred between 1450 and 1900; four periods of severe droughts occurred between 1948 and 1996, and between 1997 and 2006, a total of two drought episodes were recorded. Though droughts impacts vary across the regions, in the past few decades, water deficits and conflicts over water allocation attributed to these impacts have developed along the USA-Mexico border (Magaña et al., 2012). Since the year 2000, water systems of Mexico City have been experiencing a constant decline in their drinking water supply coverage, and these declines are expected to persist in the future (Martinez et al., 2015). With predictions showing a possible rise of $4^0$C in mean temperatures and a 20% reduction in mean precipitation by 2080 in Mexico City, it expected that the city's freshwater availability will decrease as a result of accelerated evapotranspiration rates, low precipitation run-off and decreased recharge rates In aquifers (Lankao, 2010).

Apart from the fact that Africa is highly exposed to climate change, lack of the capacity to respond or adapt to climate change impacts in many communities in Africa also triggered its high vulnerability to climate change (Pereira, 2017). Following Australia, Africa is the world's second-driest continent, and is prone to acute water scarcity problems such as water shortages, water stress and water crisis (Naik, 2016). Due to a large number of immediate and long-term impacts of climate change on water resources in several African countries, It has been generally recognised that a multitude of population in different African areas is already suffering from insufficient water supply and distribution (Akpor and Boakye, 2011). Akpor and Boakye (2011), and Naik (2016) further stated that, although the continent is rich in natural resources such as minerals, forests, wildlife and biological diversity, it still remains one of the most poorest and underdeveloped continent in the world due to countless reasons that includes lack of access to clean drinking water.

Africa is a hottest continent, with a land that consists of approximately 60% of drylands and deserts (Gan et al., 2016). Due to the effect of inadequate and unreliable rainfall, altering rainfall patterns and floods, several African countries are currently experiencing enormous water stress (Akpor and Boakye, 2011). According to Urama and Ozor (2010), about 25% of the population in Africa is living under water stress, while 69% live under conditions where water is relatively abundance, but abundance does not necessarily mean availability. Added to this, the scarcity of water resources in Africa has a very great impact on the society such as human health, agriculture, education, productivity and development, as well as in conflict resolution (Naik, 2016). Naik (2016) further argued that most of the countries in Africa do not suffer a physical water scarcity since the continent has sufficient surface and groundwater resources, but rather suffers an economic water scarcity due to its poor economy. Furthermore, Estimations based on projected precipitation changes in Africa have indicated that surface water resources across 20% of the continent will be severely affected by a decline in perennial drainage (Andersson et al., 2011).

Southern Africa is regarded as a climate hotspot due to the fact that the region is underdeveloped and marginalised, and is characterized by increasing aridity along with low adaptive capacity (Nhamo et al., 2019). Since Southern Africa has low adaptive capacity, expected increases in temperatures and projected changes in rainfall patterns will exacerbate the risk and uncertainties of the region (Mpandeli et al., 2018). However, alterations in temperatures and rainfall will vary across the region; some areas will become warmer and wetter, while others will become warmer and drier (Mpandeli et al., 2018). Furthermore, a projected 20% decrease in annual precipitation by 2080 in most Southern African countries could worsen water, food and energy insecurity if no action is taken (Conway et al., 2015).

Projections have indicated that the impacts of climate change in Southern Africa will be experienced through water resources (Jury, 2013). Bauer and Scholz (2010) reported that Southern Africa is warming up at a fast rate than other regions in the world, with land and water resources currently under stress. As a result of water stress, Southern African countries and some regions of the Sahelian strip are highly prone to drought. Matchaya et al. (2019) reported that the region is currently faced with severe water scarcity challenges because of frequent drought, declining surface water resources along with exacerbating agricultural water demand. Since 1970s the spatial extent of drought has been increasing due to stronger relationship between El Niño Southern Oscillation (ENSO) and the southern African rainfall (Edossa et al., 2014).

South Africa is a semi-arid and water scarce country dominated by low and uneven rainfall distribution, uneven distribution of surface and groundwater resources, low runoff and uncertain elevated levels of evaporation due to a hot climate (Maphela and Cloete, 2019; Molobela and Sinha, 2011). The country's water supplies are prone to altered rainfall patterns and accelerated evaporation, since large volume of water supply are stored in large dams (Herrfahrdt-Pähle, 2010). Owing to the semi-arid condition of the country, South Africa is facing enormous water resources restrictions, and the Department of Water Affairs (DWA) has estimated that the country will be declared chronically water scarce by 2025 (Herrfahrdt-Pähle, 2010). Furthermore, catastrophic climate change impacts will exacerbate the already existing challenges of water deficits, and will initiate water resources limits (DEA, 2010). MacAlister and Subramanyam (2018) further reported that the accessibility of renewable surface and groundwater resources is expected to decline in most arid and semi-arid regions, increasing water completion between different users.

According to DEA (2010), challenges brought by climate change impacts in south Africa include the following:

- Fluctuating stormflow and dry spells - projections have indicated an increase in the frequency of storm-flow events and dry spells.
- Increased cost – an estimated 10% decrease in runoff could double the value of new water schemes, therefore increasing the cost of proving water.
- Rising temperatures – projections have indicated that higher mean temperatures attributed by climate change will result in increased unreliable weather, floods, and rainfall.

In South Africa, droughts occurs frequently in the arid and semi-arid areas of the country, and are associated with devastating impacts on the economy, environment and society (Edossa et al., 2014). according Donnenfeld et al. (2018), the 2015 drought in South Africa, characterized by three successive years of below-average rainfall was the most serious and persistent drought since the 1940s, where average dam levels dropped from around 93% to 48% in 2014 and 2016 respectively. Moreover, all provinces in South Africa will probably face changes attributable to climate change in the future, and the Limpopo province is no exception (DEDET, 2016). Between 2004 and 2012, the province suffered the most severe drought conditions than all other provinces in South Africa, as a result, dams dropped to 50% full in contrast with 84% in the late 90s (Maluleke and Mokwena, 2017; Maponya and Mpandeli, 2012b). Furthermore, from 2012 to 2013, a below normal rainfall was recorded across the Limpopo province, accompanied by a strong phase of EL Nino Southern Oscillation (ENSO) and drought conditions in several parts of the province (Maluleke and Mokwena, 2017). DEDET (2016) further reported that, water deficits are so far a major concern in the province, and the situation will worsen due to climate change.

### 2.3. Climate change impacts on agriculture and food

In South Africa, agriculture is frequently seen as successful sector dominated by medium- to large-scales farms (Calzadilla et al., 2014). These farms, which make up 86% of all agricultural land are commercially oriented, capital-intensive, and typically produce surpluses which account for 90% of the value added (Zwane, 2019). The agricultural sector in South Africa is highly diverse, with the country having only 14% of arable land whereby only one fifth of this land has a high agricultural potential (Musetha, 2016). A variety of crops characterizes the country's agriculture including wheat, maize, sunflower, sugarcane, bananas, vegetables, citrus fruits (FAO, 2016). According to Cammarano et al. (2020) agriculture in South Africa provides food, income and employment to around 70% of the region's population, thereby playing an important role on food security and local economy. However, since most of the agricultural production is rainfed, which means that farmers depend on rain to grow crops and produce yields that are marketable, climate projections indicate that the agricultural production will face serious risks that will affect both commercial and small-scale farmers (Cammarano et al., 2020).

Maponya (2012) reported that, between 23% and 33% of the South Africa's gross agricultural production comes from the grain industry, making it one of the largest industries in the country. Of all crops grown in South Africa, maize is the most cultivated field crop important for food security (Choruma et al., 2022). This makes South Africa one of the nations that produces and exports the most maize in the Southern African Development Community (SADC), with more than 11 metric tons of maize produced during the 2018/2019 planting season (Akanbi et al., 2020). Choruma et al. (2022) further stated that, climate change threatens the agricultural productivity and hence food security, as well as the livelihoods of small-scale farmers who rely on maize production for a living. Moreover, the more visible impacts of climate change in the South Africa's agriculture have been felt through seasonal temperature and rainfall fluctuations, which result in changes in planting dates and irrigation scheduling of other critical activities that have implications on farmer's and rural communities' household incomes (Mdoda, 2020).

Maize is predominantly cultivated in the highveld region of South Africa, which constitutes the whole of Gauteng province, nearly all of Free State and parts of North West, Mpumalanga, Northern Cape and Limpopo Province (Akanbi et al., 2020; Matji, 2015). However, a decline in agricultural production due to climate change is being reported across different regions in South Africa. For example, a study by Cammarano et al. (2020) projected an increase in mean temperatures in the north eastern part of Free State Province which they predicted would result in a 10% to 16% decrease in maize production for commercial maize farms in the area as a result of projected climate impacts. Mdoda (2020) reported that the impact if climate change on agricultural productivity for small scale farmers in Eastern Cape Province varied across the seasons and a 10% increase in temperature recorded in summer season led to a decrease in net farm revenue per hectare by R321.40. Choruma et al. (2022) further reported a decrease in maize yield by as much as 23.8% by 2099 in the Eastern Cape province.

Olabanji et al. (2021) investigated the impact of climate change on crop production in the Olifants Catchment, South Africa. The study projected a possible increase in monthly average temperature of 1.0 °C in 2010-2039, 1.6 °C in 2040-2069, and 2.9 °C in 2070–2099 periods under RCP 4.5 scenario relative to baseline (1976-2005), as well as an increase by 2.3, 3.0, and 5.0 °C for the same three future periods respectively, under RCP 8.5 scenario. Olabanji et al. (2021) further indicated that crop yields for maize, soybeans, dry beans, and sunflower are most likely to decrease by a range of 19 to 65%, 11 to 38%, 16 to 42%, and 5 to 30%, respectively, a result of potential temperature increases under both RCPs climate change scenarios.

According to Shew et al. (2020), wheat is frequently cultivated as an additional, dryland staple crop for maize in Southern Africa, especially in South Africa. However, given the recent weather patterns, South Africa wheat may be vulnerable to extreme heat exposure (Asseng et al., 2015), due to this, wheat yield could decline posing major challenges to farmers and people who depend on regional wheat production for food security (Shew et al., 2020). The Western Cape Province is the largest producer of wheat among other commodities in South Africa (Theron et al., 2021). However, between 2015 and 2017, the Western Cape Province experienced three consecutive years of below average rain which led to long periods of drought and significant water shortages (Otto et al., 2018). Theron et al. (2021) reported that, Western cape's wheat growing areas experienced 30 years (between 1988-2018) of persistent drought with high spatiotemporal variability. A study undertaken by Shew et al. (2020), reported that 24 hours exposure to temperatures above 30 $^{0}$C will decline wheat production in Western Cape by 12.5%, and a uniform changes in temperature from +1, +2 and +3 $^{0}$C will lead to average wheat yield reduction of 8.5%, 18.4% and 28.5%, respectively.

The Western Cape is also a home to several industries such as the deciduous fruit, wine and citrus, which are important to South Africa's broader Agri-economy (Zwane, 2019).The wine industry in South Africa derives more than 50% of its GDP from the Western Cape's grape production, which also accounts for more than 8% of the province's employment, but climate variability is the main challenge with grape production in south Africa (Arku et al., 2012).

Limpopo Province is one of the provinces in South Africa that has the richest agricultural sector in terms of fruits and vegetables, cereals, sugar and tea production (Oni et al., 2012). Oni et al. (2012) further reported that, the province is characterised by different climates which allow the production of varying agricultural products ranging from fruits (bananas and mangoes) to cereals (maize and wheat) and vegetables (tomatoes, potatoes, and onions). According to Cai et al. (2017), agriculture in Limpopo Province is responsible for the country's following productions: 75% of mangoes, 66% of tomatoes, 65% of papaya, 60% of avocados, 36% of tea and 25% of bananas, citrus and litchis. The DAFF (2017) argued that although all provinces in South Africa produce tomatoes, Limpopo Province has the biggest area under tomato production which covers more than 75% of the total area under tomato plantation in the country. Although the production of tomatoes have increased for certain years, a number of decreases have also been experienced in the tomato industry due to the vulnerability of tomato crop to climate change and variability (Tshiala and Olwoch, 2010).

High variability of climate in Limpopo Province is a major problem as it is situated in a semi-arid area characterized by low, erratic rainfall (Mpandeli, 2014a). Low rainfall is received in the province accompanied by warm temperatures and substantial drought occurrences (Elum et al., 2017). Mzezewa et al. (2010) stated that the pattern and amount of rainfall are some of the principal components that influence agricultural systems. Furthermore, marginal and unreliable rainfall accompanied by high runoff and exacerbated evaporation losses in semi- arid areas are among the key factors restricting crop productivity  (Mzezewa et al., 2010).

Limpopo Province is dominated by commercial famers occupying approximately 70% of the main agricultural land, while smallholder famers especially those located in the former homelands occupies the rest (Cai et al., 2017). Considering the fact that a large number of smallholder farmers in the province are highly dependent on rain-fed agriculture, water availability is the main limiting factor (Oni et al., 2012). Furthermore, drought has severely affected the agricultural sector in the province, posing a greater impacts on rain fed agriculture (Mpandeli and Maponya, 2013). A study by of drought impacts on food scarcity in Limpopo province by Maponya and Mpandeli (2012b) showed that current weather in province is dominate by drought and as a result, Limpopo province has witnessed a decline in water availability for livestock and irrigation which posed a great impact on the agricultural sector and consequently resulting in food scarcity.

Vhembe District is responsible for the production of more than 4.4% of the total agricultural output in South Africa, as well as 8.4% and 6.3% of subtropical fruits and citrus fruits respectively (Maponya and Mpandeli, 2015). According (Phophi et al., 2020) to smallholder famers in Vhembe District rely of the production of vegetable such as cabbage, tomatoes black nightshade and cowpea as a source of income. However, a large number of small-scale farmers in the district have been facing severe climatic risks, excessive climate change and variability for many years (Mpandeli, 2014b). Furthermore, farmers in the District identified tardy rainfall, extended period of dry spells and exacerbated drought frequency as key indicators of climate change hindering vegetable production  (Phophi et al., 2020). Considering that rainfall varies considerably across the District, low rainfall will result in a decrease in agricultural activities, reduced livestock, drinking water deficits, low yield and lack of seeds for future cultivation (Mpandeli, 2014a)

**2.4. Crop water requirements (CWRs)**

Abundant water supply is a basic need for all crops at a growing stage where they are most sensitive to water shortages (Eze et al., 2020). However, not all water supplied to crops is utilized since some is lost through the process of evapotranspiration defined as combined process by which water is lost from plant surfaces to the atmosphere through evaporation and transpiration (Altalib et al., 2021; Yan and Mohammadian, 2020). CWR is defined as the depth of water (measured in millimeters) required to meet the water consumed through evapotranspiration ($ET_c$) by a crop that is free from diseases, cultivated in large fields under soil conditions that are not limiting, including soil water and fertility, and is capable of achieving its maximum production potential within the given growing environment (Pereira and Alves, 2005). Pereira and Alves (2005), further explained $ET_c$ as the daily evapotranspiration rate (measured in millimeters) of a particular crop as influenced by the crop's growth stages, the prevailing environmental conditions, and the agricultural practices used, all geared towards maximizing crop yield. In order to achieve successful irrigation management, it is crucial to understand the water requirements of crops at various management levels within the irrigated area (Ratna et al., 2016). Traditionally, CWR is estimated based on Allen et al. (1998) crop coefficient approach which estimates crop evapotranspiration ($ET_c$) under standard conditions. According to Shah et al. (2015), the values of crop evapotranspiration are equal to the values of CWRs under standard conditions. In the crop coefficient approach, the CWR is equal to the product of calculated reference evapotranspiration ($ET_0$) and the crop coefficient ($K_c$) which is determined by on the crop type and its growing stages (Gafurov et al., 2018). Allen et al. (1998) mathematical presentation of the crop coefficient approach is given by:

$$ET_c = K_c \times ET_0 \tag{2.1}$$

Where $ET_c$ is the water requirement of a given crop in mm/day, $K_c$ is the crop factor/coefficient and $ET_0$ is the reference crop evapotranspiration in mm/day.

**2.5. Reference crop evapotranspiration ($ET_0$)**

The $ET_0$ is defined as 'the rate of evapotranspiration from a hypothetical reference crop with an assumed crop height of 0.12 m, a fixed surface resistance ($r_c$) of 70 s $m^{-1}$ and an albedo of 0.23 that closely resembles the evapotranspiration (ET) from an extensive surface of green grass which is actively growing with a uniform height, shades the ground completely and is well-watered (Irmak and Haman, 2003; Rodny et al., 2016; Steidle Neto et al., 2015).

Cheshmberah and Zolfaghari (2019) defined $ET_0$ as the amount of water evaporated from small-height crops that are affected by climatic parameters. Evapotranspiration is the amount of water is lost from soil and transpired through plants (Cristea et al., 2013).

$ET_0$ is highly vulnerable to climate change effects on meteorological parameters such as temperature, relative humidity wind speed and solar radiation intensity (Cheshmberah and Zolfaghari, 2019; Lin et al., 2018). Figure 2.1 indicate the relationship between $ET_{0,}$ ET weather parameters, environmental factors, and crop characteristics. A prolonged increase in $ET_0$ will promote long-term dryness accompanied by a likely decrease in precipitation leading to a shift in climate class mainly from semi-arid to arid water-scarce zones (Cheshmberah and Zolfaghari, 2019).

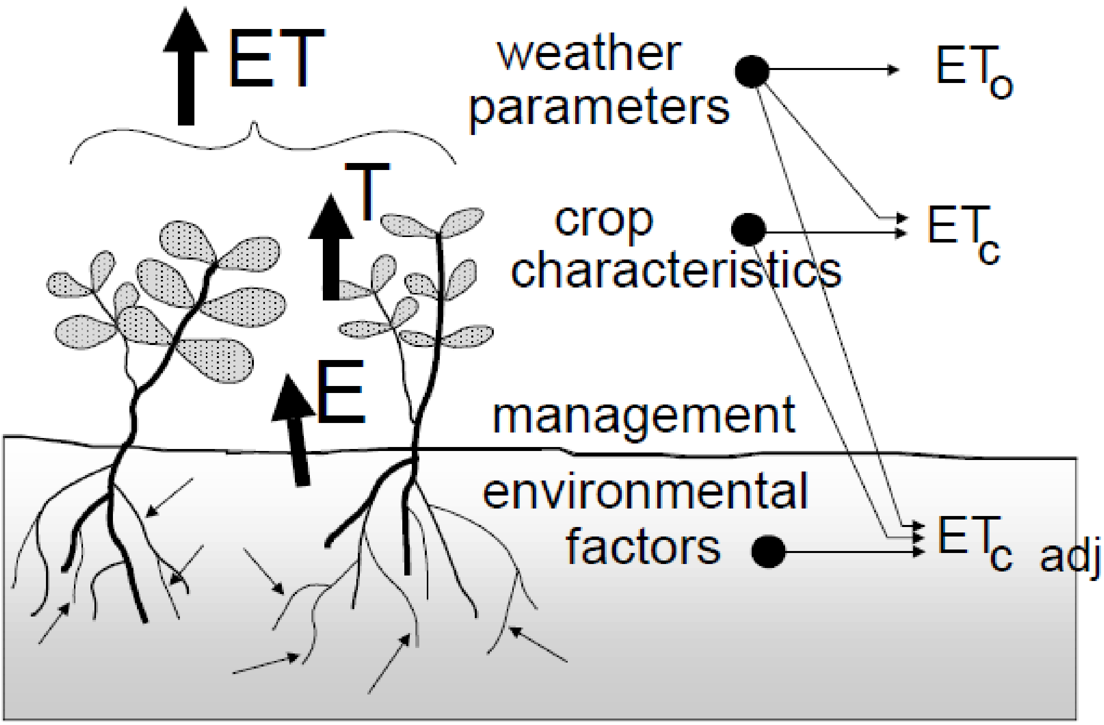


Figure 2.1: Water loss through the process of evapotranspiration and factors affecting evapotranspiration with reference to related ET concepts (Allen et al., 1998).

$ET_0$ is an important variable in hydrological, environmental and agricultural studies, that plays a key role in planning and managing irrigation projects, as well as water management in both irrigated and rain-fed agriculture (Djaman et al., 2019). Furthermore, understanding the relationship between $ET_0$ and future hydrologic process will allow the design of suitable water and vegetation management strategies in water scarce regions in the context of climate change (Lin et al., 2018). According to Steidle Neto et al. (2015) $ET_0$ is one of the first principal steps considered when estimating CWR in agricultural field under current and future climate conditions. This makes $ET_0$ a key factor in determining crop water requirements (Liu et al., 2022), and its estimation is essential for effective planning, design and management of irrigation water resources, crop water management and climate change studies (Altalib et al., 2021; Ikudayisi et al., 2022).

$ET_0$ is primarily based on climatic parameters, and can be estimated using the empirical or physical based mathematical equations on the basis of weather data (Ahmadipour et al., 2019). After $ET_0$ is calculated, it is multiplied by $K_c$ to find the CWR (Gafurov et al., 2018). The Food and Agriculture Organization (FAO) has recommended a number of methods to estimate $ET_0$ including the FAO-56 Penman-Monteith (Allen et al., 1998), FAO-24 Blaney-Criddle (Doorenbos and Pruitt, 1977), Hargreaves and Samani (1985), and Priestley and Taylor (1972) which are the mostly used methods in many regions. However, the selection and applicability of each particular method varies with climatic conditions and accessibility of meteorological data, as well as method data requirement (Gafurov et al., 2018).

### 2.5.1. FAO-56 Penman-Monteith (FAO-56 PM) method

The FAO-56 PM method has been recommended by the FAO as the most exclusive method for estimating $ET_0$ for short grass and tall-crop surfaces at different time scales (hour, day, month) depending on measured input data (Ncoyini-Manciya et al., 2022; Veste et al., 2020). According to (Djaman et al., 2019), The FAO-56 PM equation has been used in many areas of the world as a standard method for estimation of $ET_0$. This is because FAO-56 PM method can be applied without the need for local calibrations due to its physical basis, and it is a well-established method that has been tested test using numerous lysimeters (Heydari et al., 2015). To estimate $ET_0$, FAO-56 PM equation incorporates the aerodynamic effects and principle of water balance requires (Liu et al., 2022). Furthermore, it requires weather and meteorological data such as sunshine hours, solar radiation, average temperature, wind speed and relative humidity (Ikudayisi et al., 2022). Due to high number of climatic data required as input parameters, the application of FAO-56 PM equation in limited in many developing countries including South Africa because of unavailable or missing data (Altalib et al., 2021; Ikudayisi et al., 2022). This has influenced the use of equations that require only temperature to estimate $ET_0$ in regions where data are missing (Ferreira et al., 2021; Trajkovic et al., 2020). The FAO Penman– Monteith equation to predict ETo is given by Allen et al. (1998) as follows:

$$ET_0 = \frac{0.408\Delta(R_n - G) + \gamma \frac{900}{T+273} u_2 \, (e_s - e_s)}{\Delta + \gamma(1 + 0.34 u_2)} \qquad (2.2)$$

Where *ETo* is the reference evapotranspiration (mm day-1), $R_n$ is the net radiation at the crop surface (MJ m-2 day-1), *G* is the soil heat flux density (MJ m-2 day-1), *T* is the mean daily air temperature at 2 m height (°C), $u_2$ is the wind speed at 2 m height (m s-1), $e_s$ is the saturation vapour pressure (kPa), $e_a$ is the actual vapour pressure (kPa), *Δ* is the slope of the vapour pressure curve (kPa °C-1), *γ* is the psychrometric constant (kPa °C-1). The guidelines for calculating the different variables included in the FAO Penman–Monteith equation are explained in detail by Allen et al. (1998).

Trajković and Gocić (2010) evaluated the performance of seven $ET_0$ methods FAO-56 PM, FAO-24 Penman, FAO-24 Blaney-Criddle, FAO-24 radiation, FAO-24 Pan, Priestley-Taylor and Hargreaves-Samani in estimating $ET_0$ for mediterranean semiarid conditions of Policoro, Italy using minimum and maximum air temperatures, minimum and maximum relative humidity, wind speed, sunshine and pan evaporation. They found that the FAO-56 PM equation had the best results among other temperature-based formulas. Similarly, Djaman et al. (2019) analyzed the performance of FAO-56 PM equation and other 34 reference evapotranspiration equations under limited data in New Mexico. The study found that the FAO-56 PM yielded good results under missing solar radiation, relative humidity, and wind speed. However, it underestimated daily $ET_0$ due to more than one meteorological data missing. Meanwhile other equations along with the Makkink, Calibrated Hargreaves, and Abtew, Jensen-Haise equations, had best performance compared to the PM-FAO56, and could be the best alternative methods for $ET_0$ estimation. Yan and Mohammadian (2020) Forecasted daily reference evapotranspiration for Canada using the FAO-56 equation and statistically downscaled global climate model projections. The observational daily weather data for $ET_0$ calculations, including the daily air temperature, solar radiation, wind speed, and relative humidity (RH), were collected. The study concluded that with data availability, the daily $ET_0$ can be satisfactorily forecasted using the FAO-56 PM equation and statistically downscaled GCM projections.

### 2.5.2. FAO-24 Blaney-Criddle (B-C) method

The original B-C is one of the oldest temperature-based method by Blaney and Criddle (1950). This method was modified by Doorenbos and Pruitt (1977) on the FAO drainage paper no.24 to improve the effect of climate on crop water requirements. According to Poonia and Bhatnagar (2022), FAO-24 B-C method is a factor of temperature and daytime hour with less meteorological data requirements. Due to its simplicity in using only air temperature, the FAO-24 B-C can be used in many developing countries with limited data as an alternative method for estimating ETo compared with the FAO-56 PM method (Heydari et al., 2015). Although the mothed has less dependency on input parameters, its results are found to be less accurate due to less number of input parameters (Seenu et al., 2019). Furthermore, under extreme climate conditions such as in windy, dry, and sunny areas the FAO-24 B-C method underestimate $ET_0$ up by approximately 60%, while in calm, humid and clouded areas, $ET_0$ is overestimated by approximately 40% (Zarei et al., 2015). The FAO-24 Blaney Criddle method (Doorenbos and Pruitt, 1977), can be expressed as:

$$ET_0 = b\,[a\,(0.46T + 8)] \tag{2.3}$$

Where $a$ is the mean daily percentage of total annual daytime hours, and $b$ is the adjustment factor which depends on minimum relative humidity, sunshine hours, and daytime wind speed.

Rahimikhoob and Hosseinzadeh (2014) Investigated the possibility of obtaining reliable $ET_0$ estimates based on the remote sensing-based surface temperature data using FAO-24 B-C method in irrigated areas of Khezestan province, Southwest of Iran under semiarid environment. The model performance was assessed using the FAO-56 PM method as a standard reference method. The results showed a close agreement between the calibrated FAO-24 B-C method and the reference values. Farias et al. (2020) analyzed the performance of several calibrated empirical methods for estimating $ET_0$ in Para region (Brazil). The FAP-24 B-C was one of the evaluated methods. They reported that the FAO-24 B-C equation calculated the best outcomes for all performance statistical criteria and did not need calibration. Therefore, it was recommended for Estimating $ET_0$ in the area. Zhan and Lin Shelp (2009) analyzed the performance of calibrated FAO-24 B-C in estimating $ET_0$ for moderate climates and under extreme climatic conditions (windy, dry, and sunny areas) at Barrick sites worldwide. They announced that the calibrated FAO-24 B-C method can provide accurate estimates of $ET_0$ for moderate climates. However, it provides inaccurate results under extreme climatic conditions.

### 2.5.3. Hargreaves-Samani (H-S) method

The H-S method Is a temperature-based method for estimating $ET_0$ developed by (Hargreaves and Samani, 1985) as an improvement to the original radiation based equation (Hargreaves, 1975). The modified H-S method was specifically developed for estimating $ET_0$ with only maximum and minimum temperatures in arid areas (Gao et al., 2017), and its main advantage is that in areas where data is not available, the lapse rate adjustments can be used to interpolate accurate air temperatures (Tabari and Talaee, 2011). Tabari and Talaee (2011) further emphasized that interpolating weather data can be used in other $ET_0$

methods, but this procedure works best in H-S method with only air temperature data requirement since incorporating many weather variables can potentially lead to cumulative errors in $ET_0$ estimating. Furthermore, H-S method tend to overestimate $ET_0$ under high humidity. The (Hargreaves and Samani, 1985) method is expresses as follows:

$$ET_0(mm/day) = 0.0023R_a\,(T + 17.8)(T_{max} - T_{min}) \quad (2.4)$$

Where $R_a$ is the extraterrestrial radiation (MJ/m$^2$/day), $T$ is the mean temperature (°C), and $T_{max}$ and $T_{min}$ are mean maximum and mean minimum temperatures (°C), respectively.

$$R_a = \frac{24(60)}{\pi} G_{sc} d_r\,[\omega s \sin(\emptyset)\sin(\delta) + \cos(\emptyset) cos\delta \sin(\omega s)] \quad (2.5)$$

Where $G_{sc}$ is the solar constant, $d_r$ is the inverse relative distance Earth-Sun, $\omega s$ is the sunset hour angle], ϕ is the latitude and δ is the solar declination. Equations for calculating these variables are found in (Allen et al., 1998).

Moeletsi et al. (2013) investigated the ability of the H-S equation and the Thornthwaite equation for estimating monthly $ET_0$ using multi-year data from eight weather stations in the semi-arid Free State Province of South Africa. The results showed close correlation between the non-calibrated equations, with H-S equation underestimating $ET_0$ for the July to December period while the Thornthwaite equation underestimated $ET_0$ for all months of the calendar year. Gafurov et al. (2018) analyzed the $ET_0$ results calculated based on air temperature in a limited data Central Asia region by non-modified and modified Hargreaves-Samani method. The $ET_0$ results for the two methods were compared with FAO-56 PM method values. The study found that the $ET_0$ calculated by non-modified H-S method were underestimated during summer months. This was associated with higher temperatures and wind speed during these months. However, the modified H-S method had better performance which improved the accuracy of $ET_0$ estimates in the region. Awal et al. (2022) Evaluated the performance of five empirical equations (Hargreaves-Samani (H-S), Valiantzas, Priestley-Taylor, Makkink, and Stephens-Stewart) in estimating $ET_0$ for West Taxis under four climate divisions (High Plains, Low Rolling Plains, Trans Pecos, and Edwards Plateau) with limited weather data using FAO-56 PM as a standard reference method. The results showed that all the empirical equations underestimated the $ET_0$ before and after calibration. However, the H-S equation with either original or calibrated values of its parameters outperformed all tested models, and it was concluded that it is a reasonable estimator, especially under limited weather data conditions. Latif and Javed (1998) demonstrated the application of Hargreaves equation to estimating water requirements for major crops (sugarcane, cotton, and wheat) in Pakistan. ETo results from Hargreaves equation were compared with ETo results computed by Jensen-Haise, Penman-Monteith and pan evaporation methods, while computed crop water requirements results were compared with the observed values determined by the Pakistan Agricultural Research Council (PARC) in 1982. However, this study concluded that Hargreaves method produced better results and its performance criteria were within the practical range.

### 2.5.4. Priestley-Taylor (P/T) method

Priestley and Taylor (1972) method is one of the widely used methods for estimating $ET_0$ based on radiation. It was developed as a shortened version of the original Penman (1948) combination method by substituting the aerodynamic component of the original Penman equation with an empirical coefficient (α) with an estimated average value of 1.26 (Didari and Ahmadi, 2019). The modified P/T method was developed specifically for humid climates with damp surfaces (Tom–Cyprian et al., 2022). According to Tabari and Talaee (2011), the P/T method is a simple method for $ET_0$ estimation and it requires only few weather data. Due to its less data requirements, the P/T method have been widely used by crop modelers (Gao et al., 2017). However the  P/T method must be regional calibrated for acceptable performance before being used for estimating $ET_0$ (Tabari and Talaee, 2011). The Priestley and Taylor (1972) method can be expresses as:

$$ET_0 = \alpha \frac{\Delta}{\Delta + \gamma} \frac{R_n}{\lambda} \quad (2.6)$$

Where $\alpha$ is the empirically derived constant and was defined as 1.26 by (Priestley and Taylor, 1972), and λ is the latent heat of vaporization (MJ/Kg)

Tabari and Talaee (2011) evaluated the performance of Priestley-Taylor and Hargreaves method in estimating $ET_0$ before and after calibrating the models with FAO-56 PM in an arid and cold climate of Iran. They reported an improvement of $ET_0$ estimates by the methods after calibration. Overall, the priestly-Taylor had the best fit as compared with FAO-56 PM method. Gao et al. (2017) compared the performance of six $ET_0$ methods, namely, the FAO-24 Radiation, FAO-24 Blaney Criddle, Hargreaves, Priestley-Taylor, Makkink, and Turc, with FAO-56 Penman-Monteith in estimating monthly averages of daily $ET_0$, total annual $ET_0$, and daily $ET_0$ in an arid, semiarid, and humid regions of Aksu (China), Tongchuan, (China) and Starkville (United States), respectively. the results showed that the Priestly-Taylor method worked best in the arid and semiarid regions but had poor performance in humid region.

Didari and Ahmadi (2019) reported the inapplicability and underestimation of $ET_0$ in arid and semiarid areas of Southern Iran by Priestley-Tylar method after Calibrating and evaluating the performance of the FAO56-PM, FAO24-radiation, and Priestly-Taylor in estimating $ET_0$ using the spatially measured solar radiation.

### 2.6. Crop coefficient ($K_c$)

The $K_c$ is defined as the ration of  $ET_c$ to the $ET_0$, and it reflects an integration of the effects of the four key characteristics that differentiate the from reference grass, and it includes the albedo of the crop-soil surface, crop height, soil evaporation and canopy resistance (Ayyanagowdar et al., 2020; Roja et al., 2020). The $K_c$ is mostly influenced by crop type, with only small effects from the climate and soil evaporation (Shah et al., 2016). Moreover, the $K_c$ of a given crop over a growing period varies due evapotranspiration (ET) differences during the growing stages (Mebrahtu et al., 2021). The crop growth stages for $K_c$ calculations are divided into four distinct stages: initial, development, mid-season and late season stages (Ayyanagowdar et al., 2020). A correct estimation of $K_c$ at each growing stage is critical for  assessing crop water requirements of from weather variables and thereby optimize irrigation management (Machakaire et al., 2021). Most agricultural crops have a minimum $K_c$ value at planting and a maximum $K_c$ value is reached around complete canopy cover (Trivedi et al., 2018). Allen et al. (1998) used a segmented $K_c$ curve (Figure 2.2) to describe the time variation of $K_c$.

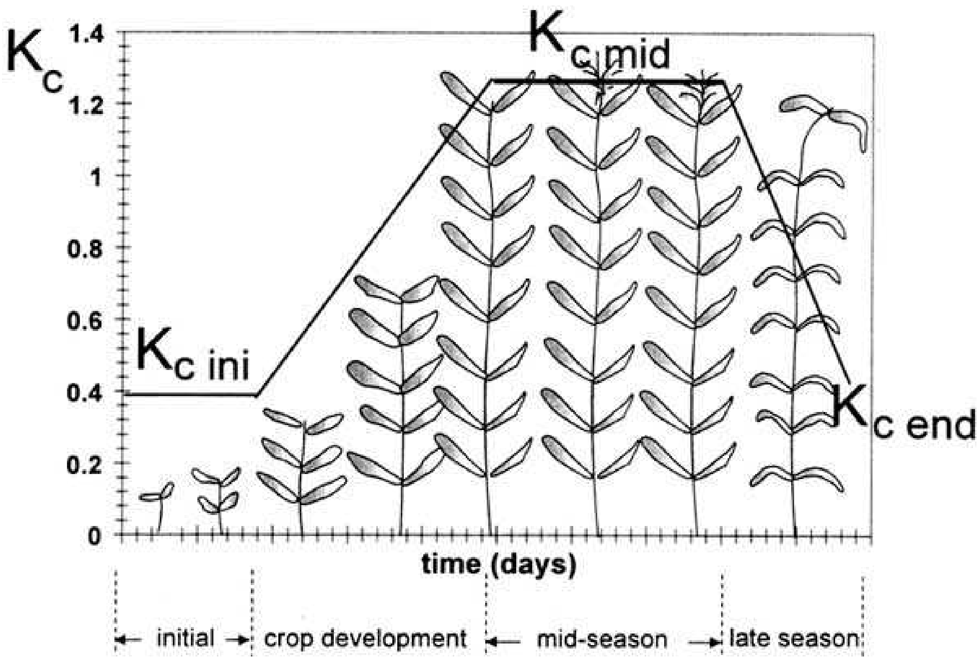


Figure 2.2: Generalized Kc curve for the single crop  (Shah et al., 2015).

As illustrated by Figure 2.2, the initial stage start immediately after planting to approximately 10% ground cover (Kc is small), development stage runs from 10% ground cover to effective full cover which usually occurs at the beginning of flowering (Kc increases), mid-season stage runs from effective full cover to the start of maturity and is often indicated by the beginning of the ageing or yellowing of leaves, leaf drop, or the browning of fruit (Kc is at maximum), while late season stage is from the start of maturity until harvest (Kc decreases) (Shah et al., 2016; Shah et al., 2015). According to Dauda and Olayaki-Luqman (2016), Kc vary by location, based on factors such as temperature, soil, crop type, crop variety, and irrigation systems.

### 2.7. Impacts of climate change on future CWRs

Agricultural water resources are declining globally as a result of changing climate conditions, with a particular emphasis on semi-arid and arid zones (Elbeltagi et al., 2020). According to Masia et al. (2021), the projected impact of climate change on agriculture in the coming years due to changes in the intensity and distribution of rainfall, soil water content, atmospheric water vapor, higher temperature leading to high rates of evapotranspiration will have a considerable impact on irrigation requirements. Furthermore, the increase in drought amount and expected increase in potential evapotranspiration due to climate change and variability could have a direct impact on crop growing season and crop water requirements (Abraham and Muluneh, 2022). Shanka and Arba (2021) stated that, water is important for crops growth as well as for food production. However, a decrease in irrigation water supplies due to climate change has been getting worse day by day with scarcity being observed in many parts of the world, and as a result, there is an increasing demand for irrigation water to be used efficiently by crops (Roja et al., 2020). According to Olabanji et al. (2020) the amount of water required to produce 1kg of food security crops such as maize, wheat and rice is estimated at 1.5 $m^3$, 1.0 $m^3$ and 2.5 $m^3$. However, the anticipated climate change especially in Africa is predicted to worsen water scarcity and the need for more irrigation, which would reduce food production (Rotich and Mulungu, 2017).

Water is gradually becoming more scarce in most parts of the world (Mebrahtu, 2021). Therefore assessing the future impact of climate change on crop water requirements is essential for local or regional water and food planning (Kobuliev et al., 2021). Parekh et al. (2013) assessed the impact of climate change on CWRs for wheat, sorghum, maize, small vegetables, tomato, gram, and cowpeas in the Sukhi command area of Vadodara district, Gujarat. CWRs were estimated for the periods 2011-2020, 2046-2065 and 2080-2099 using 2003-2009 as a baseline period. The results showed a negligible decrease in the water requirement for all crops in the period 2011-2020, but a considerable increasing water requirement in the periods 2021-2030, 2046-2065 and 2080-2099 as compared to base period 2003-2009 was observed for all crops. Ye et al. (2015) estimated the CWRs and irrigation water requirements (IWRs) for rice in Southern China under changing climate conditions. The regional CWRs and IWRs were predicted to increase respectively by 8% and 6% from 2011 to 2040, by 17% and 19% from 2041 to 2070, and by 20% and 24% from 2071 to 2100 compared with 1951–1980. Rotich and Mulungu (2017) assessed the effects of climate change on maize water requirements at Moshi Airport and Lyamungu station in Kikafu sub-catchment, Tanzania. The CWRs were assessed for the time periods 2011–2030 and 2046–2065 (named the 2020s and 2050s, respectively) using 1971-2000 as a baseline period. The CWRs were projected to increase by 3.8% in the 2020s and 7.1% in the 2050s at the Moshi Airport and by 19.9% in the 2020s and 22.4% in the 2050s at Lyamungu station relative to the baseline period. More impacts were projected to be during 70–80 days of the development stage and the entire mid-season (81–140 days) whereby the temperature will be high but with low precipitation.

Masia et al. (2021) evaluated the impacts of climate change on maize, wheat, and wine grape water requirements under past (1976–2005) and future climate conditions (2036–2065) in Mediterranean countries of Southern Europe. The study found that, the water requirements for maize, wheat, and grape production will respectively increase by an average of 13%, 16%, and 10% under future climate. Poonia et al. (2021) investigated climate change impacts on crop water requirement (CWR) and crop irrigation requirement (CIR) for maize, wheat and, rice over eastern Himalayan region. The study focused on three periods, i.e., 2021–2046, 2047–2073, and 2074–2099 taking 1998–2015 as baseline period. The results suggested that towards the end of the 21$^{st}$ century, CWR for rice and wheat will increase by 8% and 39% over the West Sikkim and by 11% and 37% over the South Sikkim. Only maize showed a decreasing trend over West and East Sikkim (- 4% and -15%).

Ogundeji and Jordaan (2017) modelled the impact of climate change on CWRs for fruit crops (apples, pears, apricots, nectarines, and plums) for the periods 1971-199 and 2046-2065 in the Western cape Province, South Africa. CWRs were estimated for two irrigation systems (sprinkler and drip) under low and high Global Circulation models (GCMs). The results suggested that CWRs will increase substantially for both types of irrigation, as such, CWRs for all fruit crops ranged between 2830 $m^3$/ha and 4130 $m^3$/ha for sprinkler irrigation in the base climate while that for the future climate ranged between 3400 $m^3$/ha and 4880 $m^3$/ha for low GCM and between 3280 $m^3$/ha and 4690 $m^3$/ha for high GCM. For drip irrigation, the values were smaller with the base climate CWR ranging between 1950 m3/ha and 2900 $m^3$/ha, while that for future climate ranges between 2320 $m^3$/ha and 3390 $m^3$/ha for low GCM and between 2190 $m^3$/ha and 3280 $m^3$/ha for high GCM.

### 2.8. Greenhouse gas (GHG) emission scenarios

Greenhouse gases (GHGs) such as carbon dioxide, water vapour, methane and nitrous oxide absorbs the Infra-red radiation and prevents heat from escaping into the outer space, thereby warming the earth's atmosphere and surface (Kweku et al., 2017). Nakicenovic et al. (2000) emphasized that the future evolution of GHGs is highly uncertain and is based on driving forces such as population growth, socio-economic growth, and technological change. However, assessing the future uncertainties of GHGs is essential for understanding the magnitude and nature of environmental threats such as climate change (Schenk and Lensink, 2007). Scenario analysis of a wide range of alternative futures is the most preferred method for assessing uncertainties associated with future GHGs emissions (Schenk and Lensink, 2007). According to Nakicenovic et al. (2000), scenarios provide a description of how the future is likely to unfold, and they effectively analyse the effect of driving forces on future emissions outcomes as well as assessing the associated uncertainties.

A set of emission and concentration scenarios referred to as the Representative Concentration Pathway (RCPs) have developed for the fifth Coupled Model Inter-comparison project (CMIP5) (Kawase et al., 2011). These scenarios were used for climate projections by the Intergovernmental Panel on Climate Change on its fifth Assessment Report (AR5) (Chaturvedi et al., 2012). There are for RCPs scenarios namely RCP2.6, RCP4.5, RCP6.0 and RCP8.5 (Chaturvedi et al., 2012; Kawase et al., 2011; Van Vuuren et al., 2011a).The name of each RCP correspond to a specific radiative forcing target level for 2100 based on the forcing of greenhouse gases and other forcing agents (Kawase et al., 2011; Van Vuuren et al., 2011a). Furthermore each RCP scenario represents a full spectrum of stabilization, mitigation and all emission scenarios available in literature (Chaturvedi et al., 2012). According to Van Vuuren et al. (2011a), RCPs provide information on all components of radiative forcing such as greenhouse gases emissions, land use, and air pollutants which are used as inputs in climate modelling and atmospheric chemistry modelling.

The RCP8.5 was developed by the Model for Energy Supply Strategy Alternatives and their General Environmental Impacts (MESSAGE) modelling team and the IIASA Integrated Assessment Framework at the International Institute for Applied Systems Analysis (IIASA), Austria (Chaturvedi et al., 2012). It is a scenario in which GHG emissions will continue to rise throughout the 21 century, and by the end of the century it will have led to a radiative forcing of 8.5 $W/m^2$ (Mirdashtvan et al., 2018; Riahi et al., 2011). Alternatively, RCP8.5 represents a future with high GHG concentration (Mbokodo et al., 2020). Its main purpose is to serve as input to the Coupled Model Inter-comparison Project Phase 5 (CMIP5) of the climate community and it assumes that a large population, slow economic development. Technological changes and energy intensity development will result in high energy demand and GHG emissions (Riahi et al., 2011). Following RPC8.5 is RCP6.0 developed by Asia-Pacific Integrated Model (AIM) modelling team at the National Institute for Environmental Studies, Japan (Chaturvedi et al., 2012). It is a scenario of long-term, global emission of GHGs that stabilize radiative forcing at 6.0 $W/m^2$ by 2100, without exceeding the value of previous years (Masui et al., 2011).

The RCP4.5 is also a stabilization scenario that represent a future of moderate GHG concentration (Mbokodo et al., 2020). In this scenario, radiative forcing is stabilized at 4.5 $W/m^2$ in the year 2100 without overshooting that target (Thomson et al., 2011). RCP4.5 was developed at the Pacific Northwest National Laboratory's Joint Global Change Research Institute by the MiniCAM modelling team (Chaturvedi et al., 2012). This scenario assumes that global population will reach a maximum of 9 billion people and then decline to 8.7 billion people in 2065 and 2100 respectively (Emanuel and Janetos, 2013).

The RCP2.6 was developed by the Integrated Model to Assess the Global Environment (IMAGE) modelling team of the Netherlands Environmental Assessment Agency (Chaturvedi et al., 2012). It is a mitigation scenario in which concentration of atmospheric $CO_2$ is to peak in the mid-21st century, and then decrease at a slow rate afterwards but, go to zero by 2100 (Caesar et al., 2012). The RCP2.6 is alternatively referred to as RCP3-PD, which indicates that radiative forcing peak at 3 $W/m^2$ before 2100 and then decline to 2.6 $W/m^2$ by 2100 (Van Vuuren et al., 2011b). This radiative forcing level will be archived by reducing the emissions of greenhouse gases and air pollutants over time (Chaturvedi et al., 2012). According to Ishizaki et al. (2012), the main aim of this mitigation scenarios is to decrease the global mean temperature to $2^0$C. Figure 2.3 shows the radiative forcing projections under different emission scenarios. Future climate projections were not carried out in this study. The already existing and freely available Conformal Cubic Atmospheric Model (CCAM) climate projections from RCP8.5 were used.

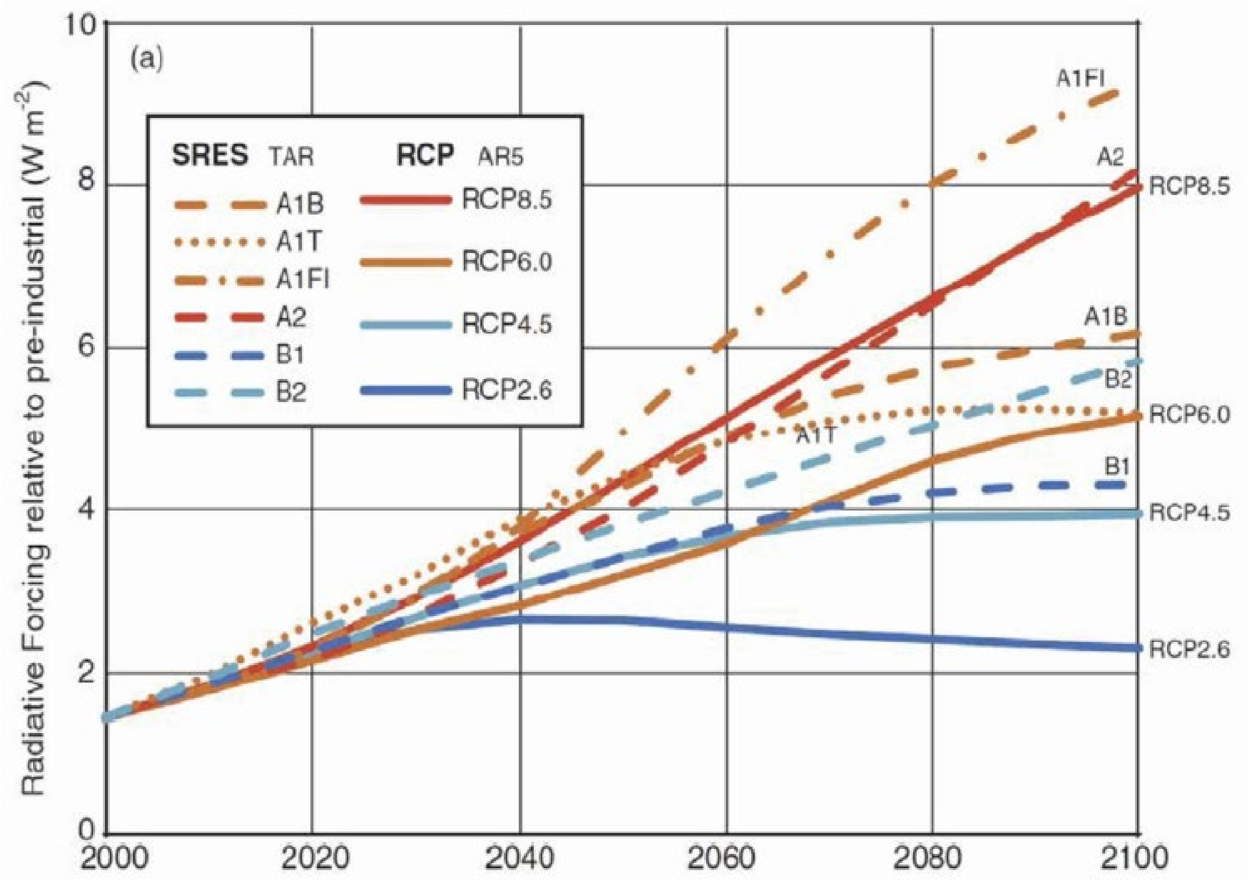


Figure 2.3: Radiative forcing projections under different emission scenarios (IPCC, 2013).

**2.9. Models used for climate change projection.**

Dynamic climate change models based on physical laws applied to earth systems have emerged the primary tools for future climate change projections (Engelbrecht et al., 2011). According to Luhunga et al. (2016), Global climate Models (GCMs) have emerged the most current highly advanced tools available for simulating the global climate system's response to increased atmospheric greenhouse gas concentrations. For example, the Commonwealth Scientific and Industrial Research Organisation (CRISO), European Center/HAMburg (ECHAM) and HADley center Atmospheric Model (HADAM) GCMs were employed in the IPCC 3rd Assessment Report (TAR), while The Geophysical Fluid Dynamics Laboratory (GFDL), Model for Interdisciplinary Research on Climate (MIROC). and Meteorological Research Institute- coupled global climate model (MRI-CGCM) GCMs from the Coupled Model Intercomparison Project Phase 3 (CMIP3) multi-model dataset were employed in the 4th Assessment Report (AR4) (Lumsden, 2009). GCMs provide a description of relevant physical processes in the atmosphere, oceans, land, and ice surfaces that make up the climate system (Luhunga et al., 2016)

The spatial resolution of current GCMs which is around 100-200 km provides an opportunity to successfully address the general circulation of the atmosphere and the ocean, as well as sub-continental patterns such as temperature and precipitation (Rummukainen, 2010). Although GCMs can provide sufficient simulations for atmospheric general circulation at a continental scale, they in most cases fail to capture comprehensive processes associated with regional variability and changes in local climate necessary for assessment of regional and national climate change (Endris et al., 2013). Furthermore, GCMs are unable to represent the fine-scale detail that characterises the climate in many regions world-wide due to their relatively coarse space resolution (Luhunga et al., 2016), and this influenced the use of regional modelling in Southern Africa (Engelbrecht et al., 2011).

Regional climate models (RCMs) are highly favourable research method which permits a more comprehensive process studies and simulation of regional and local conditions, and as a result, they contribute to climate impact studies and adaptation planning (Rummukainen, 2010). The RCMs functions under the guidance of GCMs but, they have the potential to represent small-scale processes and features (Spinoni et al., 2020). These models are applied at a high resolution over selected areas of interest with the aim of obtaining comprehensive observations (Engelbrecht et al., 2011). Furthermore, all RCMs use a similar domain, have a spatial resolution of 50 km, and are driven by the Interim European Centre for Medium-Range Weather Forecasts (ECMWF) Re-Analysis (ERA-Interim; 1989–2008) (Kalognomou et al., 2013; Nikulin et al., 2012).

In Africa, only a few number of climate-change studies based on RCMs have been carried out (Engelbrecht et al., 2009). However, the World Climate Research Program have currently initiated the Coordinated Regional Climate Downscaling Experiment (CORDEX) program, which is a modelling framework that provides an opportunity produce high-resolution regional climate projections necessary for assessing future climate change impacts on regional scales (Endris et al., 2013; Giorgi et al., 2014). The development of CORDEX program was targeted on the African region due to its high vulnerability to climate and weather variability (Dosio et al.,2015; Dosio et al.,2019). These models provide a framework to assess and benchmark the performance of a model, as well as a framework for climate projections used in impact and adaptation studies (Giorgi et al., 2009). Added to this, the Global climate models participating in the CMIP5 are downscaled by CORDEX RCMs so as to support international collaboration to generate an ensemble of high resolution historical and future climate projections at regional scale (Dosio et al., 2019; Dosio et al., 2015). Giorgi et al. (2009) highlighted that the climate projection framework within the CORDEX is based on simulations of Global climate models that supported the IPCC fifth assessment report (referred to as CMIP5).

The CORDEX have been used in previous studies to simulate future climates over Africa (Dosio et al., 2019; Endris et al., 2013; Hernández-Díaz et al., 2013). Nikulin et al. (2012) presented the first results of CORDEX- Africa by evaluating an ensemble of 10 RCMs simulations covering the whole African continent. All models were run at a resolution of 50 km and were driven by ERA-Interim; 1989–2008. Kim et al. (2013) also evaluated the CORDEX models and presented systematic biases across all models for different regions, mainly precipitation in drier regions such as South Africa. According to Giorgi et al. (2009), most of current studies are running RCMs using a higher grid spacing of up to 10 km for climate projections. Meanwhile, a study by Engelbrecht et al. (2011) has indicated that a variable-resolution global model, known as the Conformal-Cubic Atmospheric model (CCAM) which offers an opportunity to obtain acceptable future climate change projections over Southern Africa can be successfully applied at spatial scales ranging from relatively low-horizontal resolution global simulations, to a micro-scale at ultra-high 1 km resolution over selected areas of interest.

The Conformal-Cubic Atmospheric Model (CCAM) is a variable-resolution global atmospheric model (Landman et al., 2018; Sipayung et al., 2018), It was developed by the Commonwealth Scientific and Industrial Research Organisation (CSIRO) in Australia (Mbokodo et al., 2020). The CCAM is formulated on the conformal cubic grid which enables the model to avoid problems related to lateral boundaries when modelling the atmosphere in limited areas (Sipayung et al., 2018). Furthermore, CCAM uses a semi-Lagrangian and semi-implicit dynamic core to produce solutions for hydrostatic primitive equations (Engelbrecht et al., 2015; Mbokodo et al., 2020). The model functions as a global circulation model when applied at quasi-uniform resolution. It can also be applied alternatively in stretched-grid mode using the Schmidt (1977) transformation, to produce high-resolution simulations over selected areas of interest (Landman et al., 2012; Landman et al., 2018). According to Landman et al. (2012), CCAM has been illustrated to effectively allow simulations of current climatology condition over Southern Africa and tropical Africa.

Rummukainen (2010) stated that the implementation of all RCMs was motivated by the concept of downscaling with the aim of obtaining regional and local detail from scattered observations or low-resolution numerical simulations. For example, Sipayung et al. (2018) emphasized that the development of CCAM was also focused on regional climate downscaling. Engelbrecht et al. (2011) applied a CCAM in stretched grid mode to perform a downscaling procedure over Southern Africa. The aim was to obtain simulations of about 60 km resolution (Figure 2.2). However, the resolution declined to approximately 400 km in the far-field. Simulations were carried out in South Africa, on the Sun Hybrid System of the Centre for High Performance Computing (CHPC).

For the past 10 years, CCAM and Division of Atmospheric Research Limited-Area model (DARLAM) of CSIRO have been employed to provide simulations of present-day climate and future climate change over Southern Africa and Tropical Africa (Engelbrecht et al., 2011). It has been highlighted that CCAM provide adequate rainfall and temperature distribution simulations, including intra-annual rainfall and circulation cycle throughout the region (Engelbrecht et al., 2009). Furthermore, this model can also accurately represent the daily climatic statistics that have been observed (Engelbrecht et al., 2011). It has been used for operational short-range weather forecasting in South Africa (Landman et al., 2012).

Mbokodo et al. (2020) used CCAM to analyse heat waves projection under the influence of climate change in South Africa over the of 1983-2099. Simulations were carried out under RCP 4.5 and RCP 8.5 scenarios. The study found that average maximum temperature is likely to rise by about $6^0$C in South Africa by 2070-2099. Engelbrecht et al. (2011) forced CCAM with sea-ice and bias-corrected sea-surface temperature of six coupled global climate models (CGCM) projections from the IPCC forth Assessment Report (AR4) to project summer rainfall changes over southern Africa, Simulations were performed at a quasi-uniform resolution of about 200 km and were downscaled at resolution of about 60 km. The study projected drier summers over the region, with Zimbabwe and Botswana to be the most severely affected. Malherbe et al. (2013) also applied CCAM to simulate present and future climate over Sothern Africa and Southwest Indian Ocean. The study found that tropical cyclones occurrence will decrease over the Southwest Indian Ocean. Projections also indicated a simultaneous increase in rainfall from January to March in the Northern Mozambique and Southern Tanzania, as well as a decline in semi-arid areas of further South such as Limpopo River basin.

### 2.10. Uncertainties of climate models

The IPCC (2014) addresses uncertainty as lacking complete information, including incomplete knowledge or lack of agreement on what is known. It plays an important part in environmental change research globally, climate science and climate change impact science, as well as in hydrology and water resources. In climate systems, uncertainties is attributed to two potential sources, which include human activities, unknown future GHGs and aerosols emissions concentrations (Foley, 2010). In climate changes impacts studies, it is important to consider uncertainty in order to avoid restriction of the hydrologic projection value if no adequate assessment of related uncertainty is taken into consideration (Troin et al., 2018). Moreover, assessing uncertainty attributed to climate change impacts on hydrology is essential for model predictions improvement and enables a successful development of water resources management strategies (Sellami et al., 2016).

When quantifying climate change impacts on water resources, uncertainties may arise from a number of sources including greenhouse gas emission scenarios, selection of GCMs, downscaling methods (RCMs), structures and parameterization of hydrological models (Chen et al., 2011; Kundzewicz et al., 2018; Troin et al., 2018). According to Kundzewicz et al. (2018), uncertainties are introduced by transfer function, in such that, GCMs are derived by primary inputs provided by emission scenarios (Foley, 2010), the GCMs will produce climate projections on a course resolution scale (110-250 km) and will need to be downscaled by RCMs so that they can be suitable for the application of hydrological models (Sellami et al., 2016). Given that RCMs can only downscale climate projections to only 25-50 km resolution, although the output of GCMs can be downscaled, the associated uncertainty will still remain since their simulations hardly match the patterns of climate variables observed at local scale (10-0.1 km) (Sellami et al., 2016), Uncertainty will then be transferred to impacts on water resources (Kundzewicz et al., 2018).

Minville et al. (2008) compared statistics on historic (1961–1990) and future discharge (2020, 2050 and 2080) to study climate change impacts on the Chate-du-Diable watershed (Quebe,Canada) using ten climate projections obtained from five GCMs, two greenhouse gas emission scenarios (GHGES), one downscaling method and one hydrological model. The study concluded that the choice of GCMs was the source of uncertainty out of all sources considered in the study.

Chen et al. (2011) used six GCMs under two GHG emission scenarios, five GCM initial conditions, four downscaling techniques, three hydrological models and ten sets of hydrological model parameters to investigate overall uncertainty of climate change impacts on hydrology in the Canadian watershed. Their results show that the potential contributor to uncertainty was the choice of GCMs. They further indicate that the selected hydrological variables influenced by variability are also a major source of uncertainty.

Vetter et al. (2017) applied five CMIP5-GCMs under four RCPs and nine hydrological models to evaluate the sources of uncertainty in projected runoff under climate change in 12 large-scale river basins across the world. Analysis of Variance (ANOVA) method which permits for the decomposition of variances and identification of the potential sources of uncertainty along the GCM-RCP-HM model chain was used to analyse three major contributors to uncertainty. The results indicate that GCMs is a major source of uncertainty contributing to runoff projections followed by RCPs and the hydrological models.

In climate modelling, uncertainties are not clearly summarised within the differences between climate models available for impact assessment, which lead to difficulties when distinguishing climate model simulations uncertainties from an ensemble of multiple available GCMs, as well as when reducing uncertainties in global climate model simulation (Clark et al., 2016). However, in hydrological applications, balancing evaporation with precipitation at global scales can be considered as a basic test for climate models fitness (Clark et al., 2016)

Kundzewicz et al. (2018) introduced a framework by which some of the uncertainties arising from different sources can be reduced, including those from climate models and hydrological model. The framework outlined that the uncertainties associated with climate models can be reduced by using a much finer resolution GCMs and RCMs, this will improve scale similarity between climate models and impact models. Added to this, using an ensemble of GCMs and the RCMs along with improved testing of these models can also minimize uncertainty. In hydrological models, the framework states that, forcing an improved hydrological model with finer resolution climate input data and using an ensemble of hydrological models to improve the reliability and robustness of future projections can assist in reducing the uncertainty associated with these models.

### 2.11. Hydrological modelling for climate change impacts

Hydrological modelling involves the use of small-scale physical models, mathematical analogous and computer simulations to represent real hydrological features and processes such as precipitation, snowmelt, interception, infiltration, evaporation, surface and sub-surface flow, as well as the way they interact with each other (Bello, 2020; Islam, 2011). Hydrological models have emerged essential tools that mathematically represent hydrological processes and human-induced impacts on hydrologic systems (Cardoso de Salis et al., 2019; Dwarakish and Ganasri, 2015). The application of hydrological models is essential for water resources planning, development and management, flood prediction and design, and coupled systems modelling including such as, water quality, hydro-ecology and climate (Pechlivanidis et al., 2011). These models provide a detailed description on the distribution and movement of water resources, as well as the amount of water stored in the soil and in natural bodies of water and their exchange (Bello, 2020). They also provide users with the opportunity to generalise both spatial and temporal information on the area of interest (Pechlivanidis et al., 2011). Although hydrological modelling is an important task, its application in arid and semi-arid environments is challenging since most of the catchments within these environments are ungauged and have a distinctive feature of the hydro-climatological variables (Mengistu et al., 2019).

According to Paul et al. (2021) hydrological models have a unique and common characteristics which makes their classification important. One of the most important classifications of hydrological models is physically based (e.g. Soil and Water Assessment

Tool, and MIKE SHE), empirical (e.g. Water Evaluation and Panning Model), and conceptual (e.g. Hydrologiska Byrans Vattenbalansavdelning) models (Kwakye and Bárdossy, 2020; Soleimanian et al., 2022). Devi et al. (2015) and Kwakye and Bárdossy (2020) explained these classifications as follows: Physically based models represent the real system and uses state variables which are measurable and functions of both space and time, and perform well especially in small scales, conceptual models describes all components of the hydrological process and performs well in large scales, while empirical models are data driven models that use information from available data ignoring the features and processes of the hydrological system.

### 2.11.1. The Soil and Water Assessment Tool (SWAT) model

The SWAT model has been applied as an effective assessment model for hydrological modelling and water resources management worldwide (Vilaysane et al., 2015). SWAT is a river basin or watershed scale model of the United States Department of Agriculture - Agricultural Research Service (USDA -ARS) (Querner and Zanen, 2013). SWAT is based on the principle of water balance equation which is the principal driving force of all processes in the model due to its effects on pant growth, and sediments distribution (Arnold et al., 2012; Ayivi and Jha, 2018). The model simulates the hydrological cycle based on the following water balance equation (Vilaysane et al., 2015):

$$SW_t = SW_0 + \sum_{i=1}^{t}(R_{day} + Q_{surf} - E_a - W_{seep} - Q_{gw}) \qquad (2.7)$$

Where: $SW_t$ and $SW_0$ are the final and initial soil water contents (mm), $t$ is time (days), $R_{day}$ is the amount of precipitation (mm), $Q_{surf}$ is the amount of surface runoff (mm), $E_a$ is the amount of evaporation (mm), $W_{seep}$ is the amount of percolation and bypass flow exiting the soil profile bottom (mm), and $Q_{gw}$ is the amount of return flow (mm).

The main objective of SWAT model is to assess the effects of land management practices on water resources, sediments and contamination transport in large complex agricultural watershed characterised by different soil, land use and management conditions (Nursugi and Windari, 2014; Park et al., 2011). In order to fulfil this objective, the SWAT model is physically based, make use of accessible data, it is computationally effective and can be applied for an extended period of time (Querner and Zanen, 2013).

During SWAT model set up, the catchment is divided into sub-catchments which are further divided into Hydrological Response Units (HRUs), The HRUs represent unique combinations of land use, vegetation and soil characteristics (Gayathri et al., 2015; Ncube and Taigbenu, 2014). The model will therefore quantify relevant hydrological constituents for each HRUs

(Vilaysane et al., 2015). To perform simulations on catchment hydrologic processes, SWAT requires several inputs data such as, digital elevation model (DEM), soil types, land use, land cover, rainfall, temperature (minimum and maximum), solar radiation, relative humidity and wind speed (Mengistu et al., 2019). According to Nursugi and Windari (2014), SWAT model is data intensive but, integrating the model into GIS permits the use of accessible datasets from governmental sources on climate, soil, topography, and land use. The main components of SWAT are water resources, climate, nutrient cycling, soil temperature, sediment transport, crop growth, agricultural management, and pesticide dynamics (Abbaspour et al., 2009)

The SWAT model has been internationally accepted as a powerful interdisciplinary tool for watershed modelling as evidenced by SWAT international conferences, A number of SWAT associated papers introduced at numerous other scientific gatherings and multitudes of articles published in many journals (Akoko et al., 2021; Ang and Oeurng, 2018; Gassman et al., 2007; Mengistu et al., 2019; Obiero et al., 2011; Odiyo et al., 2020; Sirodoev et al., 2022). The international acceptance of SWAT is related to the model's flexibility in addressing water resources problems as a consequence of the models comprehensive nature, robust model support and open access status of the model (Gassman et al., 2014). According to Montecelos-Zamora et al. (2018), SWAT has been applied for different purposes in many regions worldwide, this include estimations of water resources and effects of climate change on water balance components. The model can also be applied in a watershed for streamflow predictions thorough preliminary model performance evaluation, then calibration and validation in order to initiate its performance in the selected catchment (Obiero et al., 2011). Furthermore, the model allows the division of a watershed or a river into sub-watershed or sub-basins which enables the model to simulate streamflow with a high level of spatial detail (Santhi et al., 2006). Gyamfi et al. (2016) applied SWAT model to assess the impacts of land use and land cover changes on hydrology in the Olifants Basin, South Africa. Faramarzi et al. (2013) fed the calibrated SWAT model with future climate projections from five global circulation models (GCMs) to analyse climate change impacts of on water resources availability in Africa, using a sub-basin as a hydrologic unit.

### 2.11.2. MIKE SHE model

The MIKE SHE (Abbott et al., 1986) is a deterministic, fully distributed and physically-based hydrological model, that has the ability to simulate simulated the critical processes of water cycle on both surface and subsurface (Papadimos et al., 2022). The MIKE SHE a derivative of Système Hydrologique Européen (SHE), was developed by the Institute of Hydrology (the United Kingdom), SOGREAH (France) and DHI (Denmark) (Sandu and Virsta, 2015). It is based on natural laws and representative data from the site where the hydrological model is being applied (Ikhwali and Pawattana, 2022). The MIKE SHE model includes validated empirical relations in addition to the finite difference representation and solution of the theoretical partial differential equations of mass and energy balance (Arrey et al., 2019; Papadimos et al., 2022). Furthermore, it incorporates modules such as advection-dispersion or geochemical modules, as well as the water movement module which is an fundamental part of the model responsible for combining various process-oriented components, each of which describes the main processes in each part of the hydrological cycle (Arrey et al., 2019). According to Rebelo et al. (2022), MIKE SHE covers major hydrological processes including overland flow, saturated and unsaturated flow, overland-groundwater, evapotranspiration, and irrigation and drainage. In MIKE SHE, watershed can be divided into basic units such as by dividing the areas as a grid network where water flows from one point to another when draining through the watershed (Ikhwali and Pawattana, 2022).

To simulate channel flow, the MIKE SHE model uses MIKE Hydro River module coupled to it (Rebelo et al., 2022). However, the original module for channel flow within the MIKE SHE does not support representation of hydraulic structures such as culverts and weirs which affects river flow simulation, especially in areas where watershed is affected by human activities (Sandu and Virsta, 2015). This problem was addressed by Refsgaard and Sørensen (1997) through the coupling of MIKE SHE with MIKE 11 hydraulic modelling system. This is achieved through river links, which are located on the margins separating adjacent grid cells (Sandu and Virsta, 2015). MIKE 11 is a 1-dimensional hydraulic modelling system based on the complete dynamic wave formulation of the Saint-Venant equations for modelling water flow in channel or rivers, as well as lakes and estuaries (Papadimos et al., 2022). Furthermore, It has extensive modeling tools for complex channel networks, reservoirs, and river structures like weirs, culverts, bridges and gates (Ramteke et al., 2020). The Sait-Venant equations for channel flow are expressed as two equations describing mass and momentum, and can be written as follows (Moussa and Bocquillon, 2000):

$$W^2 \frac{\partial t}{\partial y} + \frac{\partial Q}{\partial x} = 0 \tag{2.8}$$

$$\frac{\partial v}{\partial t} + V \frac{\partial Q}{\partial x} + g \frac{\partial y}{\partial x} + g.\left(S_f - S\right) = 0 \tag{2.9}$$

Where: y is the flow depth (m), V is the flow velocity (m $s^{-1}$), g is the acceleration due to gravity (m $s^{-2}$), S is the riverbed slope, $S_f$ the slope of energy line, Q the discharge ($m^3$ $s^{-1}$), x is the longitudinal distance (m), and t is time (s). a more detailed description these equations can be found in (Moussa and Bocquillon, 2000).

During MIKE SHE model setup, a number of dataset  is required including Digital Elevation map, land use/ land cover data, soil data, and climate data Initial groundwater head, bottom elevation of the aquifer system, geological units, time series, overland and channel flow component, saturated sone component etc.(Ramteke et al., 2020; Shu et al., 2018). However, data requirements may vary depending on hydraulic components simulated. Abbott et al. (1986) and  Refsgaard and Sørensen (1997) gives a detailed description of the MIKE SHE model.

According to Rebelo et al. (2022), the MIKE SHE is not commonly used in South Africa. However, the model has been successfully applied to relevant studies globally, i.e., Ikhwali and Pawattana (2022) used MIKE SHE model coupled with MIKE 11 model to calculate every component of water resources in order to evaluate the effects of climate change on water resources in Haui Luang watershed for baseline period (1986-2015) and future period (2021-2050). Malamataris et al. (2020) projected the implications climate change on the water balance of Volvi and Koronia lakes of the Mydonia basin aquifer until 2100 using hydrological and hydraulic models, such as MIKE SHE, MIKE HYDRO River, MIKE HYDRO Basin and the UTHBAL.  Papadimos et al. (2022) combined the MIKE SHE/MIKE 11 model and Global Circulation Models (GSMs) to assess the response of a Greek lake in terms of its water balance and water level under climate change.

### 2.11.3. Water Evaluation and Panning (WEAP) Model

The WEAP model is a type of decision system developed and supported by the Stockholm Environmental Institute (SEI) (Ashofteh et al., 2017). It is a lumped continuous hydrological model based on rainfall-runoff method (Abera Abdi and Ayenew, 2021). According to Tena et al. (2019) WEAP model operates based on the principle of water balance which makes it applicable to complex transboundary river systems, single catchments, and municipal and agricultural systems. Furthermore, it addresses a wide range of issues, including groundwater and streamflow simulations, reservoir operations, hydropower generation and energy demands, sectoral demand analyses, water conservation, water rights, water allocation priorities, ecosystem requirements, pollution tracking, and project benefit-cost analyses (Ikegwuoha and Dinka, 2020). The WEAP modeling tools capable of simulating hydrological processes and water management practices at the catchment level for the current status as well as for various alternative scenarios support quantitative estimations of water availability, water demand, and water consumption on both a temporal and spatial scale (Tena et al., 2019). Furthermore, the model calculates the hydrological cycle components by modeling the rainfall-runoff process at the catchment area's surface using climate time series (Ahmadaali et al., 2018). According to Abera Abdi and Ayenew (2021) climate datasets such as precipitation, temperature, relative humidity, and wind speed is one of the most important input data in the WEAP model.

Different methods are available in WEAP for rainfall-runoff modeling of the basin, which include rainfall-runoff (simplified coefficient method), rainfall-runoff (soil moisture method), irrigation demands only (simplified coefficient method), plant growth (daily; CO2, water and temperature stress effects), and MABIA (FAO 56, dual KC, daily) (Khalil et al., 2018). The rainfall-runoff method (soil moisture method) is the most preferred method when modelling hydrological processes of basins (Ahmadaali et al., 2018; Ikegwuoha and Dinka, 2020; Oti et al., 2020). The soil moisture method is based on a one-dimensional - two-soil-layer conceptual model algorithm for estimating surface runoff, evapotranspiration, deep percolation, and sub-surface runoff for a given unit area of land (Teklu et al., 2020). In soil moisture method, The catchment is divided into two soil layers known as buckets: an upper soil layer with shallow water capacity and a bottom soil layer with deep water capacity (Oti et al., 2020). Oti et al. (2020) further stated that the water balance of a catchment divided based on varying fractional land use and/or soil type areas is computed for each fraction area. Figure 2.4 shows a conceptual diagram and main equations in the soil moisture method. A detailed description of soil moisture method equations are given by Ahmadaali et al. (2018).

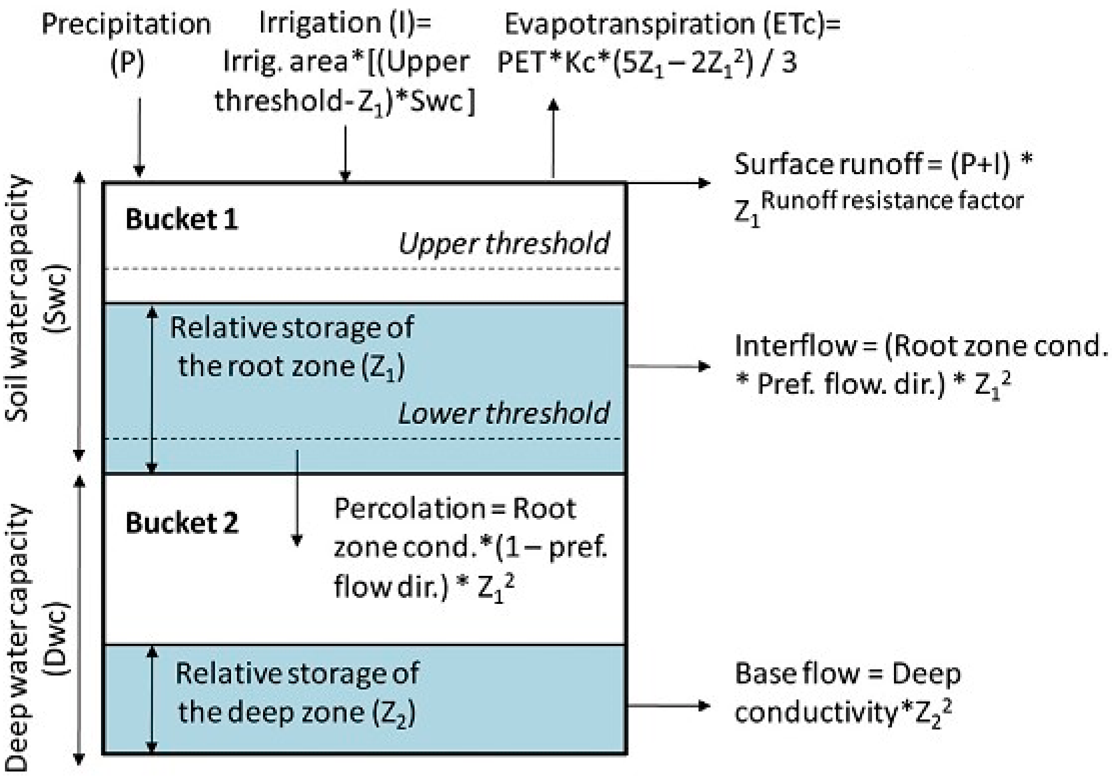


Figure 2.4: Conceptual diagram and equations incorporated in the soil moisture method (Ahmadaali et al., 2018).

### 2.11.4. Hydrologiska Byrans Vattenbalansavdelning (HBV) model

The HBV is a semi-distributed conceptual rainfall-runoff water balance model developed by Bergström and Forsman (1973). It was further improved as HBV-6 and HBV-96 by Bergström (1992) and Lindström et al. (1997), respectively. The HBV model takes into account key permafrost hydrological processes such as surface energy balance, snow routine, snow melt, soil moisture, and infiltration (Bui et al., 2020). In HBV model, The whole catchment is divided into sub-catchments, which are further subdivided into various elevation and vegetation zones (Devi et al., 2015). According to Tibangayuka et al. (2022) the main advantage of the HBV model is that it is simply structured, has less data requirements and computer facilities. The model uses precipitation, temperature, and potential evapotranspiration time series as input data, and to simulate daily discharge (Grimaldi et al., 2019; Pauwels et al., 2013). The Theissen polygons is used to average these input dataset over the watershed (Bui et al., 2020). However, The Thiessen polygon approach ignores the basin's elevation and temperature gradients, and as a result, the interpolation method used in the HBV model could produce unacceptable modeling results.(Bui et al., 2020). In the HBV model, precipitation is considered as a snow or rain depending on weather the temperature on the corresponding day is above or below the temperature threshold (TT), as such, when temperature is below TT, all precipitation is deemed to be a snow and when actual temperature is above, there will be snow melt (Parra et al., 2018). To simulate streamflow, the model divides precipitation into three reservoirs (slow, fast and soil), and then a triangular hydrograph is used to direct the modeled streamflow to the catchment (Grimaldi et al., 2019). Figure 2.5 shows a conceptual diagram and main equations incorporated in the HBV model based on Bergström (1992) and Lindström et al. (1997).

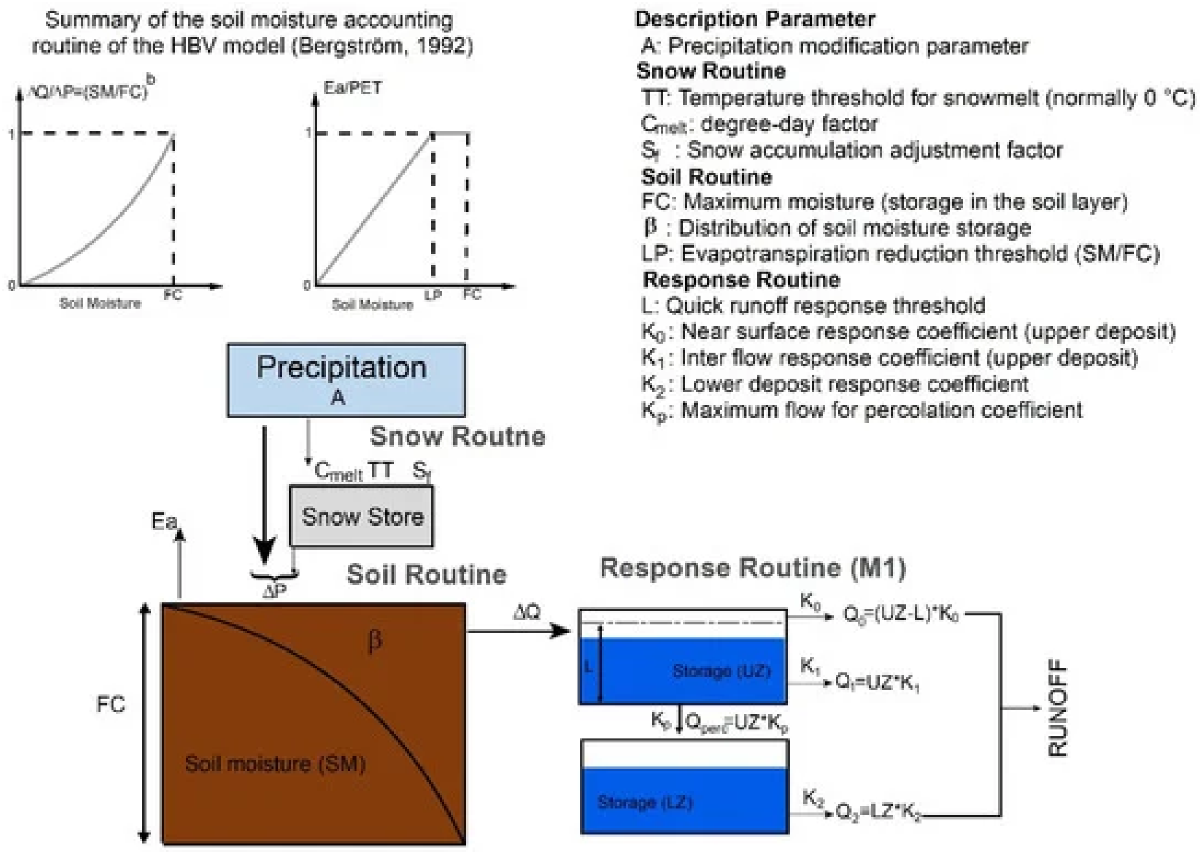


Figure 2.5: Simplified diagram of HBV model, including its parameters description and main equations. (Parra et al., 2018).

Tibangayuka et al. (2022) evaluated the performance of HBV model and Artificial Neural Network (ANN) in simulating streamflow in a data limited catchment in Tanzania. All models were reported to be able to simulate streamflow in the catchment. Similarly Kwakye and Bárdossy (2020) applied HBV model to simulate low flows in Black Volta basin in West Africa. They announced that the HBV model was stable and reacted well to precipitation signals. Heyi et al. (2022) fed the HBV model with projected future rainfall and mean monthly potential evapotranspiration to simulate future streamflow for 2050s and 2080s under changing climate conditions in upper Awash River sub-basin, Ethiopia. The model showed a good performance for streamflow forecasting. (Huang et al., 2019) highlighted that, although the HBV model is extensively used with good performance, the model still needs to improvements to better quantify the impacts of climate changes and land used changes. Furthermore, there is growing a debate about whether conceptual rainfall-runoff models can accurately simulate the water balance in response to changing climatic conditions (Coron et al., 2014; Fowler et al., 2016; Merz et al., 2011).

## 2.12. Summary

In this chapter, the literature reflects on the concept of climate change being long-term changes in global and regional weather patterns, or a change in the properties of the climate that prevails for a prolonged period. It has been scientifically recognized that global climate change is produced by human-induced emissions of greenhouse gases such as methane, carbon dioxide, and nitrous oxide into the atmosphere. Previous studies highlighted that climate change is perceived in terms of long periods of extreme heat, and rainfall scarcity. climate change impacts on water resources were discussed on an international, continental, regional and national scale as well as impacts on agriculture in Limpopo province and Vhembe District municipality.

The concept of crop water requirements, crop reference evapotranspiration as well as the impacts of climate change of future crop water requirements were also reviewed. The chapter further explained a set of emission and concentration scenarios known as the RCPs used for climate projections. Climate change projection models were also reviewed. This include the GCMs, and regional climate models such as CORDEX and CCAMs provide the opportunity to simulate reginal and local climate of selected areas at a high resolution. However, when quantifying climate change impacts on water resources, uncertainties from climate models may arise from several sources including greenhouse gas emission scenarios, selection of GCMs, downscaling methods (RCMs), structures and parameterization of hydrological models.

The last section of this chapter reflets on the concept of hydrological modelling. Several hydrological models including SWAT, MIKE SHE, HBV and WEAP were reviewed. it was also emphasized that SWAT has been applied as an effective assessment model tool for hydrological modelling and water resources management worldwide, and It has been worldwide accepted as a powerful interdisciplinary tool for watershed modelling as proven by SWAT international conferences, hundreds of SWAT-related papers introduced at multiple other scientific gatherings, and multitudes of publications published in many journals.

# CHAPTER 3: MATERIALS AND METHODS

## 3.1. Preamble

This chapter covers information about methodologies used to achieve the study objectives, data collection, data sources and data analysis.

## 3.2. Hydrological analysis for climate impact modelling

The SWAT model was used in this study to assess the impacts of climate change on water resources availability for agriculture with the aim of proposing practical adaptive measures to alleviate future climate change impacts for small-scale farmers within the study area. The SWAT model was selected for this study due to its acceptance as a powerful tool for watershed modelling as evidenced by SWAT international conferences, tons of SWAT associated papers presented at numerous scientific gatherings and multitudes of articles published in many journals (Ang and Oeurng, 2018; Obiero et al., 2011). A study by Ncube and Taigbenu (2014) reported the ability of SWAT model to represent South African watershed and produce streamflow time series adequately, and can be applied to areas with limited data like in this study area. The SWAT model was set to project future climate change impacts on water resources based on inflows for two future scenarios: near future (2023-2052) and far future scenarios (2053-2082). Figure 3.1 shows the structure of methodology of modelling under Arc-SWAT.

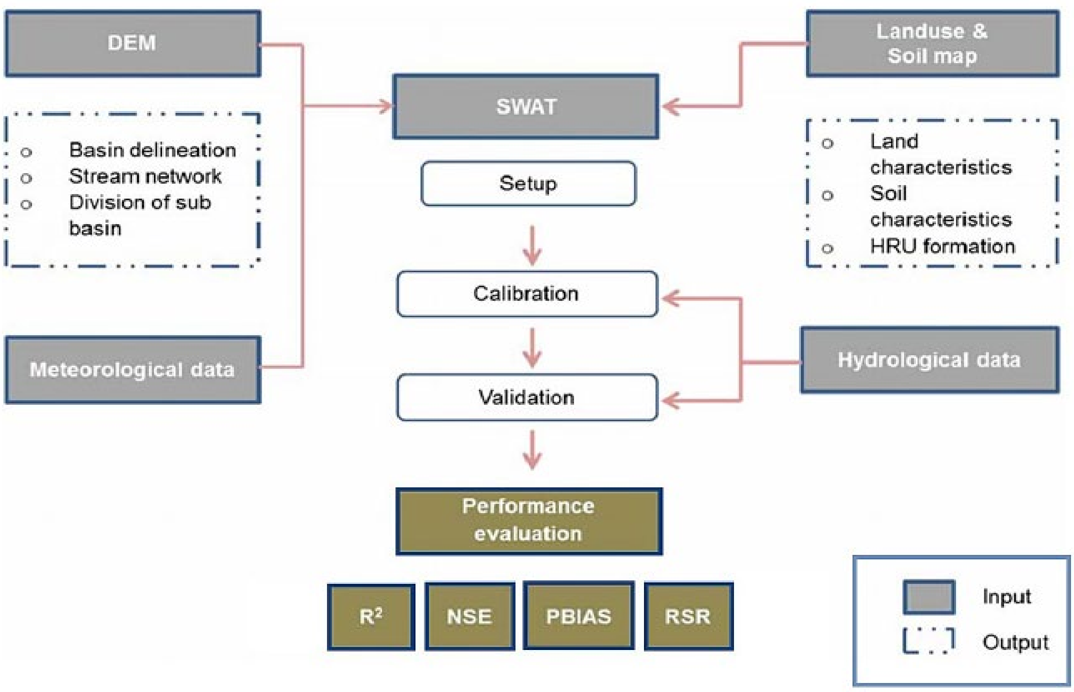


Figure 3.1: Structure of methodology of modelling under Arc-SWAT (Aqnouy et al., 2019).

The SWAT model was setup to project future inflows using CCAM climate data on rainfall and temperature to simulate future inflows based on predicted climate scenarios. The format suitable for SWAT model input data requirement was taken into consideration during data preparation. Historical data on rainfall, minimum and maximum temperature, relative humidity, solar radiation, and wind speed from several weather stations within Nzhelele area were assessed to establish their status, such as the period in which data available and data status. This allowed the selection of model simulation, calibration, and validation periods. Digital Elevation Model (DEM), Soil data, Land cover data and observed streamflow data are also required as inputs parameters for SWAT model set up. The Figure 3.2 shows the processes involved in SWAT model data input, setup, model calibration and validation, as well as streamflow simulation using ArcSWAT. This involves the selection of installed ArcSWAT extension, delineation of the watershed, HRUs definition, databases editing, defining weather data, default input files application, including setting up and running the model. Graphical tools which are installed within the model interface can then be used to present the simulated results.

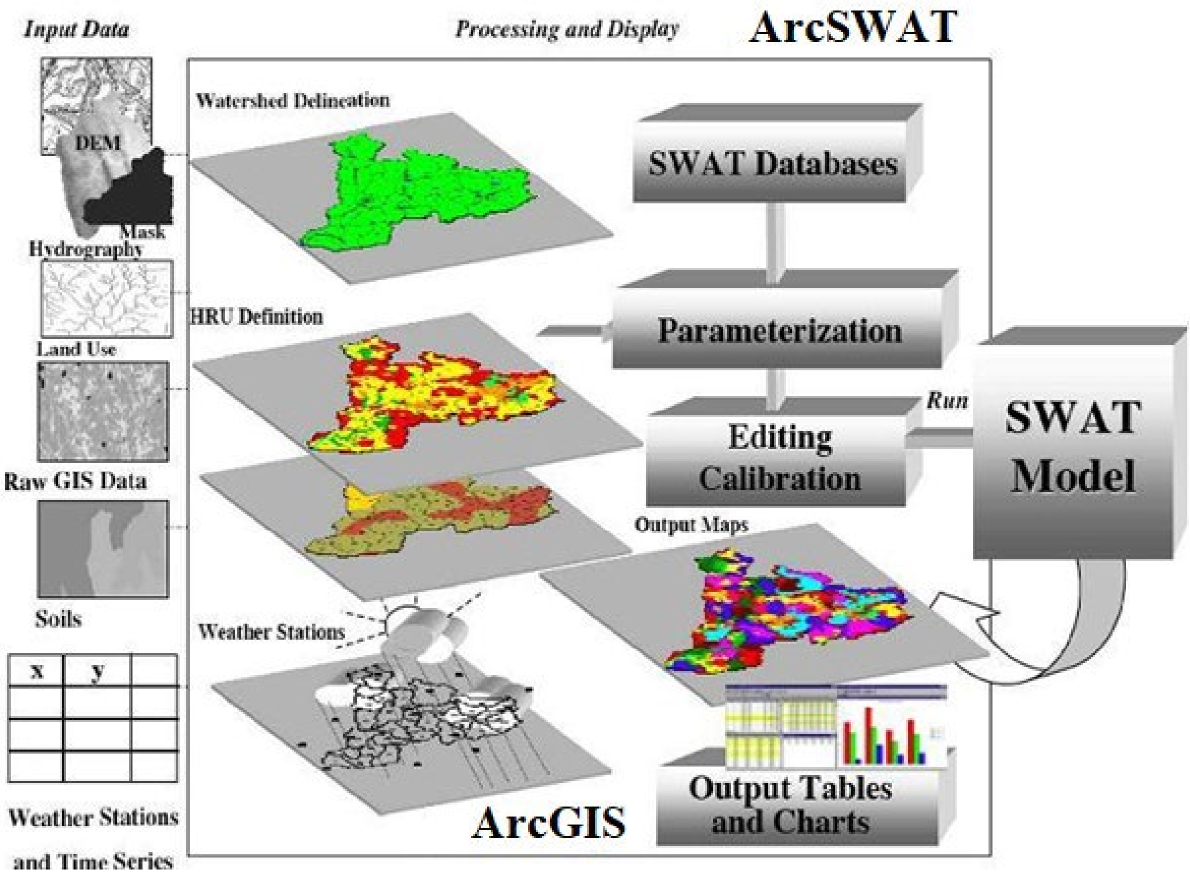


Figure 3.2: Arc-View Interface showing processes in SWAT during flow simulation (Odiyo et al., 2020).

### 3.2.1. SWAT model data requirements and setup

The SWAT model is comprehensive and requires a diversity of information and data to run. According to (Chordia et al., 2022) The SWAT model requires inputs data related to watershed characteristics such as the Digital Elevation Model (DEM), Land Use Land Cover (LULC), soil data, hydrological data and climatic factors (such as precipitation, temperature, wind speed, relative humidity, and solar radiation). Statistical techniques and trend analyses aided identification of relationships within and between data sets.

- **Rainfall and temperature data**

Rainfall and temperature (minimum and maximum) data from SWAT gridded station 229303 for the period 1987-2009 were collected as input variables to the SWAT model. Rainfall data for the period 1987-2009 from three real ground rainfall stations (Mphephu, Jouberstroom and Veermedling) obtained from South African Weather Service (SAWS) were also added as input variable to the SWAT model to supplement the SWAT gridded station and to show real presentation of rainfall in the study area. Figure 3.3 Shows the location of the rainfall and temperature stations within the study area. However Gauging stations used in this study were selected depending on the availability and quality of data.

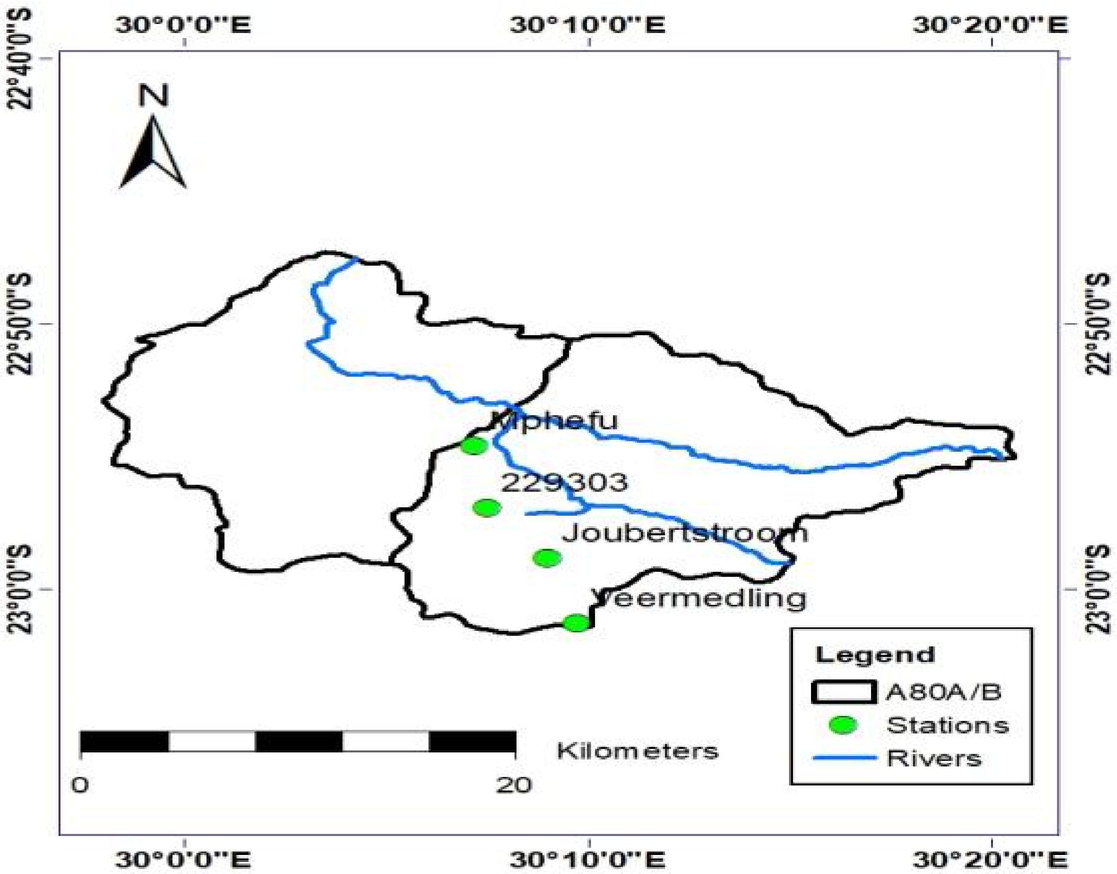

Figure 3.3: Location of rainfall (Mphephu, Jouberstroom , Veermedling and 229303) and temperature (229303) stations

- **Land cover**

Land cover map for quaternary catchments A80A and A80B within Nzhelele area was prepared by the Department of Environmental Affairs (DEA). The map was generated based on the 2018 South African National Land-cover dataset produced by GEOTERRAIMAGE as a commercial data product from digital, multi-seasonal Landsat 8 multispectral imagery. More than 600 Landsat images were used to generate the land-cover information, based on an average of 8 different seasonal image acquisition dates, within each of the 76x image frames required to cover South Africa. The land-cover dataset, which covers the whole of South Africa, is presented in a map-corrected, raster format, based on 30x30m cells equivalent to the image resolution of the source Landsat 8 multi-spectral imagery. The dataset contains 72 x land-cover / use information classes, covering a wide range of natural and man-made landscape characteristics. The original land-cover dataset was processed in UTM (north) / WGS84 map projection format based on the Landsat 8 standard map projection format as provided by the USGS. Figure 3.4 shows the land cover map of the study area.

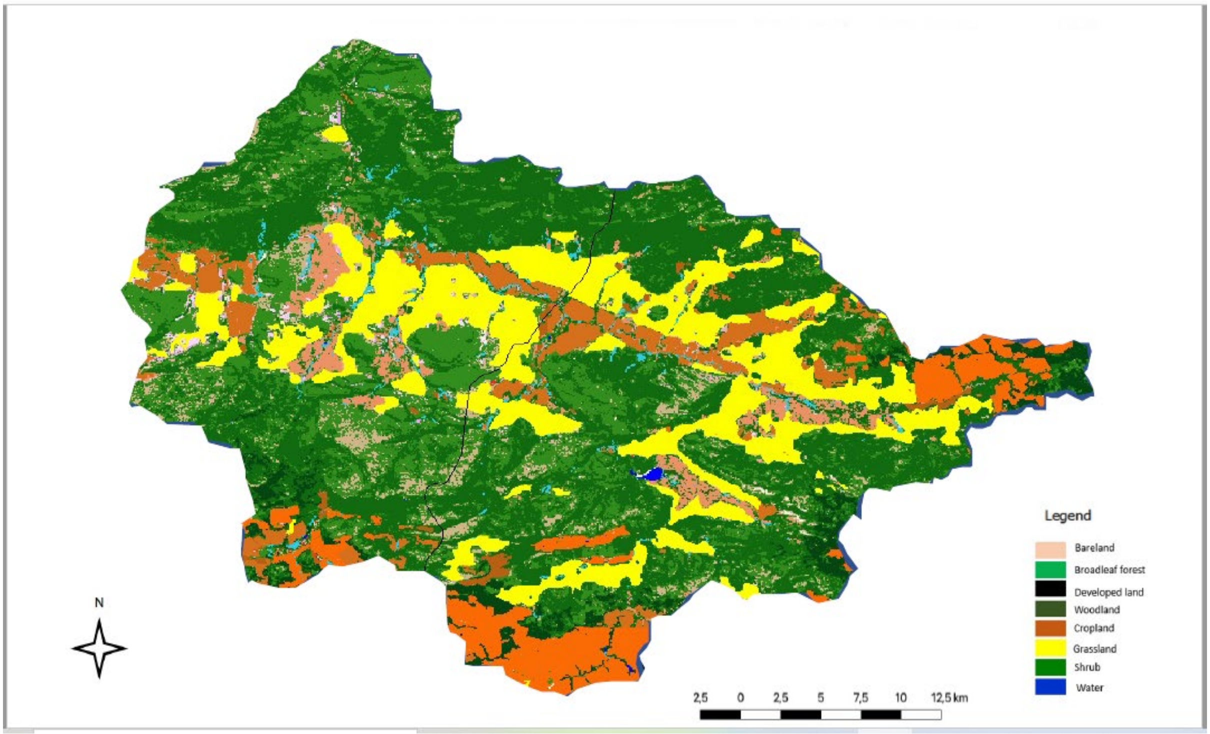


Figure 3.4: Study area land cover map

- **Digital Elevation Model (DEM)**

In hydrological modelling, the DEM is the most critical spatial input parameter (Sukumaran and Sahoo, 2020), that represent the ground surface topography or terrain in a digital raster form (Abrams et al., 2020). It provides information about the hydrological parameters of the watershed such as area of the subbasins, slope and stream information (location, length, depth, and width). The DEM (Figure 3.5) was downloaded from the United States Geological Servery's EROS Data Center. The Shuttle Radar Terrain Model (SRTM) was the source of the 30 meters DEM used in this study. The dataset was derived through mosaicking of individual SRTM tiles for a particular country and clipping the mosaicked tiles using the country (South Africa) boundary extent. DEM was used to generate the delineated quaternary catchment A80A and A80B within Nzhelele area for the purpose of hydrological modelling. The DEM was further delineated into sub-basins.

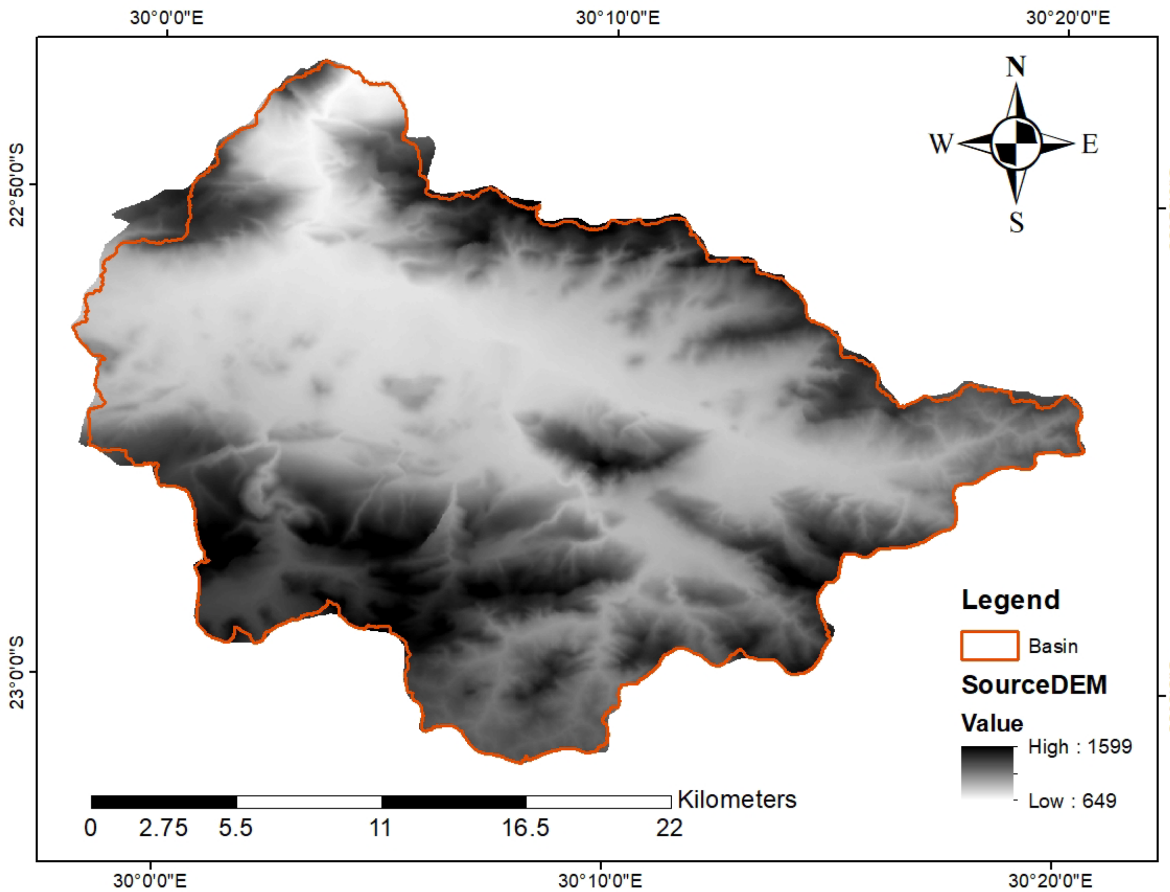


Figure 3.5: Study area Digital Elevation Map (DEM)

- **Soil infomation**

SWAT model requires soil property data such as texture, physical properties, chemical composition, hydraulic conductivity, moisture content, bulk density and organic carbon content for different layers of each soil (Mango et al., 2011). However, the SWAT database inbuilt within ArcSWAT model only contains soil types for the United States. Thus, a coarse soil map of 1:50 000 scale acquired from the Agricultural Research Council's (ARC) land type map (ARC-ISCW, 2006), was used to generate soil type map for the for quaternary catchments A80A and A80B. Land type map for the study area was formed by digitising boundaries of different soil textures and assigning various polygons to represent different soil categories. Figure 3.6 present the land type of the study area, and Figure 3.7 indicates an example of soil component and layers parameters that were manually inserted into ArcSWAT based on information from the land types. Table 3.1 shows the description of soil properties for each land use class.

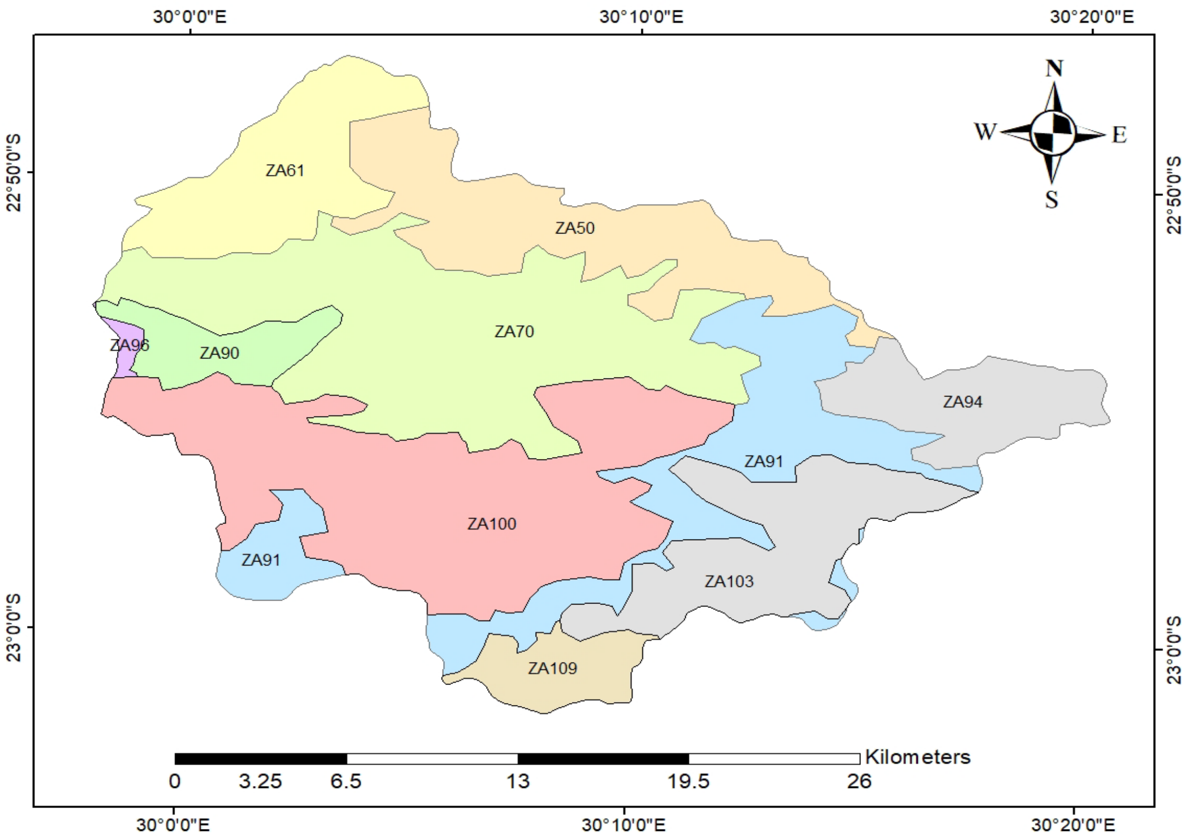


Figure 3.6: Study area land type map

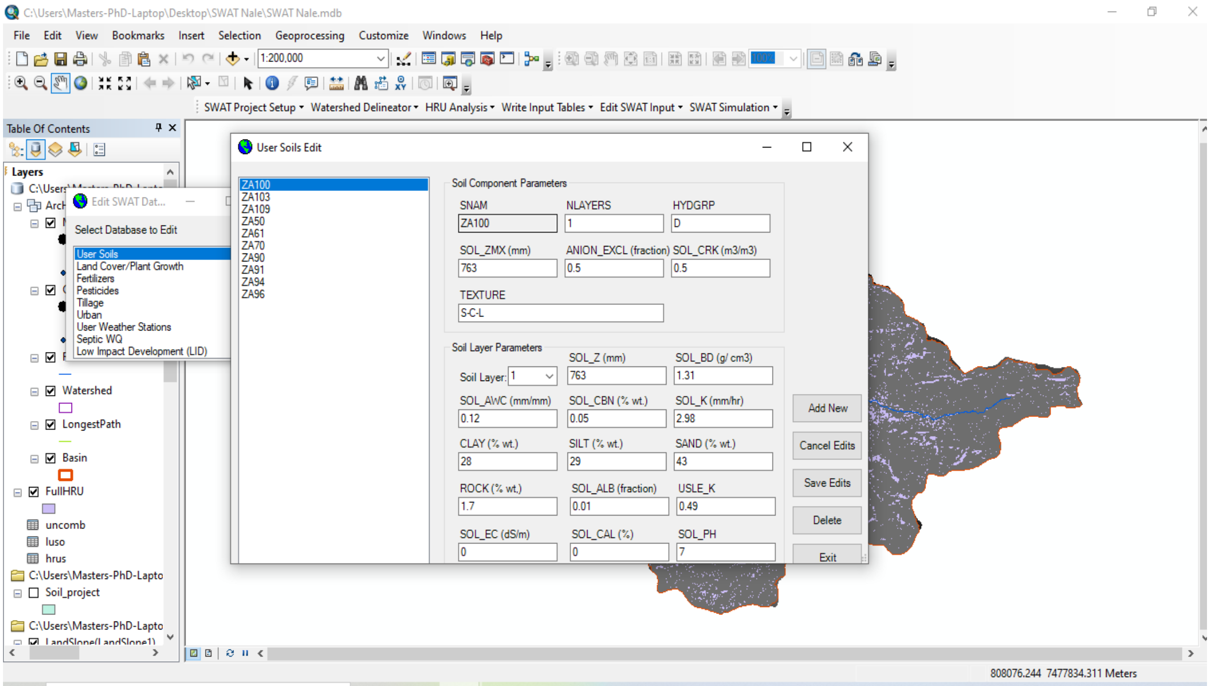


Figure 3.7: An example of soil component and layers parameters that were manual input into ArcSWAT

Table 3.1: Soil properties for different land types inserted in SWAT model obtained from ARC-SWAT software.

| Item no | Land type | Approx. Texture | | | | Soil properties | | | | | |
|---|---|---|---|---|---|---|---|---|---|---|---|
| | | Depth (mm) | Ave. % clay (given) | % Silt | % Sand | Bulk density (g/cm$^3$) | Ks (mm/h) | AWC (mm/mm) | Rock % | Texture | HYDGRP |
| 1 | ZA100 | 763 | 28 | 29 | 43 | 1.26 | 2.28 | 0.12 | 1.7 | Clay loam | D |
| 2 | ZA103 | 763 | 28 | 29 | 43 | 1.31 | 2.98 | 0.12 | 1.7 | Caly loam | B |
| 3 | ZA109 | 763 | 36 | 18 | 46 | 1.26 | 2.98 | 0.12 | 1.7 | Sandy clay | C |
| 4 | ZA50 | 763 | 28 | 29 | 43 | 1.31 | 2.98 | 0.2 | 1.7 | Sandy clay loam | D |
| 5 | ZA61 | 763 | 19 | 29 | 52 | 1.37 | 2.98 | 0.12 | 1.7 | Sandy loam | B |
| 6 | ZA70 | 763 | 19 | 7 | 74 | 1.4 | 2.98 | 0.12 | 0.1 | Sandy loam | A |
| 7 | ZA90 | 763 | 19 | 29 | 52 | 1.37 | 2.98 | 0.12 | 1.7 | Sandy | B |

| | | | | | | | | | | | |
|---|---|---|---|---|---|---|---|---|---|---|---|
| | | | | | | | | | | loam | |
| 8 | ZA91 | 763 | 22 | 19 | 59 | 1.4 | 2.98 | 0.12 | 1.7 | Sandy clay loam | C |
| 9 | ZA94 | 763 | 19 | 29 | 52 | 1.37 | 2.98 | 0.12 | 1.7 | Sandy loam | B |
| 10 | ZA96 | 763 | 15 | 18 | 67 | 1.48 | 2.98 | 0.12 | 1.7 | Sandy loam | A |

- **Land use/cover**

Figure 3.8: indicate land use classes in the study area. In total, six land uses were classified based on land cover classes. The classification process was done using the existing SWAT codes. Table 3.2. shows the description of codes and percentages of areas covered by each land use class. The codes are representing how land cover classes appears on the SWAT model. The codes were obtained on the SWAT model database, and they are spelled out under the "Land cover" header on the table.

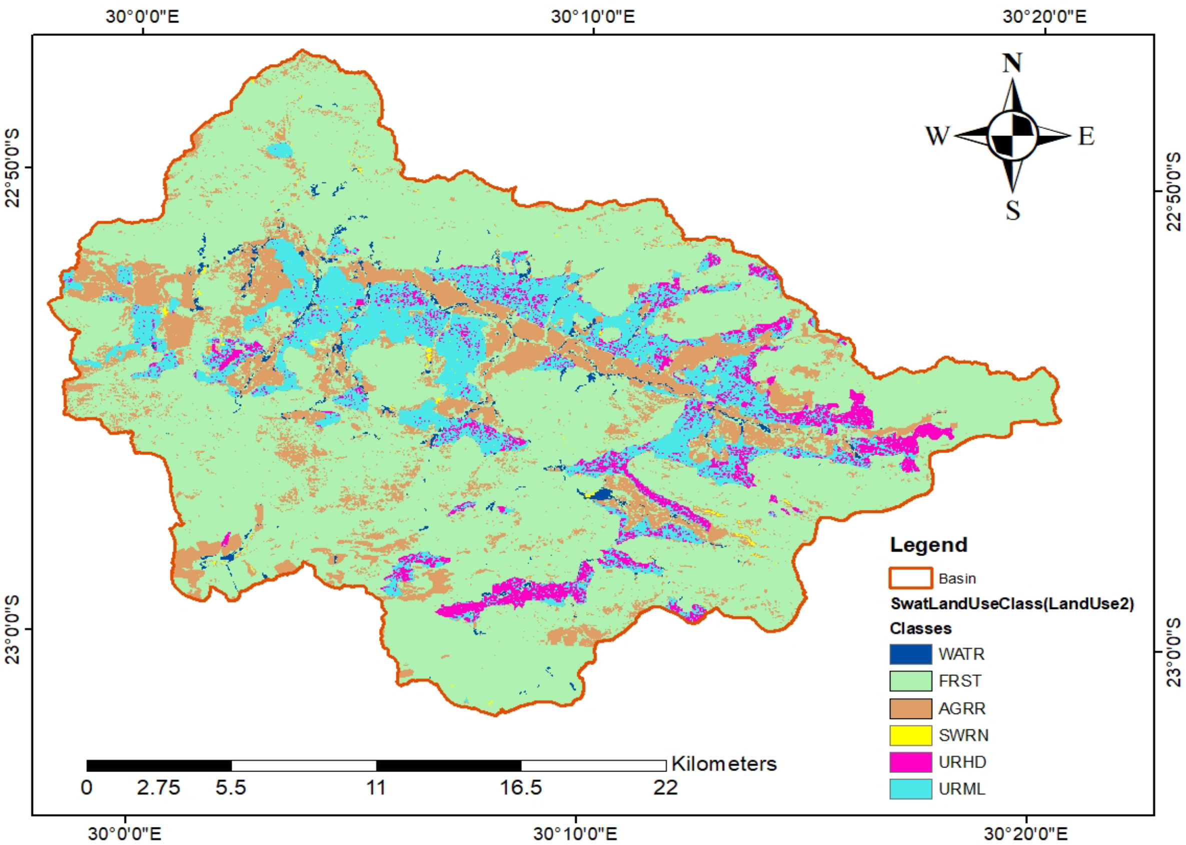


Figure 3.8: Land use/cover classes

Table 3.2: Description of land use/cover classes for the study area

| Land cover | SWAT code | Area (%) |
|---|---|---|
| Water | WATR | 1.05 |
| Forest-Mixed | FRST | 68.08 |
| Agricultural Land-Row Crops | AGRR | 14.36 |
| Barren land (rock/sand/clay) | SWRN | 0.19 |
| Urban high density | URHD | 4.58 |
| Urban medium density | URML | 11.74 |

### 3.3. SWAT model setup

The collected data were pre-processed in a format that suites SWAT model data requirements before it was uploaded in the model. The following datasets were prepared for Nzhelele area as inputs required for SWAT model setup.

- Rainfall, temperature (minimum and maximum), relative humidity, wind, and solar data for the study area for the period 1987-2009 were obtained from SWAT database (station 229303).
- CCAM projections from the CSIR (rainfall and temperature)
- Digital Elevation map (DEM)
- Watershed delineation
- Sub-division of the model into hydrological response units (HRUs)

The SWAT model was setup for the baseline period (1987-2009) to determine future water availability for agriculture under changing climatic conditions based on inflows into Raliphaswa irrigation weir for two future scenarios 2023-2052 (near future) and 2053-2082 (far future) using projected rainfall and temperature data from CCAM virtual stations p-229300, p-229301 and p-229301 (Figure 3.9).The study determined both future scenarios for a period of 30 years which is a minimum recommended period for any hydrological study by the World Meteorological Organization.

### 3.4. Model calibration, and validation

In this study, SWAT model was setup using the DEM, soils, and land cover data which were in GIS format. This was accomplished in the ArcGIS 10.7's ArcMap software utilizing the ArcSWAT added as an extension. In order comply with ArcSWAT's requirement of using the same projection to minimize dataset mismatches during processing, all the spatial datasets used for the purpose of this study were projected to UTM 35 south and WGS84 datum. The model was set based on the step-by-step procedure adopted from Jayakrishnan et al. (2005) and Durães et al. (2011).

After model setup, the user must determine and adjust the most sensitive parameters for a given watershed or sub-watershed, this is typically the first step in SWAT calibration and validation process (Arnold et al., 2012). In this study, sensitivity analysis was carried out first to determine the most sensitive parameters for calibration and validation. After sensitive parameters were identified, the model was then calibrated fist. According to Vilaysane et al. (2015) calibration is the modification or adjustment of model parameters within the recommended ranges to optimize the model output so that it matches with the observed data. The study performed both manual and auto-calibration, whereby model parameters were appropriately adjusted to fit the observed data. Auto-calibration was done using SWAT-CUP which is a computer program developed by Abbaspour et al. (2007), to integrate calibration, validation, sensitivity and uncertainty analysis procedures of SWAT model in a single interface (El Harraki et al., 2021). For parameter calibration and uncertainty analysis, the Sequential Uncertainty Fitting Version 2 (SUFI-2) algorithm within SWAT-CUP was used. This was because SUFI-2 approach has been identified as the most appropriate method for determining SWAT uncertainty under condition that the parameter range are specified (Guug et al., 2020). The SWAT model used in this study was calibrated for a period of 10 year (1991-2000) and the model output used for calibration was streamflow.

After calibration, the model was validated. Validation is the process of demonstrating that a given site-specific model is capable of making sufficiently accurate simulations although “sufficiently accurate” can vary based on the given project (Arnold et al., 2012). The observed stream flow data for a 9-year period (2001-2009) was used to validate the model.

### 3.5. SWAT model performance evaluation

A model cannot be applied for scenario analysis and policy development without a statistical analysis of its reliability (Tan et al., 2019). In general the Coefficient of determination ($R^2$) and Nash-Sutcliffe Efficiency (NSE) are the most popular statistics used to evaluate SWAT model performance (Tan et al., 2019). The percent bias (PBIAS) and ratio of the root mean square error to the standard deviation of measured data (RSR) recommended by Moriasi et al. (2007) for SWAT model performance evaluation in watershed simulations were also additional criteria used for model evaluation in this study.

### 3.5.1. Nash-Sutcliffe Efficiency (NSE)

The NSE is the most widely used evaluation criterion for testing the goodness of fit between the observed and simulated values (Obiero et al., 2011). Moreover, It shows how closely the plot of observed and simulated data fits the 1:1 line (Ang and Oeurng, 2018; Nursugi and Windari, 2014). According to  Gyamfi et al. (2016), NSE ranges from –Inf to 1, where 1 denotes the perfect agreement between the simulated and observed variables. Montecelos-Zamora et al. (2018) further stated that, NSE index values greater than 0.75 are considered “good” and those between 0.75 and 0.36 are considered “satisfactory”. NSE is calculated as follows:

$$\mathrm{NSE} = 1 - \frac{\sum_{i=1}^{n}(O_i - S_i)^2}{\sum_{i=1}^{n}(O_i - \bar{O})^2} \qquad (3.1)$$

Where: where $O_i$ is the observed variable, $S_i$ is the simulated variable, $\bar{O}$ is the mean of the observed variable, $\bar{S}$ is the mean of the simulated variable, n is the number of observations under consideration (Gyamfi et al., 2016), this is also the same for equation 3.2 and 3.3.

### 3.5.2. Coefficient of determination ($R^2$)

The $R^2$ represents the percentage of variance in the measured data that is explained the simulated data which varies between 0 and 1(Reungsang et al., 2010). According to (Obiero et al., 2011) $R^2$ describes the degree of collinearity between simulated and observed data. If the value of value of $R^2$ is close to 0, the model prediction is considered unacceptable but if it approach or is close to 1, the model predictions become highly accurate (Reungsang et al., 2010).  Generally, a model is considered acceptable if the $R^2$ is greater than 0.5 (Gyamfi et al., 2016). $R^2$ is calculated as follows:

$$R^2 = \left[\frac{\sum_{i-1}^{n}(O_i - S_i)(S_i - \bar{S})}{\left(\sum_{i-1}^{n}(O_i - \bar{O})^2\right)^{0.5}\left(\sum_{i-1}^{n}(S_i - \bar{S})^2\right)^{0.5}}\right]^2 \qquad (3.2)$$

### 3.5.3. Percent bias (PBIAS)

The PBIAS is a measure of how much (in percentage) the observed variable is either underestimated or overestimated (Gyamfi et al., 2016). Positive or negative values indicate that the model overestimates or underestimates the simulated flows respectively (Cardoso de Salis et al., 2019). According to Raksmey Ang and Oeurng (2018), the optimal value of PBIAS is zero, indicating exact simulation of observed values. Raksmey Ang and Oeurng

(2018) further stated that, in general, a lower value of PBIAS signifies accurate model simulation. It is calculated as follows:

$$\mathrm{PBIAS} = \frac{\sum_{i=1}^{n}(O_i - S_i)}{\sum_{i=1}^{n} O_i} \times 100\% \quad (3.3)$$

### 3.5.4. Ratio of the root mean square error (RMSE) to the standard deviation of measured data (RSR)

The RSR incorporates the advantages of error index statistics and includes a scaling/normalization factor, allowing the resulting statistic and reported values to be applicable to a wide range of constituents (Amin and Nuru, 2020). RSR has a range of 0.0 to +1, with low values suggesting good model performance (Ang and Oeurng, 2018). Ang and Oeurng (2018) further stated that RSR = 0 implies that the model simulation fits perfectly to the measured data, whereas large positive RSR values imply poor model performance. Gyamfi et al. (2016) gave the mathematical expression of RSR as follows:

$$\mathrm{RSR} = \frac{\mathrm{RMSE}}{\mathrm{STD_{obs}}} = \frac{\sqrt{\sum_{i-1}^{N}(O_i - S_i)^2}}{\sqrt{\sum_{i=1}^{n}(O_i - \bar{O})^2}} \quad (3.4)$$

where $O_i$ is the observed variable, $S_i$ is the simulated variable, $\bar{O}$ is the mean of the observed variable, $\bar{S}$ is the mean of the simulated variable, n is the number of observations under consideration, RMSE is the root mean square error, $\mathrm{STD_{obs}}$ is the standard deviation of the observed variable.

## 3.6. Climate change modelling and estimation of future inflows

Future climate projections were not carried out in this study. The already existing and freely available CCAM climate projections (meteorological data) were obtained from the Council for Scientific and Industrial Research (CSIR). The CSIR-CCAM projections were chosen for this study because of their 8 km resolution in contrast to the course resolution (50 km) regional models forced by CORDEX. This makes COEDEX not suitable for application within small catchments. A project by Engelbrecht (2019) on detailed Projections of Future Climate Change over South Africa highlighted that CCAM performed at 8 km resolution are more advantageous than 50 km resolution simulations, this is because convective rainfall is partially resolved in 8 km resolution and main topographic features such as southern and eastern escarpment are much better resolved which indicate that the model does not highly depend on statistics to simulate the complex aspect of the atmospheric dynamics and physics (convective rainfall), and that the topographic forcing of temperature, wind patterns and convictive rainfall can be simulated realistically (Engelbrecht, 2019). Inflows were projected for the periods 2023-2053 and 2053-2082 relative to the baseline period 1987-2009. Rainfall and temperature data from CCAM virtual station p-229300, p-229301 and p-229300 was used to project future inflows. Figure 3.9 shows the location of CCAM virtual stations used in this study.

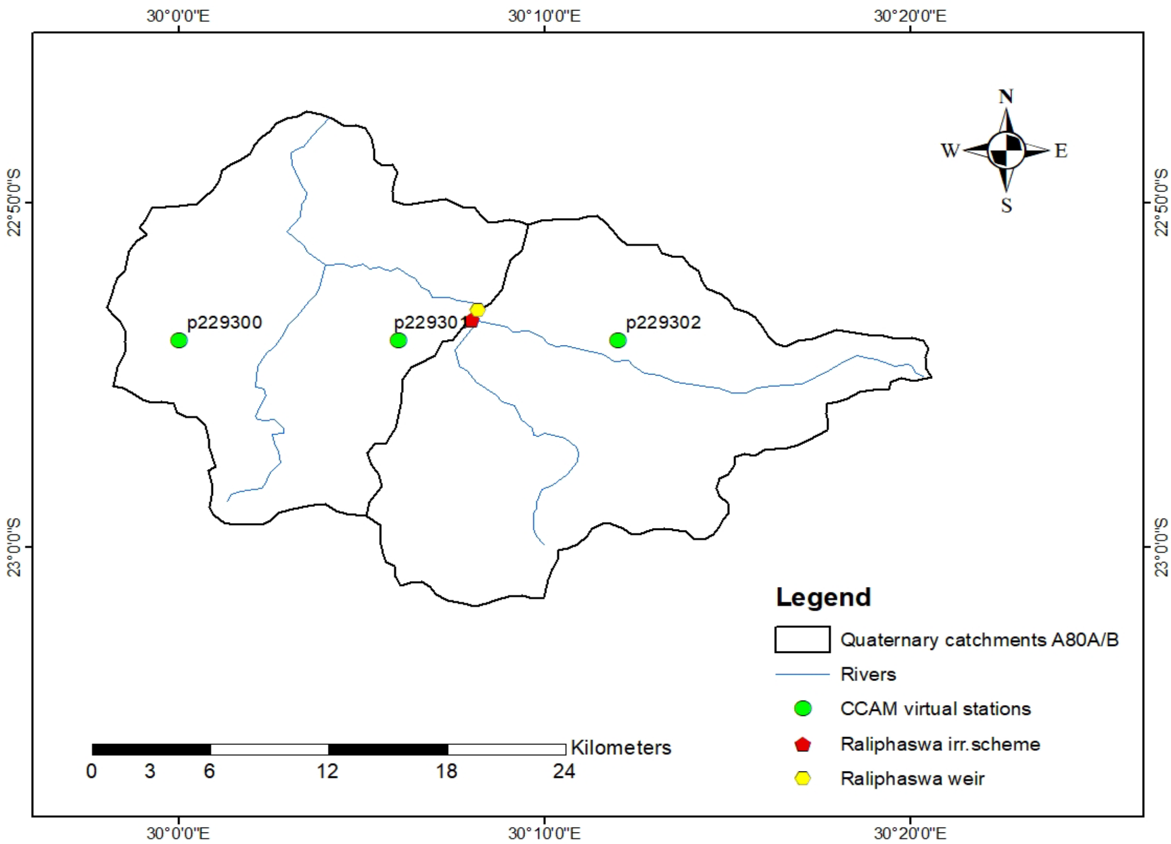


Figure 3.9. Location of CCAM visual station in the study area

### 3.7. Analysis of rainfall and temperature trends

Analysis of long-term changes in historical and future climate data (rainfall and temperature) in the context of climate change was carried out in this study. Historical temperature data for station 299300 and rainfall data for stations 299300, Mphephu, Jouberstroom and Veermedling used to set up SWAT model were analysed for the period 1987-2009 to understand their trends. Future rainfall and temperature data from CCAM virtual station p-299301 was also analysed. Sation p-229301 was selected for analysis because it is located near Raliphaswa irrigation scheme and was used for estimating future CWRs for comparison with inflows to determine if future inflows into the irrigation weir will meet crop water requirements under changing climatic conditions. Monthly and annual changes in rainfall and temperature for station p299300 were analysed for the baseline period (1993-2022), near future (2023-2052) and far future (2053-2082) to determine their changes with time. The results from the analysis were presented in graphs showing historical and future rainfall, and maximum and minimum temperatures patterns throughout the years, as well as their trends.

Linear regression is a statistical technique that can be used to determine the relationship between the dependent variable and one or more independent variables and can be expressed as follows (Daniya et al., 2020):

$$Y = \beta 0 + \beta 1 \times \varepsilon \tag{3.5}$$

Where, Y is the dependent variable (or output variable), X is the independent variable (or input variable), β0 is the intercept, β1 is the slope, and Ɛ is random error component. Equations for calculating these variables are found in Daniya et al. (2020).

In regression analysis, the p-value is used to determine whether the relationship between the independent and dependent variables is statistical significance (Gareth et al., 2013). In this study, the p-value was calculated to determine statistical significance of the historical and future trends. The $p<0.05$, also referred to as alpha ($\alpha$=005) is the most common error threshold for determining statistical significance (Andrade, 2019; Thiese et al., 2016). The p-value of less than or equal to 0.05, showed that the trends were statistically significant, while the p-value of greater than 0.05 suggested that the trends were not statistically significant (Wasserstein and Lazar, 2016). The trends were considered to be highly significant if the observed p-value is equals or lower than 0.01.

### 3.8. Estimation and comparison of future CWRs with projected inflows

Future CWRs of selected crops were estimated for three periods: Historical period (1993-2022), near future (2023-2052) and far future (2053-2082) based on Allen et al. (1998) Kc approach (Equation 2.1). The $ET_0$ was estimated based on the Hargreaves and Samani (1985) method (Equation 2.4) in Chapter 2.5.3 due to limited data availability in the study area. Downscaled temperature data from CCAM station t-299301 (Figure 3.9) which is located near to the irrigation schemes were used to estimate $ET_0$ for from which crop water requirements are estimated. To get the CWRs, the calculated $ET_0$ was multiplied by Kc value that is defined for each of the four growth stages of the crop (Equation 3.6).

$$CWR = K_c \times ET_0 \tag{3.6}$$

Where *CWR* is the water requirement of a given crop in mm/day, $K_c$ is the crop factor and $ET_0$ is the reference crop evapotranspiration in mm/day (Allen et al., 1998).

Figures 3.10 to 3.13 show the Kc values at different crop growth stages used in estimating crop water requirements in this study. Kc values at each crop growing stage are based on FAO Irrigation and Drainage paper No.24 by Allen et al. (1998) which provides general crop data for various climates and locations.

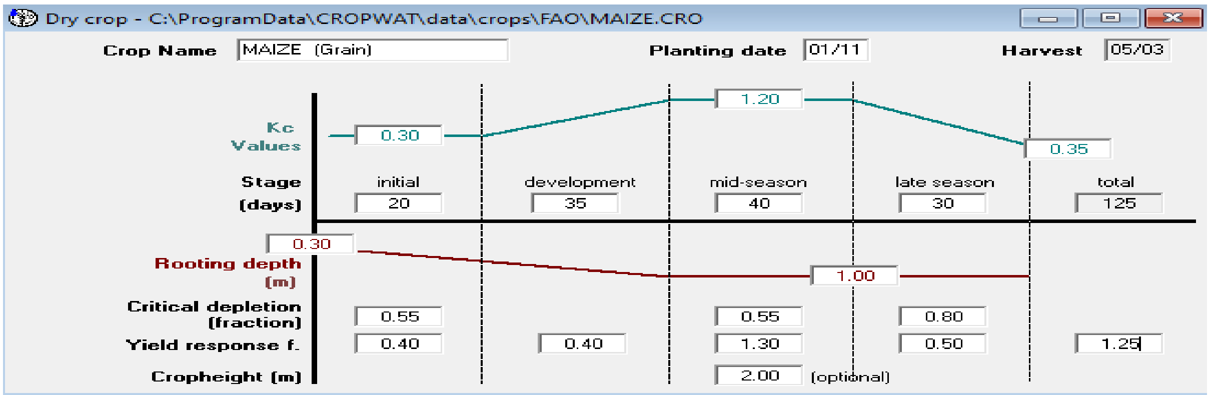


Figure 3.10: Kc curve and crop growth stages for maize

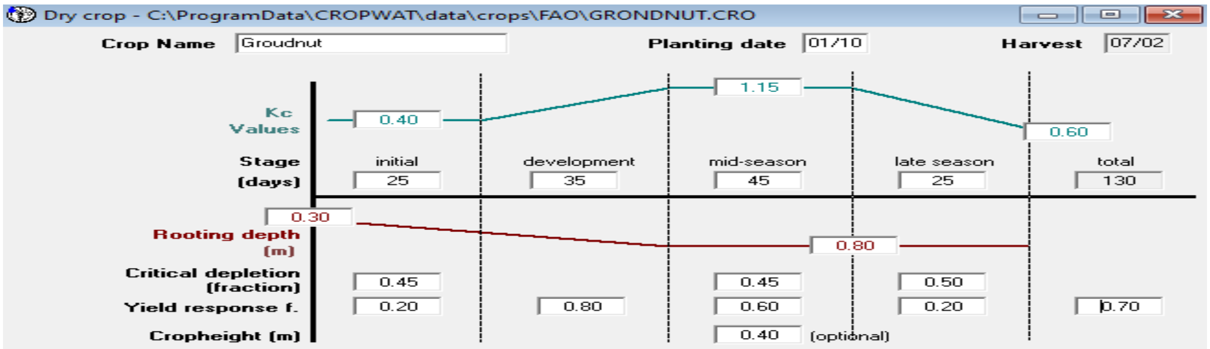


Figure 3.11: Kc curve and crop growth stages for groundnuts

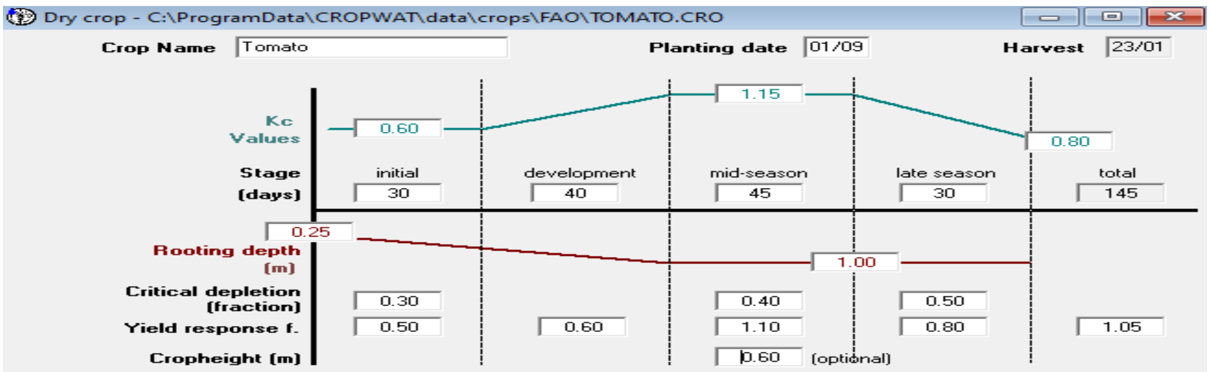


Figure 3.12: Kc curve and crop growth stages for tomato

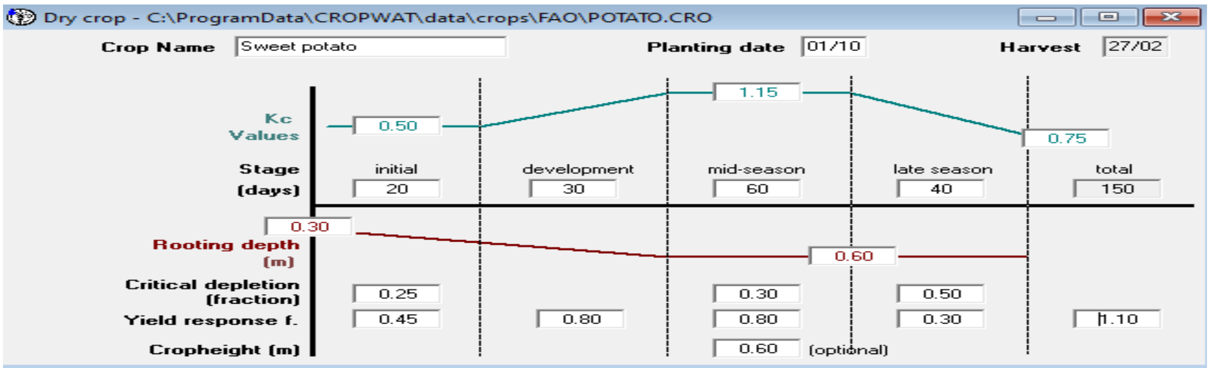


Figure 3.13: Kc curve and crop growth stages for sweet potato

In this study, water requirements for selected crops in Raliphaswa irrigation scheme were calculated for two growing seasons: wet season (summer) and dry season (winter) under changing climatic conditions. The volume of water required ($V_{wr}$) by each type of crop was obtained by converting CWRs to m/day and then multiplying them by area ($m^2$) under cultivation in each season (Equation 3.7). These were compared to the projected inflows into the Raliphaswa irrigation weir using graphical plots to determine the adequacy of future inflows into meeting future CWRs.

$$V_{wr} = CWR \times A \qquad (3.7)$$

The projected inflows ($m^3/s$) were also converted to $m^3/day$ to ensure compatibility of the units with those of $V_{wr}$.

# CHAPTER 4: RESULTS AND DISCUSSION

## 4.1. Introduction

This chapter presents the results of the impacts of climate change on future water resources availability for agriculture in Raliphaswa irrigation scheme in Nzhelele area. Climate change impacts on agricultural water availability were determined for near future (2023-2052) and far future (2053-2082) based on inflows into the irrigation scheme, and their ability to meet future crop water requirements. The results are then used to propose adaptation strategies that can be taken to alleviate impacts of climate change and variability on the availability of future irrigation water requirement.

## 4.2. Historical rainfall and temperature trends

Long-term trends and changes in temperature and rainfall were investigated in this study. Historical temperature trends for station 299303 and rainfall trends for stations 229303, Mphephu, Jouberstroom and Veermedling used to set up SWAT model were analysed for the period 1987-2009.

### 4.2.1. Historical rainfall trends

Figures 4.1 to 4.4 show the observed rainfall changes and trends for stations 229303, Mphephu, Jouberstroom and Veermedling for the period 1987-2009, respectively. The graphs presented in Figures 4.1 to 4.4 indicate that rainfall variability in all stations has been intensifying throughout the years with most of the years showing very low peaks (low rainfall) and few years showing high peaks (high rainfall), which resembles extreme climatic events such as droughts and floods. The variation line shows that rainfall is increasing in station 299303, Mphephu and Veermedling with the positive slope line equation of $y = 8.5627x+500.36$, $y = 7.5764x+346.36$ and $y = 11.071x+633.23$, respectively. The negative slope variation line equation $y = -0.1513x+935.04$ in Jouberstroom station shows a decrease in rainfall throughout the years. The annual rainfall recorded in all stations was highest during the year 2000 and lowest rainfall in 1994. A similar study by Musakwa et al. (2020) analysed rainfall trends for Nzhelele and Luvuvhu River catchment from 1968 to 2017 and also found that rainfall was highest during the year 2000 which was associated with extreme weather event Cyclone Leon-Eline. Musakwa et al. (2020) further highlighted that the two river catchments were affected by drought events in the early 1990s which was associated with the El Niño Southern Oscillation (ENSO) events.

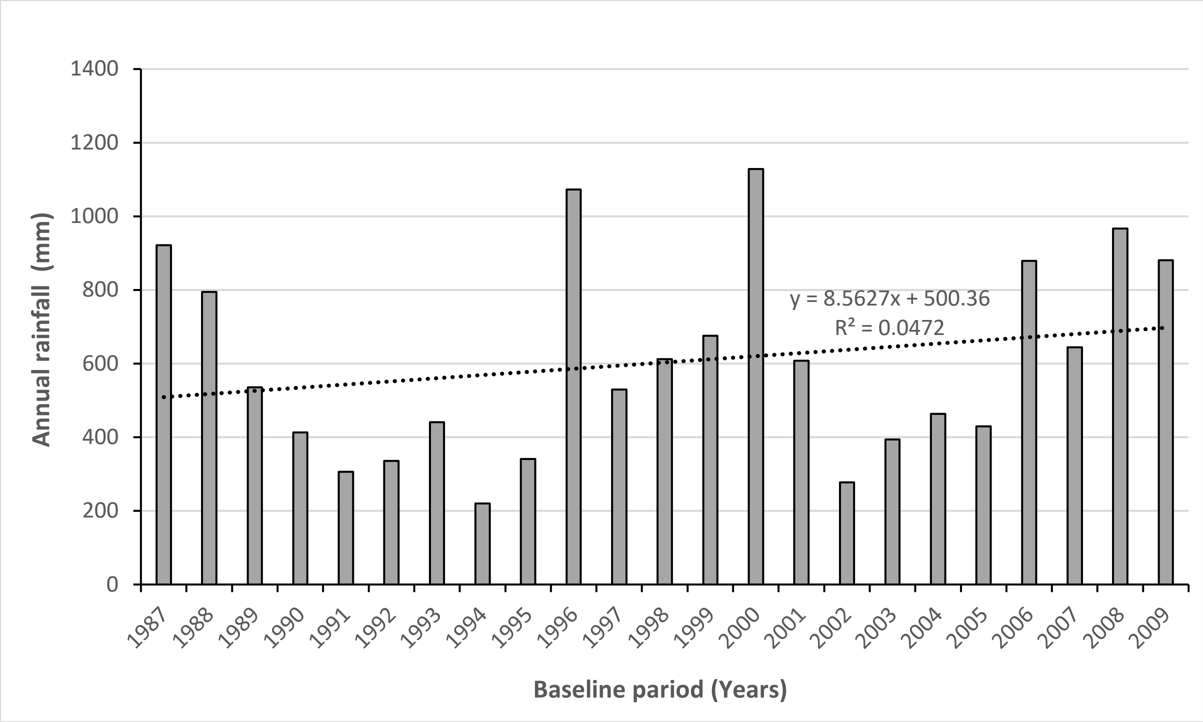


Figure 4.1: Total annual rainfall pattern and trend for station 229303

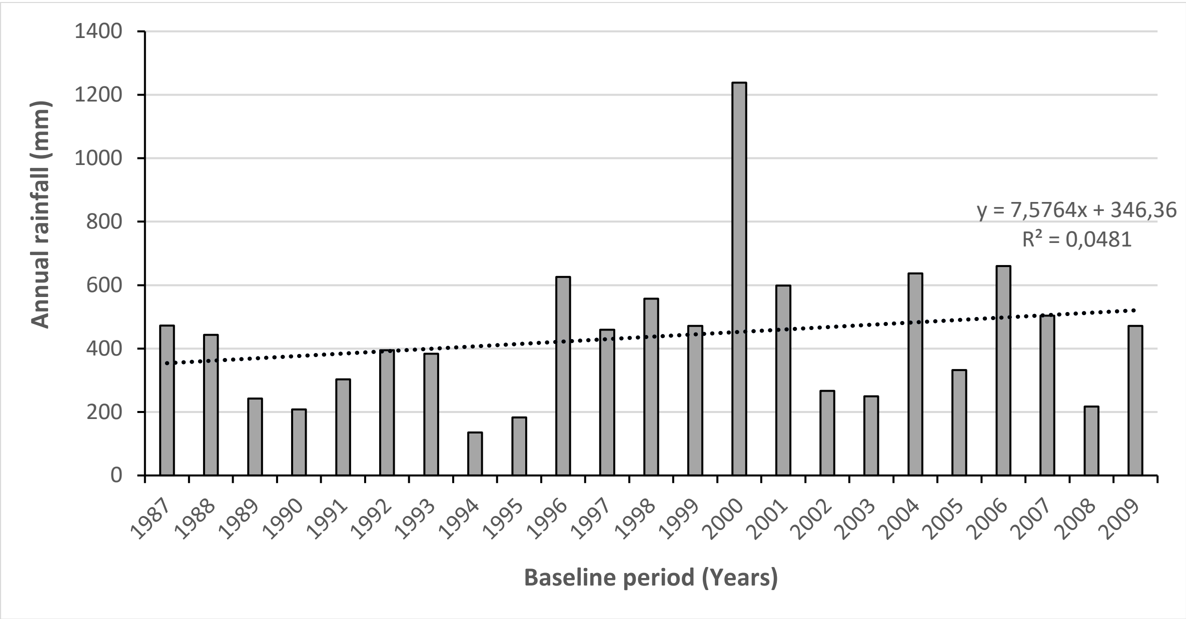


Figure 4.2: Total annual rainfall pattern and trend for Mphephu station

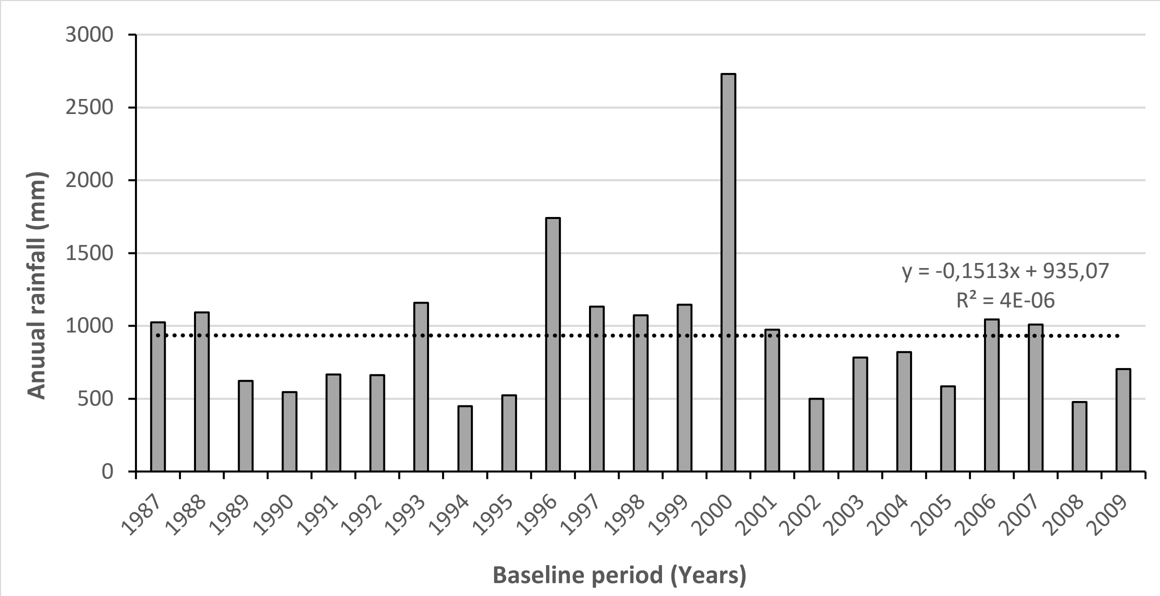


Figure 4.3: Total annual rainfall pattern and trend for Jouberstroom station

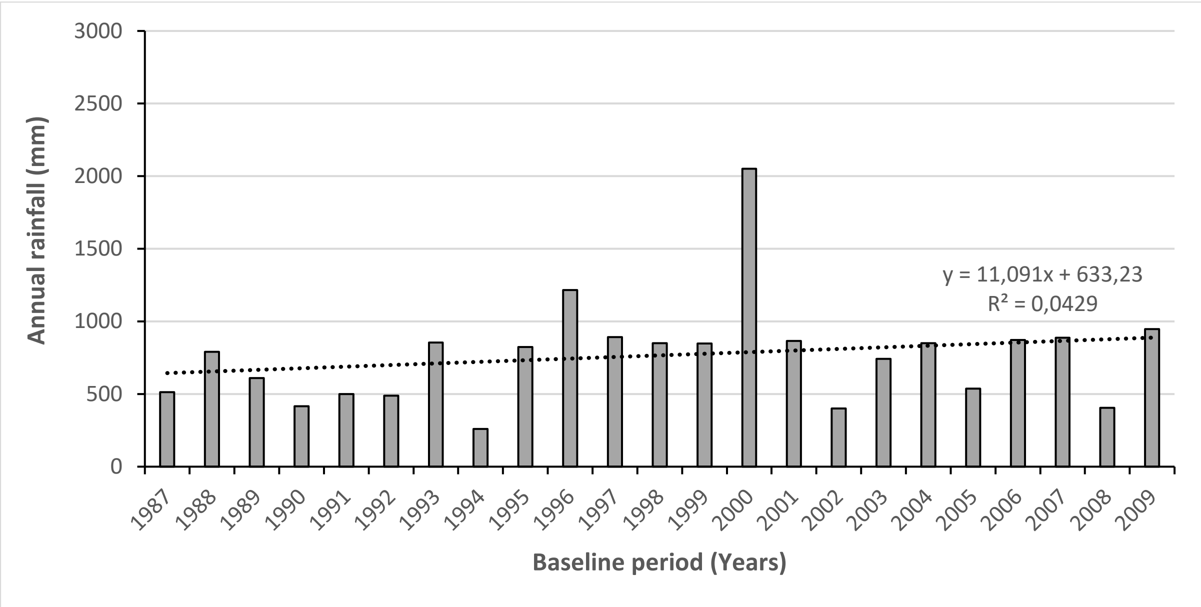


Figure 4.4: Total annual rainfall pattern and trend for Veermedling station

### 4.2.2. Historical temperature trends

Figures 4.5 and 4.6 show the trends for maximum and minimum temperatures for station 229303. respectively. Just like rainfall, average maximum temperatures have been highly variable along the years, while Figure 4.6 shows that minimal changes in average minimum temperatures were recorded throughout the years. Both maximum and minimum temperatures show increasing trend line. From the graphs, it can also be observed that temperature in the study area varies from mild to hot ranging from averages below 14°C minimum and close to 29°C maximum. Shikwambana et al. (2021) investigated the trends in temperature from 1960 to 2018 in the in the Mopani and Vhembe Districts of Limpopo Province. The study found that average minimum and maximum temperatures in Mopani district have increased by 3.0°C and 3.2°C, respectively, and In Vhembe district, minimum temperature increased by 2.3 °C and maximum temperature by 1.6°C. Tshiala et al. (2011) analysed the trends in annual and seasonal minimum and maximum temperatures, along with diurnal temperature range, over the Limpopo Province for the period 1950 to 1999 using daily data from 30 catchments. The results showed an overall increase in mean annual temperature by 0.12°C per decade for the 30 catchments, while a seasonal increase in mean temperature of approximately 0.18 and 0.09°C per decade in winter and summer was observed, respectively. Long Term Adaptation Scenarios (LTAS) technical report by DEA (2013) have indicated that between 1960-2010, Maximum and minimum temperatures in South African increased significantly each year and in practically all seasons.

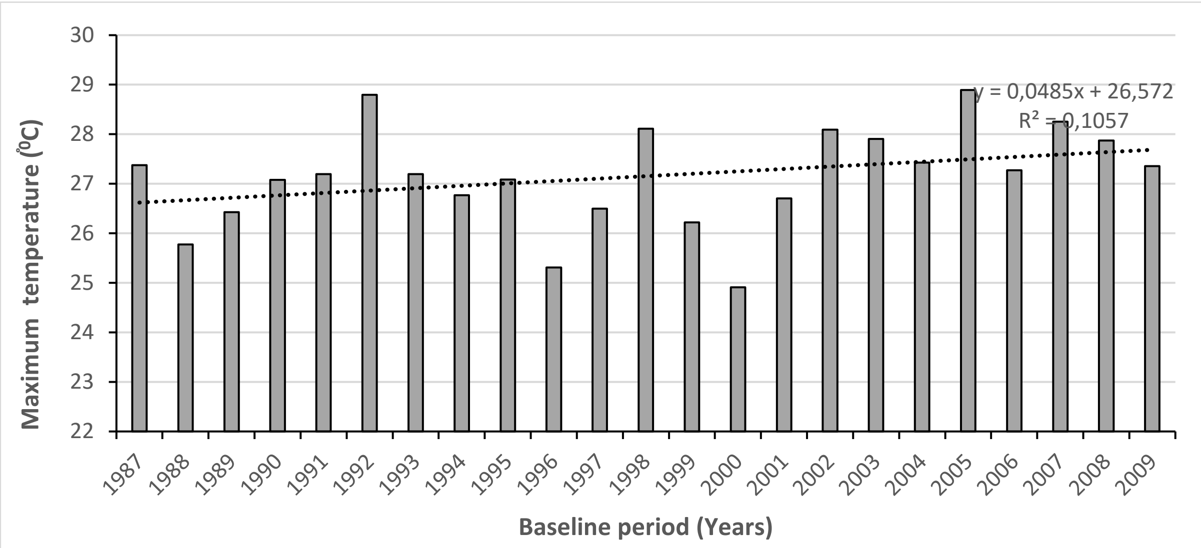


Figure 4.5: Average maximum temperature for station 229303

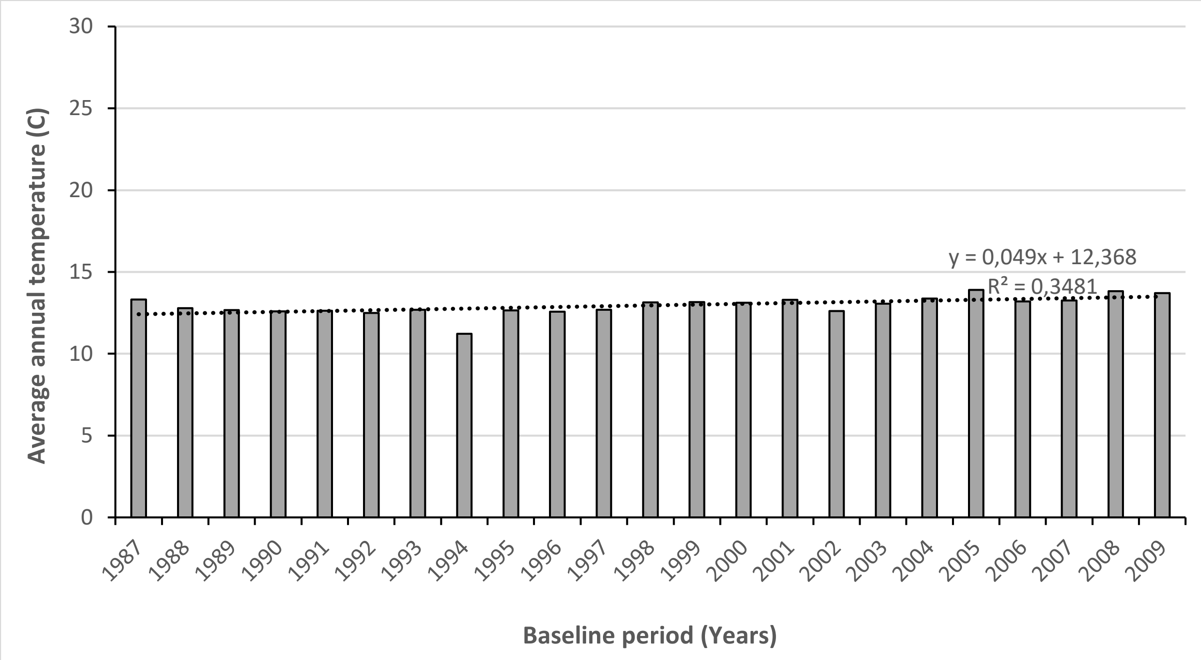


Figure 4.6: Average minimum temperature for station 229303

**4.2.3. Statistical significance of historic rainfall and temperature trends**

The results of testing the statistical significance of the trends for rainfall stations 229303, Mphephu, Jouberstroom and Veermedling, and temperature station 299303 for the period 1987-2009 are presented in Table 4.1. The estimates show a positive trend for all the stations except for Jouberstroom station which indicated a decreasing trend. The results also indicates that the trends for all rainfall stations are not statistically significant because their p-values (299303 = 0.320; Mphephu = 0.313; Jouberstroom = 0.993; and Veermedling =0.343) are greater than the common significance level of 0.05. According to Kaewmesr and Varnakovida (2018), the p-value resulting from the analysis represents the significance test at a level of α = 0.05. Maximum temperature trend for station 229303 is also not statistically significant because its p value is 0.13. While minimum temperature is showing a very statistically significant trend with a p value equal to 0.00304. this also suggests that the slope is not zero.

Table 4.1: Statistical significance test results for rainfall stations 299303, Mphephu, Jouberstroom, and Veermedling, and temperature station 299300 (* = p < 0.05, ** = p < 0.01, *** = p < 0.001)

| Stations | Variable | Estimate | Std. Error | t value | *p* value |
|---|---|---|---|---|---|
| 229303 | Annual rainfall | 8.563 | 8.399 | 1.019 | 0.320 |
| Mphephu | Annual rainfall | 7.576 | 7.357 | 1.03 | 0.315 |
| Jouberstroom | Annual rainfall | -0.1513 | 16.0717 | -0.009 | 0.993 |
| Veermedling | Annual rainfall | 11.09 | 11.44 | 0.970 | 0.343 |
| 229303 | Temp Max | 0.04848 | 0.03078 | 1.575 | 0.13 |
| | Temp Min | 0.04904 | 0.01464 | 3.349 | 0.00304 ** |

**4.3. Future rainfall and temperature patterns and trends**

Monthly changes in rainfall and temperature records for CCAM station p229301 used for future projections were also analysed for a period baseline period (1993-2022), near future (2023-2052), and far future (2053-2082). Annual rainfall and temperature patterns and trends for near future and far future.

**4.3.1. Rainfall patterns and trends**

Figure 4.7 shows the comparison of total monthly rainfall changes for historical, near future and far future for station p229301 for the period of 30 years. The graph shows high rainfall variability for all the months in all periods. In January, high rainfall was recorded in near future and low rainfall in far future. From February to April, rainfall was respectively decreasing from baseline period to near future and far future, and from September to December rainfall was increasing but with fluctuations within these months. High rainfalls were recorded in November, December, January, and February, while December recorded the highest rainfall in both future periods than all the months. The recorded high rainfalls can be linked to high temperatures in the summer season leading to high rates of evaporation during these warm months. Although rainfall may vary within local areas (Nenwiini and Kabanda, 2013), previous studies conducted in Limpopo Province, particularly in Vhembe district where the study is located have found that high rainfall is received during the summer season in the months October to March (Kom et al., 2020; Maponya, 2012; Nenwiini and Kabanda,2013). From the results, it can be observed that lowest rainfall is recorded in May, June, and July in all periods which can be linked to low evaporation during these cold months. The projections indicated a 5.7% increase in rainfall in near future and a 15.57% decrease in rainfall in far future relative to the baseline period. According to Daron (2014), rainfall projections for South Africa indicate both potential increases and declines characterised by wetting in the southwest regions with summer rainfall and drying in the northern and eastern regions with winter rainfall.

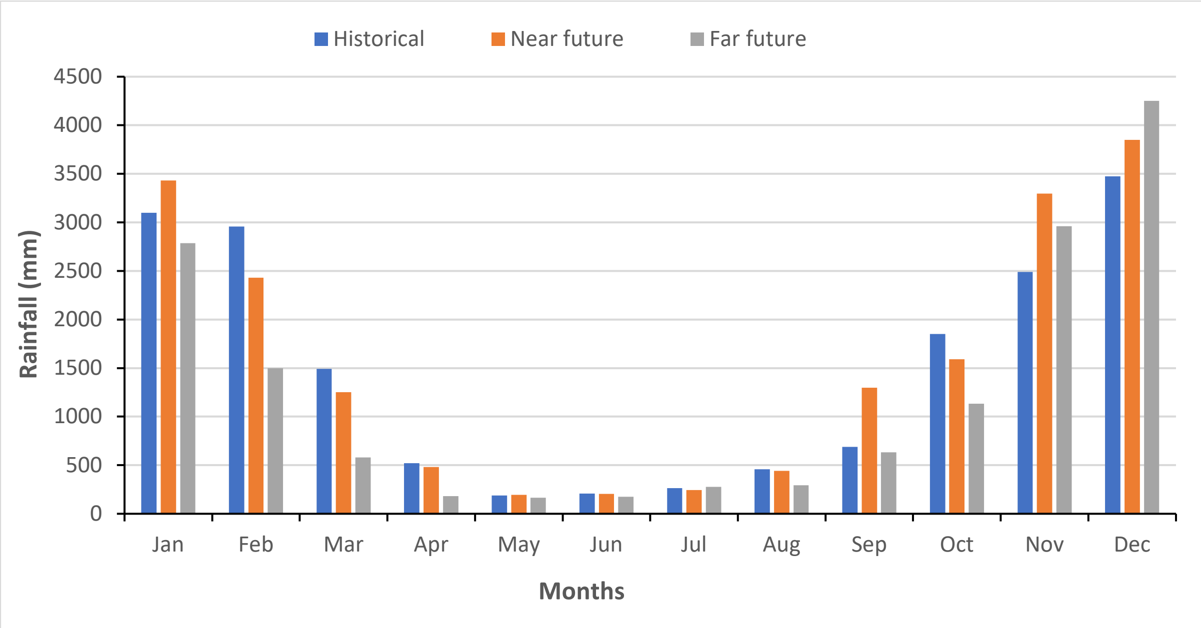


Figure 4.7: Total monthly rainfall for station p299301

Figures 4.8 and 4.9 illustrate total annual rainfall trends (mm) for station p299301 in near future and far future for the period of 30 years, respectively. Based on the graphs, there is a frequent occurrence of rainfall variability throughout the years at both future scenarios with some years showing high rainfall and low rainfall. In near future, lowest and highest rainfall was projected for the year 2028 and 2049 with an average of 279mm and 939 mm, respectively. In far future, highest rainfall is 937mm and lowest rainfall is 196 mm projected for the year 2055 and 2071, respectively. It can also be observed from the graphs that high rainfall was projected in near future than in far future. The trendline on Figure 4.3, also shows that the intensity of rainfall will decrease in far future. From near future to far future, rainfall is projected to decrease by 20.2% which will result in high incidences of drought events. Rainfall projections  in Limpopo Province are imprecise, however, there is evidence of decreasing annual rainfall (LEDA, 2019).

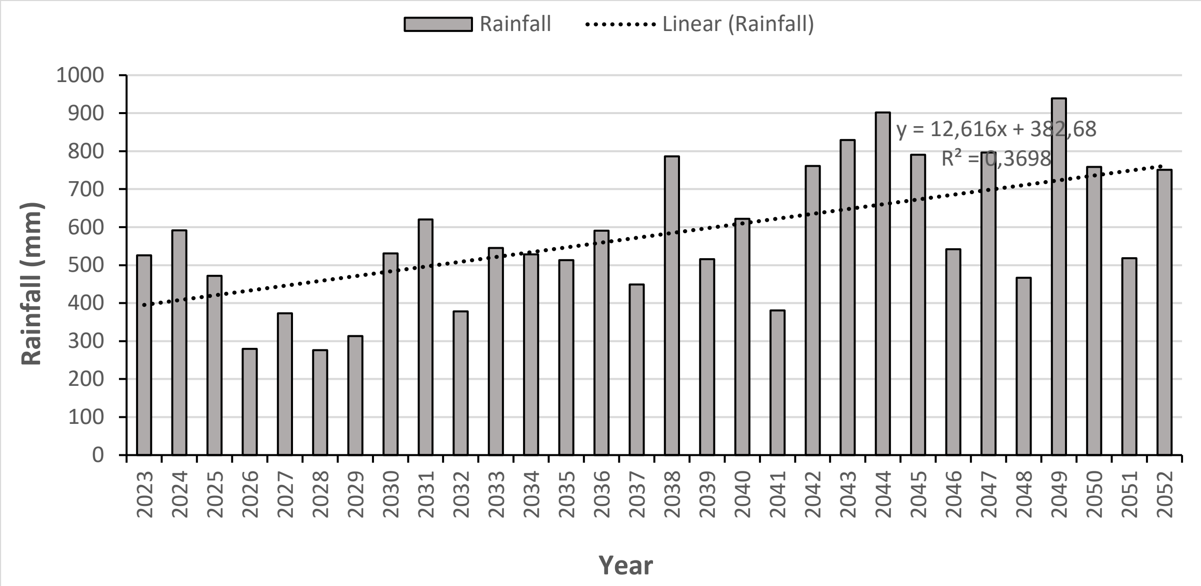


Figure 4.8: Total annual rainfall pattern and trends in near future for station p299301

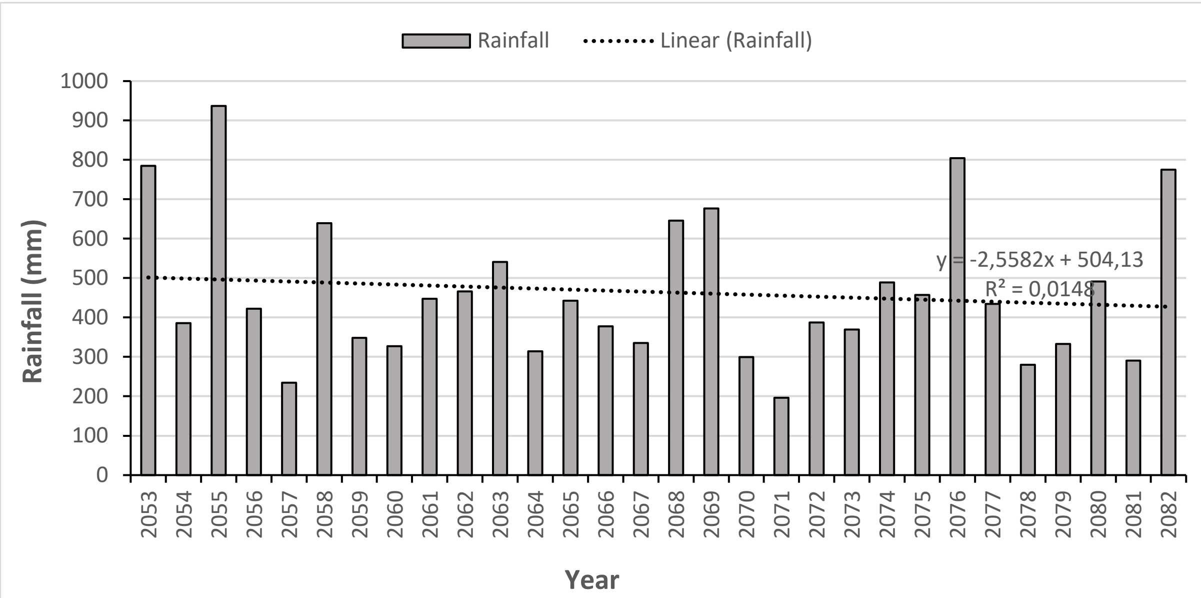


Figure 4.9: Total annual rainfall pattern and trends in far future for station p299301

#### 4.3.2. Maximum temperature pattern and trend

Figure 4.10 shows comparison of average monthly maximum temperature for baseline period, near future and far future. The graph shows that maximum temperature will increase from the baseline period to near future and far future for all the months except for April which had a slightly higher temperature in baseline period than in near future. Maximum temperature is projected to increase from 24.7 °C in baseline period to an average of 25.7 °C in near future and 28.7 °C in far future, which is an increase by 1 °C in near future and 3 °C in far future. Temperature projections for the Limpopo province show a potential increase in temperature by as much as 2 °C by 2035 with further temperature increase projected by much as 6 °C to 7 °C between 2080 and 2100 (LEDA, 2019).

A study by Engelbrecht (2019) found that, under low mitigation, maximum temperature over much of the northern interior of South Africa are likely to increase by 3 °C for in 2021-2050 relative to the baseline period 1961-1990, and over the southern parts of the country, especially over the Cape south coast, maximum temperature is likely to increase by as small as less than 2 °C. The findings of this study further revealed that for the period 2070-2099 relative to the baseline period 1961-1990, maximum temperature exceeding 4 ℃ is projected over most of the interior with the possibility of exceeding 7 °C over some areas in the northern interior.

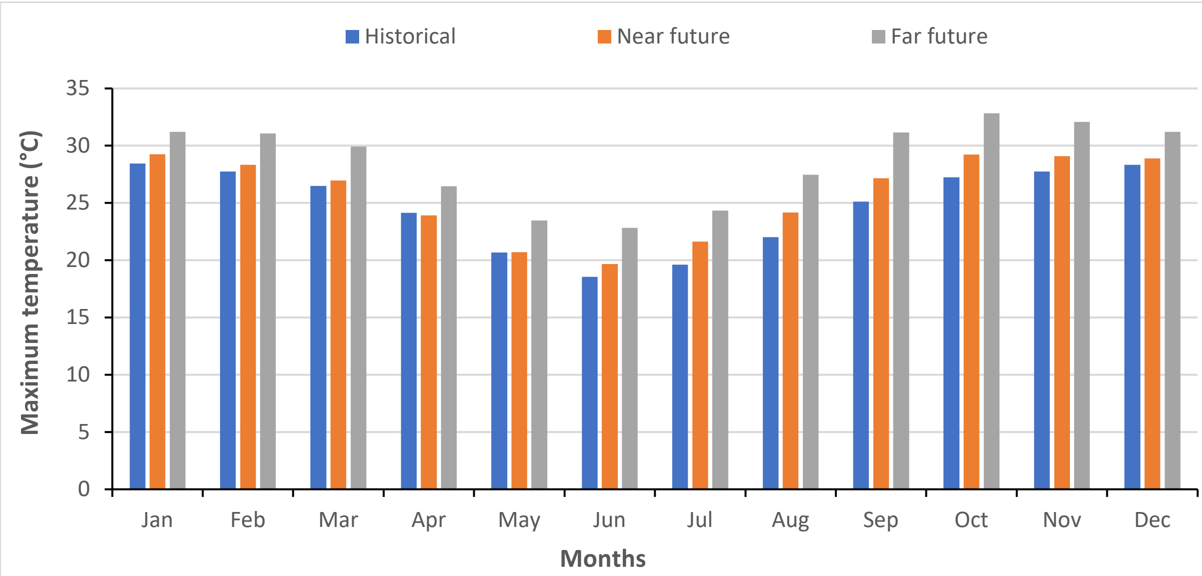


Figure 4.10: Average monthly maximum temperature for station p299301

Figures 4.11 and 4.12 show the trends of maximum temperature in the study area for near future and far future. Just like rainfall, the graphs show high variability in maximum temperatures throughout the years. The trends line in both figures indicate that maximum temperatures will be increasing in both future scenarios. According to Zhao et al. (2017), changes in temperature because of climate change has the most direct negative impacts on crops. As a result of projected increase in temperature in Nzhelele area, the rate of evapotranspiration from a reference surface will increase, and with water shortages already identified as the main problem to successful crop production in this study, the increase in temperatures will also lead to crop yield reduction since there is limited water availability to compensate for water losses by crops.

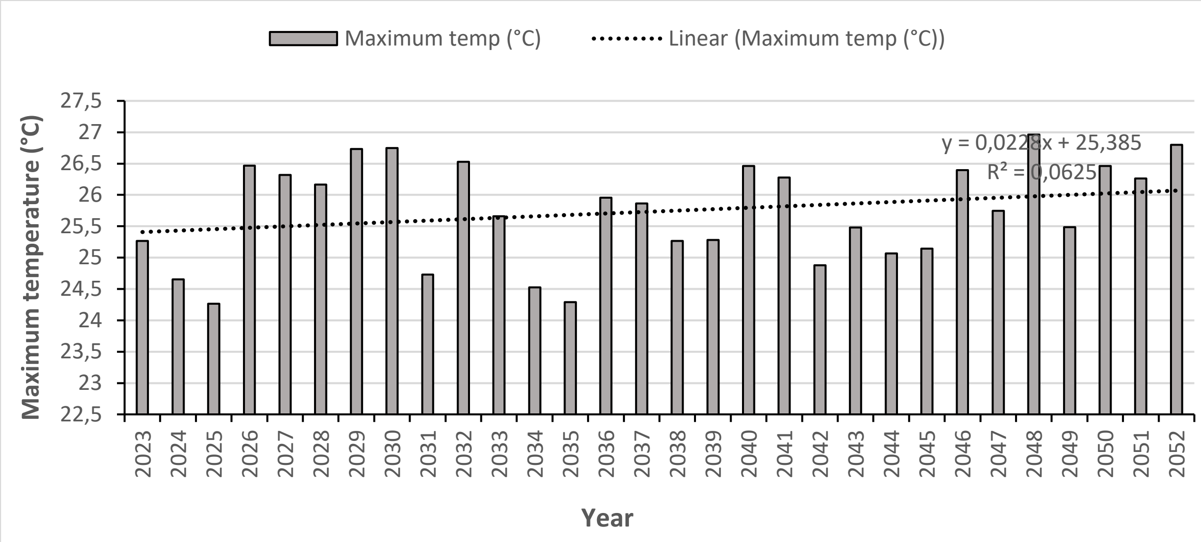


Figure 4.11: Average annual maximum temperature pattern and trend in near future for station p299301

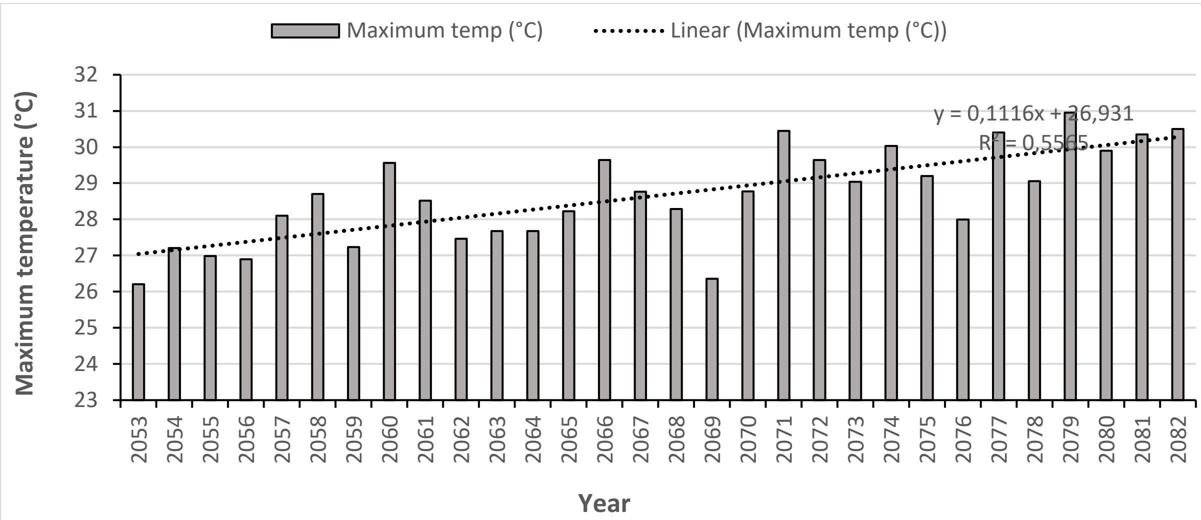


Figure 4.12: Average annual maximum temperature pattern and trend in far future for station p299301

### 4.3.3. Minimum temperature pattern and trend

Figure 4.13 shows the comparison of average monthly minimum temperatures for baseline period, near future and far future. Just like maximum temperature, minimum temperature will increase from baseline period to near future and far future in all the month. Furthermore, highest temperature is recorded in far future in all the month. Based on future projections, minimum temperature will increase from 13.3 °C in the baseline period to 14.7 °C and 16.7 °C in near future and far future, respectively, which is 1.4 °C increase in near future and a 3.4 °C increase in far future. Future projections show that under low mitigation, minimum temperature over South Africa will increase by 2 to 3 °C in 2021-2050 with reference to the period 1961-1990, and in 2071-2099 temperature will increase by more than 4 °C over much of the interior with the possibility of exceeding 7 °C in most parts of the northern interior, smaller changes where however projected for the southern coastal regions of the country only (Engelbrecht, 2019).

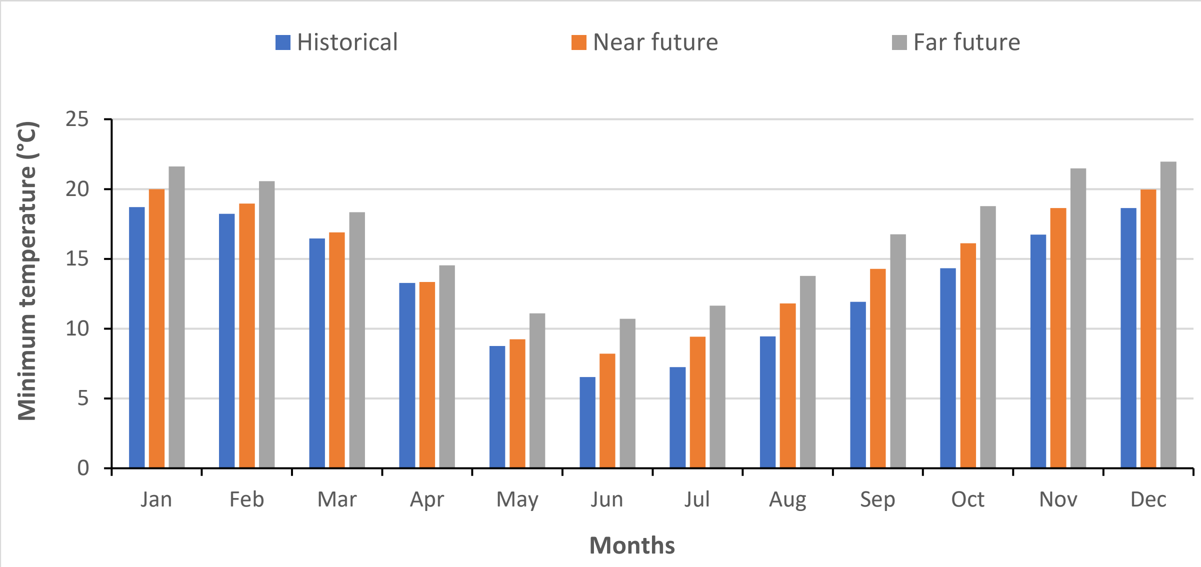


Figure 4.13: Average monthly minimum temperature for station p299301

In the study area, the presentation of minimum temperature patterns and trends for both the near future and far future is encapsulated within Figure 4.14 and Figure 4.15, respectively. In contrast to the anticipated high variability in temperature and rainfall within the region, the analysis revealed a consistent and noteworthy observation: both bear future and far future minimum temperatures exhibit a discernible trend characterized by a modestly undulating but overall positive trajectory over the years. Remarkably, the projections indicate a consistent upward trend in minimum temperatures spanning from the near future to far future periods. This trend signifies a gradual but consistent increase in minimum temperatures across the years, suggesting a warming trend within the study area. Notably, a substantial rise in minimum temperatures by approximately 2°C from the near future to the far future is projected in the study area.

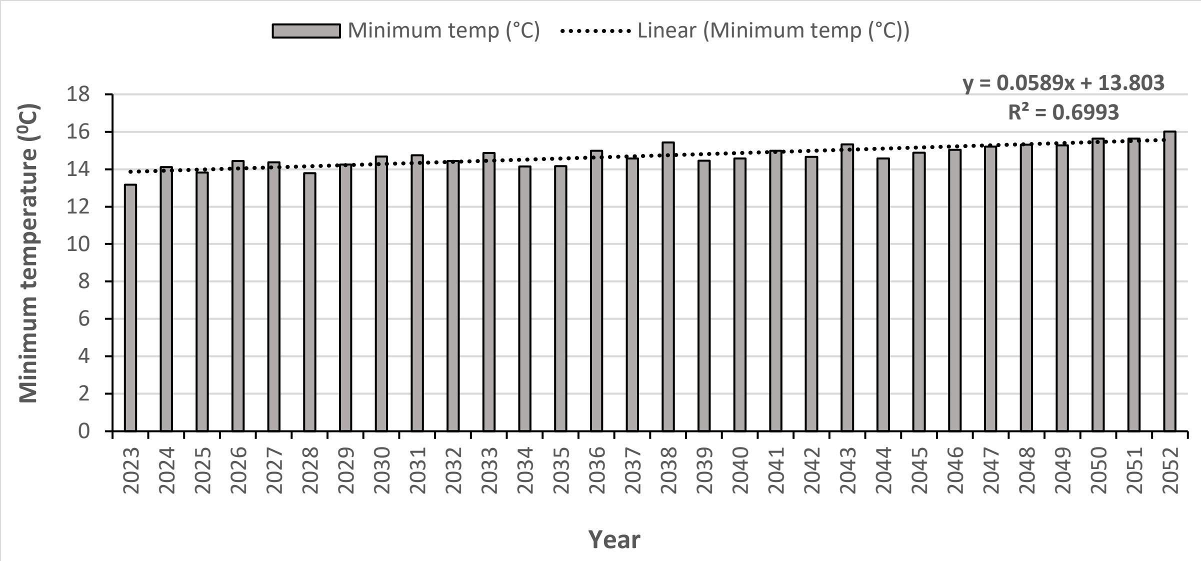


Figure 4.14: Average annual minimum temperature pattern and trend in near future for station p299301

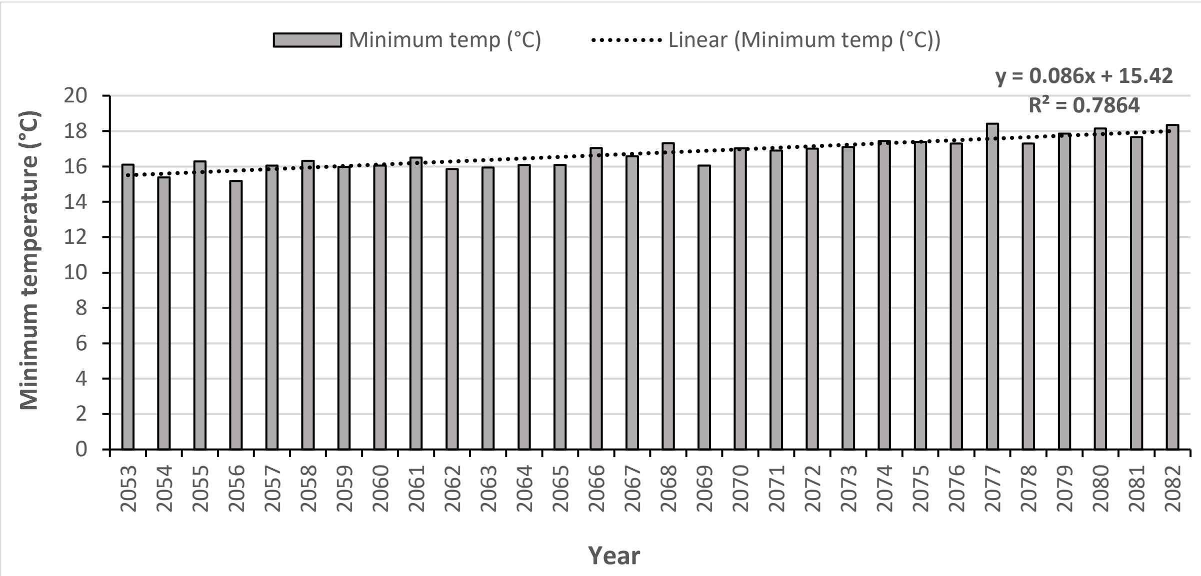


Figure 4.15: Average annual minimum temperature pattern and trend in far future for station p229301

### 4.3.4. Statistical significance of future rainfall and temperature trends for station p299301

The statistical significance analysis of rainfall and temperature trends for station p299301 for both near future (2023-2052) and far future (2023-2082) is presented in Table 4.2. The p-values are extensively employed in both social and natural sciences to assess the statistical significance of observed outcomes (Shrestha, 2019). The significance level is established at 0.05 for comparison with the p-value, whereby a p-value below 0.05 is considered "significant," and a p-value above 0.05 is deemed "not significant (Kwak, 2023). Based on the results, rainfall trend in near future is highly statistically significant with a p-value of 0.000364, meanwhile the trend is not statistically significant in the far future because its p-value (0.521) is greater than 0.05. Trends of maximum temperature in far future, and minimum temperature in both near future and far future are also highly significant with p-values of 2.22 X $10^{-06}$, 8.73 X $10^{-09}$, and 6.86 X $10^{-11}$, respectively. Maximum temperature in far future has a p value of 0.183 which indicate a non-statistically significant trend.

Table 4.2: Statistical analysis of rainfall and temperate trends for station p 299301 (* = p < 0.05, ** = p < 0.01, *** = p < 0.001).

| Station | Variable | **Period** | **Estimate** | **Std. Error** | **t value** | ***p* value** |
|---|---|---|---|---|---|---|
| p229301 | Annual rainfall | Near future | 12.616 | 3.112 | 4.053 | 0.000364 *** |
| | | Far future | -2.558 | 3.939 | -0.650 | 0.521 |
| | Maximum temperature | Near future | 0.02280 | 0.01669 | 1.366 | 0.183 |
| | | Far future | 0.11157 | 0.01882 | 5.927 | 2.22 X $10^{-06}$ *** |
| | Minimum temperature | Near future | 5.888 X $10^{-02}$ | 7.298 X $10^{-03}$ | 8.069 | 8.73 X $10^{-09}$ *** |
| | | Far future | 8.604 X $10^{-02}$ | 8.473 X $10^{-03}$ | 10.154 | 6.86 X $10^{-11}$ *** |

**4.4. SWAT modelling for predicting historical and future inflows**

As detailed in the precious chapter, SWAT model was calibrated and validated for the period 1991-2009 for the study area (quaternary catchment A80A and A80B). This was conducted to identify model problems in the initial stage of the modelling process. In watershed modelling using SWAT model, delineation of watershed (also known as basin) based on DEM is the initial phase of the entire process (Śliwiński et al., 2022). During model setup, the watershed was delineated into a total of 23 sub-basins as indicated in Figure 4.16, based on the DEM in Figure 3.5.

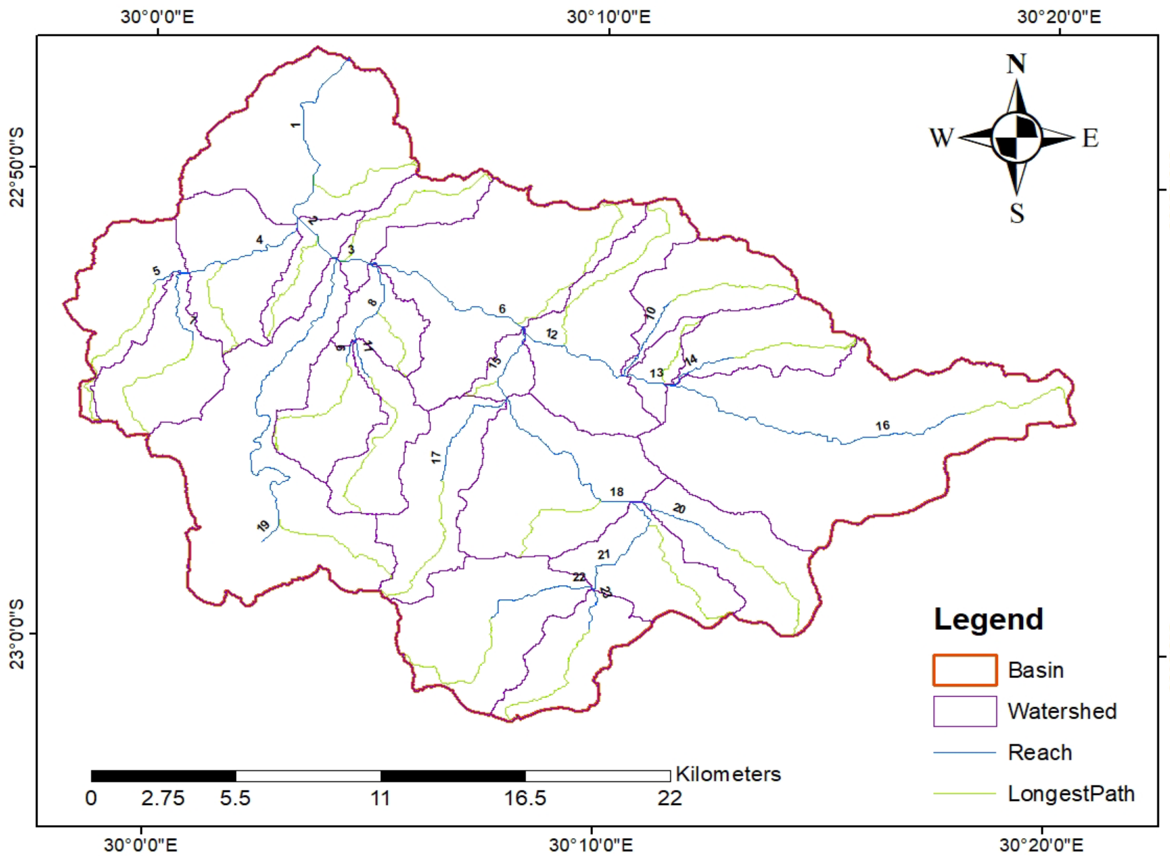


Figure 4.16: Sub-basins delineated for quaternary catchment A80A and A80B

After SWAT model divided the target watershed into sub-basins linked by the channel network, several lumped areas known as the hydrological response units (HRUs) which have uniform land-use, slope, and soil characteristics are further separated into each sub-basin (Teklay et al., 2021). To improve processing and limit the number of HRUs in each sub-basin in this study, a minimum threshold of 10% was utilized to eliminate minor land uses, soils, and slopes in each sub-basin in this study, and as a result, a total of 294 HRUs for the 23 sub-basins were produced. Figure 4.17 shows the HRUs map of the study area and Figure 4.18 shows the slope and land use combined map. The delineated sub-basins of the study area are illustrated in Figure 4.16.

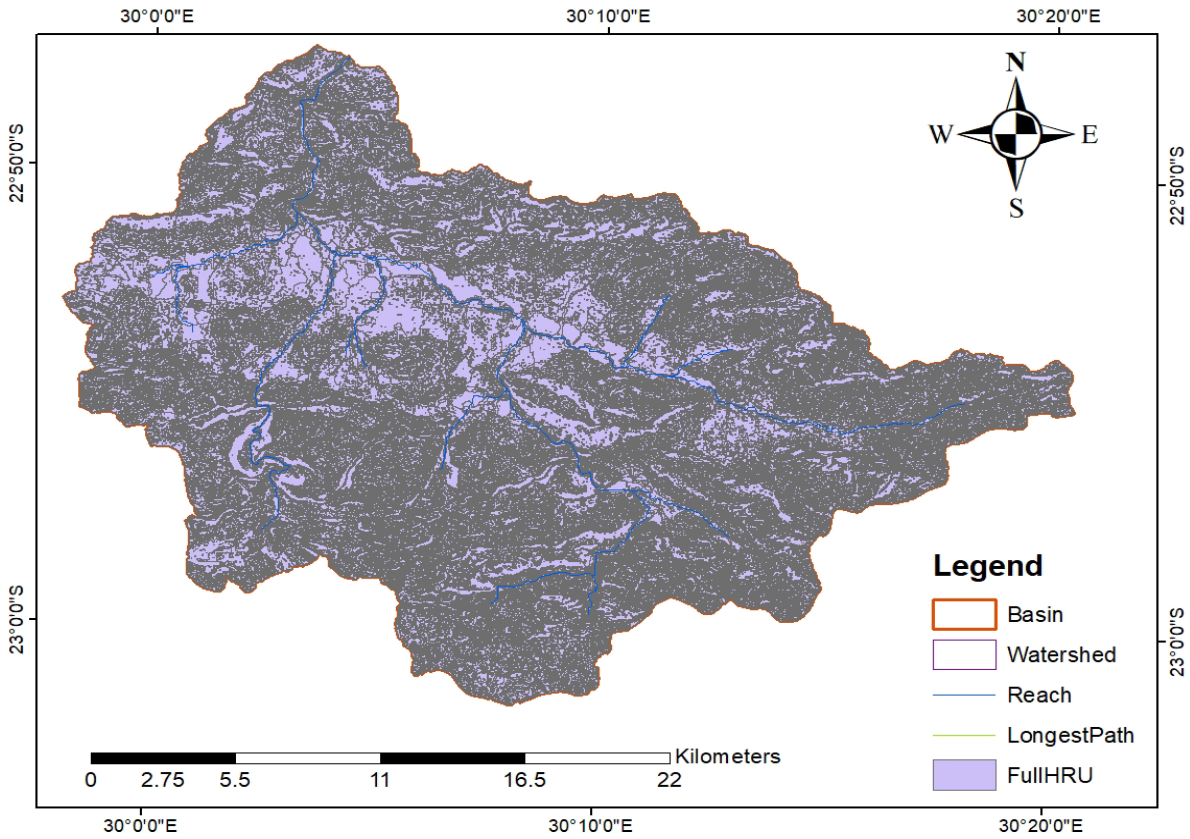


Figure 4.17: HRUs map for the delineated sub-basins for quaternary catchment A80A and A80B

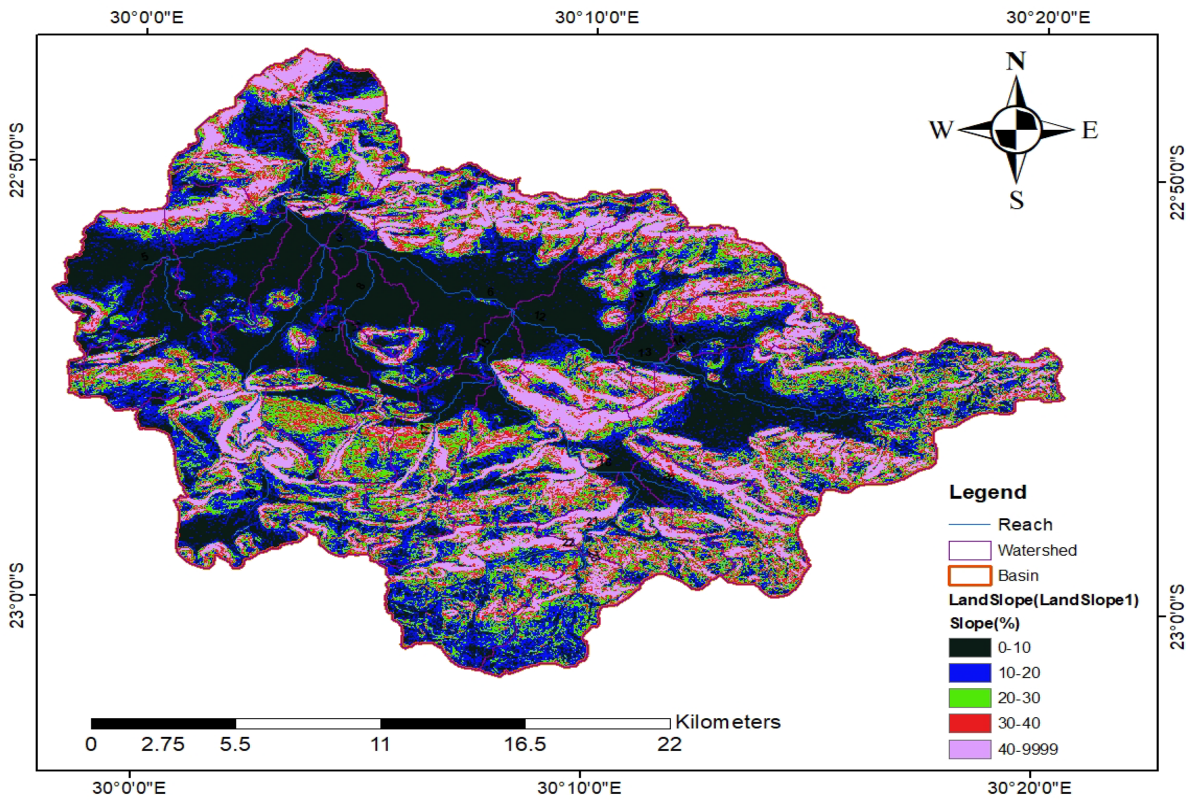


Figure 4.18: Slope and land use combined map.

Figure 4.19 shows the hydrological cycle of the study area after the model was run for quaternary catchment A80A and A80B for the period 1978-2009. This allows for identification of model problems in the initial stages of the modelling process. It further shows the water balance components for each HRUs computed on a daily time step. Table 4.3 lists 14 hydrological parameters that were automatically selected by the model during sensitivity analysis for streamflow calibration. These parameters were adjusted using the SUFI-2 algorithm at the same time and at specific calibration location. The results indicated that the Curve number (CN2) and Soil Evaporation compensation factor (ESCO) are the most sensitive parameters in this study. According to Lenhart et al. (2002), soil parameters and curve number are in most cases the most sensitive parameters to streamflow. Similar results were also found by Obiero et al. (2011). The model performance was evaluated based on the performance parameters in Table 4.4 which generally shows satisfactory to very good model performance.

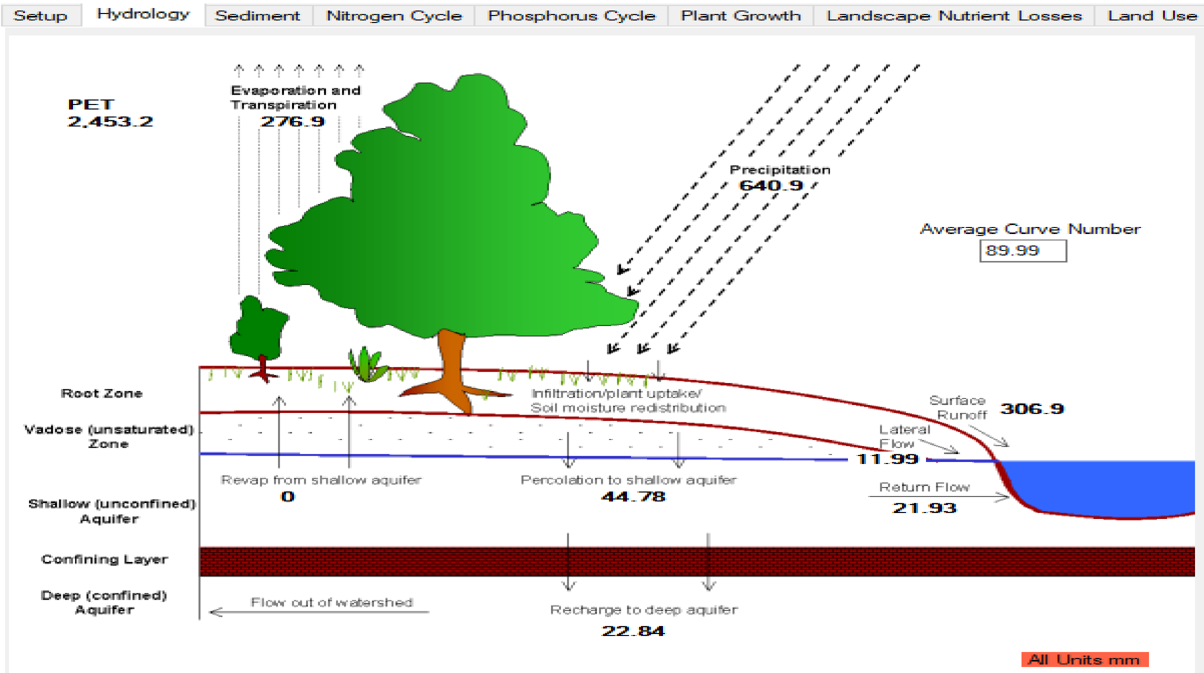


Figure 4.19: Hydrological cycle of the study area

Table 4.3: SWAT model parameters

| **Parameter** | **Parameter description** | **Fitted value** | **Minimum value** | **maximum value** |
|---|---|---|---|---|
| r_CN2.mgt | Initial soil Conservation Service (SCS) runoff curve number for soil moisture condition II | 85.954 | 1.000 | 90.000 |
| v_ESCO.hru | Soil Evaporation compensation factor | -0.890 | -0.000 | 1.000 |
| r_SOL_K (..).sol | Saturated hydraulic conductivity | 0.436 | -0.000 | 0.800 |
| v_GWQMN.gw | Threshold depth of water in the shallow aquifer required for return flow to occur (mm) | 201.363 | -10.00 | 300.000 |
| r_REVAPMN.gw | Water threshold depth in shallow aquifer for revap to occur (mm) | 6834.090 | 50.000 | 10000.000 |
| v_GW-REVAP.gw | Groundwater “revap” coefficient | 3.409 | 0.000 | 5.000 |
| r-SLSUBBSN.hru | Average slope length (m) | 1.205 | -0.500 | 2.000 |
| r_SOL_AWC (..).sol | Available water capacity of the soil layer | -7.729 | -10.000 | -0.010 |
| v_SURLAG.bsn | Surface runoff lag coefficient (day) | 9.579 | 0.980 | 22.000 |
| v_ALPHA_BF.gw | Baseflow alpha factor (day) | 0.622 | 0.050 | 0.650 |
| v_GW_DELAY.gw | Groundwater delay time (day) | -0.121 | -0.150 | 0.480 |
| v_MSK_CO1.bsn | Calibration coefficient used to control impact of the storage time constant for normal flow | 1.640 | 1.330 | 8.150 |
| v_SHALLST.gw | Initial depth of water in the shallow aquifer (mm) | 6113.636 | 500.000 | 10000.000 |
| v_RCHRG_DP.gw | Deep aquifer percolation fraction | 0.123 | 0.0100 | 0.500 |

Table 4.4: SWAT model performance statistics

| Performance measure | Calibration period | Validation period | Total model performance | Evaluation criteria (Amin and Nuru, 2020; Ang and Oeurng 2018) |
|---|---|---|---|---|
| NSE | 0.56 | 0.56 | 0.56 | 0.50<NSE≤0.65 Satisfactory |
| $R^2$ | 0.78 | 0.60 | 0.71 | 0.60<$R^2$≤ 0.75 Good<br>0.75<$R^2$≤ 1.00 Very good |
| RSR | 0.67 | 0.66 | 0.66 | 0.60≤RSR≤0.70 Satisfactory |
| PBIAS | +7.7% | -8.3% | +0.6% | PBIAS≤ ±1 Very good |

Figures 4.20 and 4.21 show the scatter plot between simulated and observed streamflow for the calibration period (1991-2000) and validation period (2001-2009), respectively. The scatter plot between simulated and observed streamflow during the calibration period (Figure 4.14) shows a very strong relationship between the simulated and observed streamflow since both values tend to be close to 1:1 line, while the scatter plot between simulated and observed streamflow during the validation period (Figure 4.21) shows a slight relation between simulated and observed streamflow. As indicated in Table 4.1, the calibration showed better response than validation in which the $R^2$, NSE, PBIAS and RSR were 0.78, 0.56, +7.7% and 0.67, respectively. For the validation period, the $R^2$, NSE, PBIAS, and RSR were 0.60, 0.56, -8.3% and 0.66, respectively.

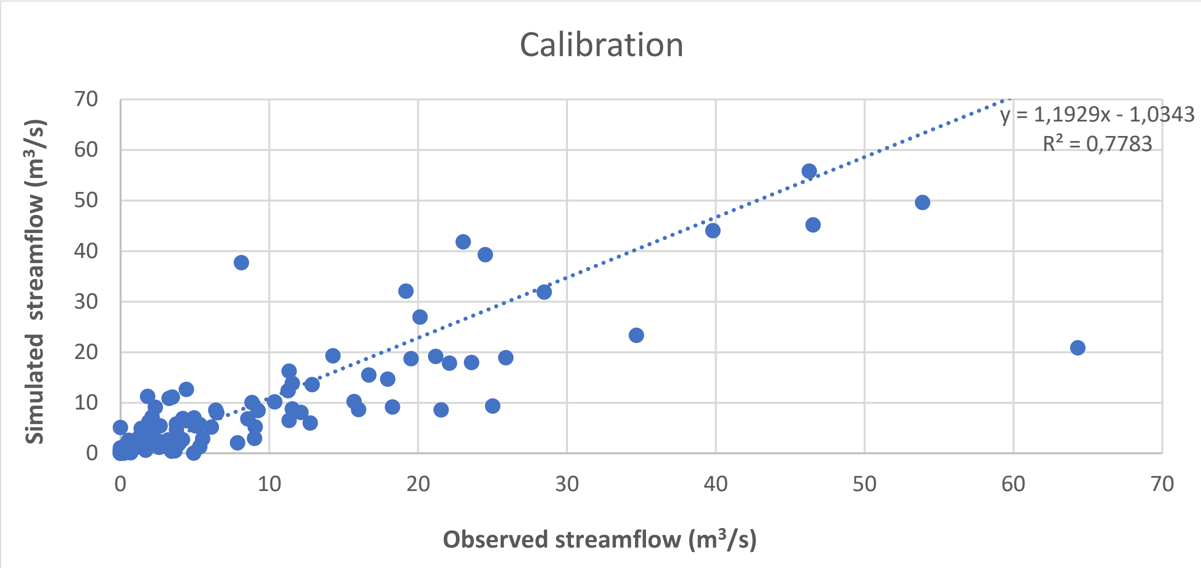


Figure 4.20: Scatter plot of average monthly simulated and observed streamflow for calibration period (1991-2000)

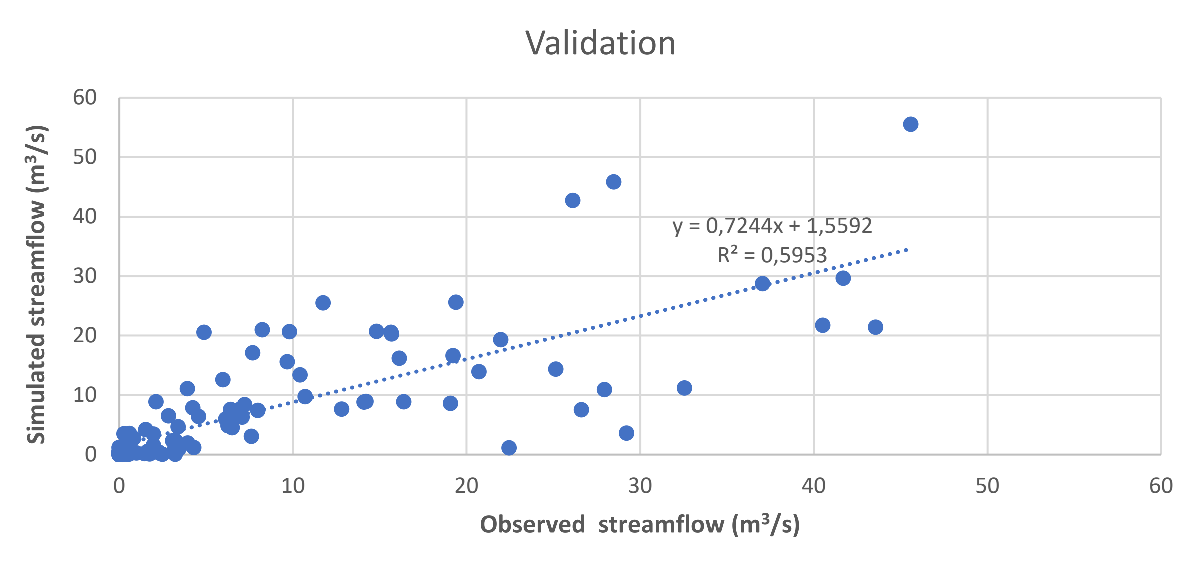


Figure 4.21: Scatter plot of average monthly simulated and observed streamflow for validation period (2001-2009).

Figure 4.22 show the simulated and observed hydrographs after calibration and validation. The model performance was evaluated based on the performance statistics in Table 4.3. The model performed well with NSE and $R^2$ values of 0.56 and 0.71, respectively. Subsequently, It can also be observed from Figure 4.22 that observed streamflow is generally lower than the simulated streamflow. However, both hydrographs maintained a similar pattern and the model was able to predict a peak flow for the year 2000. This indicate that the model will be able to project future inflows into the irrigation weir.

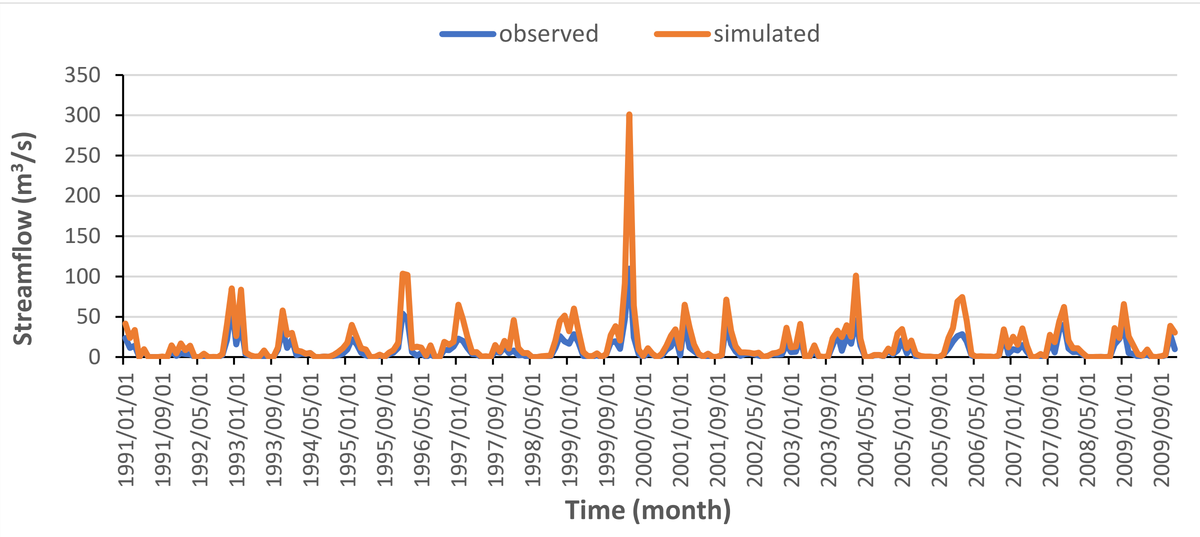


Figure 4.22: Observed and simulated streamflow

## 4.5. Impacts of climate change on water resources availability and implications on crop water requirements

### 4.5.1. Impacts of climate change on projected inflows into Raliphaswa irrigation weir

Rainfall and temperature data from CCAM stations p-229300, p-229301 and p-229302 were used as inputs to the calibrated SWAT model to project inflows for near future (2023-2052) and far future (2053-2082) with reference to historic period (1987-2009). Figure 4.23 indicate comparisons of monthly historic and projected inflows for near future and far future scenarios. The results show a more frequent occurrence of low inflows and less frequent of occurrence of high inflows for both future periods. The same changes in inflows were also observed in the historic period. High inflow events were recorded during November, December, and February, potentially because these are the wet season months associated with rainfall and runoff occurrence. Consequently, the amount of precipitation during these months had a great influence on inflow changes. February had the highest flow (2.9 $m^3$/s) in the historic period, this can also be linked to the flood event in the year 2000. During the dry season, little or no rainfall is received in the area. This resulted in very low inflows during June, July, August. Therefore, inflow in these dry season months can be associated with discharge contributions into the dam allowing very little inflows into the irrigation weir. August recorded the lowest inflows 0.021 $m^3$/s, 0.007 $m^3$/s, 0.003 $m^3$/s for historic period, near future and far future, respectively. Both near future and far future scenarios shows a decrease in inflow as compared to the historic period. The simulated monthly inflows declined from 11.9 $m^3$/s at historic, to 8.5 $m^3$/s in near future and 6.2 $m^3$/s in far future. This is a decrease by 28.7% and 48% in near future and far future, respectively, from the historic period. The deceases in projected inflows can be linked to a projected decrease in rainfall and increases in temperatures in the study area, together with the semi-arid conditions of the area. According to Makungo et al. (2010), Nzhelele River Catchment is characterized by low flows as a result of dry rainfall years dominating the catchment.

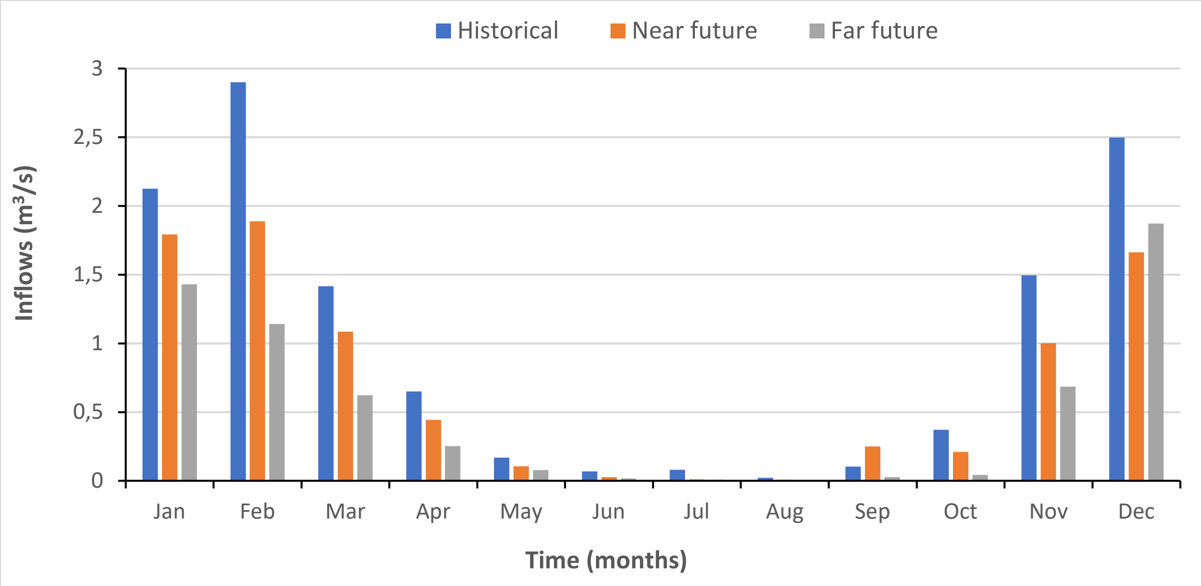


Figure 4.23: Simulated monthly inflows into the irrigation weir

### 4.5.2. Projected future crop water requirements

Future CWRs were estimated for historical (1993-2022), near future (2023-2052) and far future (2053-2082) periods based $ET_0$ and $K_C$ values. Water requirements for prioritized crops in Raliphaswa irrigation scheme were estimated for two growing seasons: wet season (summer) and dry season (winter). The description of the crops from which future CWRs are estimated are presented in Table 4.5 as well as the preferred planting dates by Raliphaswa farmers and the area under cultivation in summer and winter. This information was obtained after a questionnaire survey conducted with farmers.

Table 4.5: Selected crops for water requirements estimation

| **Crops** | **Reason for selection** | **Description** | **Preferred planting dates (summer)** | **Preferred planting dates (winter)** | **Area under cultivation in summer (Acres)** | **Area under cultivation in winter (Acres)** |
|---|---|---|---|---|---|---|
| Tomato | Prioritised | -high sensitivity to very low and very high temperatures (Odiyo et al., 2020) | September–November | April – May | 0.8 | 1.52 |

| | | | | | | |
|---|---|---|---|---|---|---|
| | | -20ºC to 24ºC. At temperatures below 12ºC and above 35ºC, flowers shed leading to poor fruit set, and the quality of the fruit produced may be detrimentally affected (Stevens et al., 2012). | | | | |
| Maize | Prioritised (staple food) | -Being a warm weather crop, daily mean temperatures > 22°C are required with a January mean > 19°C and < 24°C being ideal (Schulze and Walker, 2006).<br>-The critical temperature harming yield is approximately 32ºC (Stevens et al., 2012). | October-December | May | 18.94 | 0.25 |
| Groundnuts | common | -Optimum temperatures for growing groundnut are 25-30°C, Temperatures above 35°C are | Mid-October to mid-November | Not preferred during winter | 3.25 | 0 |

| | | | | | | |
|---|---|---|---|---|---|---|
| | | detrimental to groundnut production while low temperatures delays germination (Desmae and Sones, 2017) | | | | |
| Sweet potato | Common | -A warm season crop sensitive to low temperatures, especially frost (Agricultural Research Council, 2013). | October to November | May | 10.92 | 2.4 |

### 4.5.3. Estimated reference evapotranspiration ($ET_0$)

Figure 4.24 indicate comparisons for monthly estimated $ET_0$ for the period 1993-2022 (historical), 2023-2052 (near future) and 2053-2082 (far future). Based on the results, high $ET_0$ was estimated in warmer months (October, November December, January, and February) and low $ET_0$ was estimated in cold months (May, June, and July) for all periods. However, October recorded the highest $ET_0$ of 20.23 mm/day and 22.9 mm/day in near and far future, respectively, while for historic period high $ET_0$ of 18.6 mm/day was observed in November. The lowest $ET_0$ was found in June for all the periods ranging from 7.17 mm/day in the historical period to 8.31 mm/day in near future and 9.33 mm/day in far future. The results further show a continuous increase in $ET_0$ from the historical period to near future and far future in all the months. Average $ET_0$ will increase from historical period (13.9 mm/day) to near future by 8.31% (15.16 mm/day) and far future by 20.14% (16. mm/day). According to Mebrahtu (2021), different values of $ET_0$ are influenced by different changes that occur in weather condition such as wind speed, relative humidity sunshine hours and temperature. Therefore, high values of reference evapotranspiration recorded in both future scenarios might be linked to high temperature combined with low relative humidity. Inversely, low reference evapotranspiration values were due to low temperatures and high relative humidity. Estimated $ET_0$ was linked to the crop's coefficient (Kc) for each growing stage to estimate the water requirements.

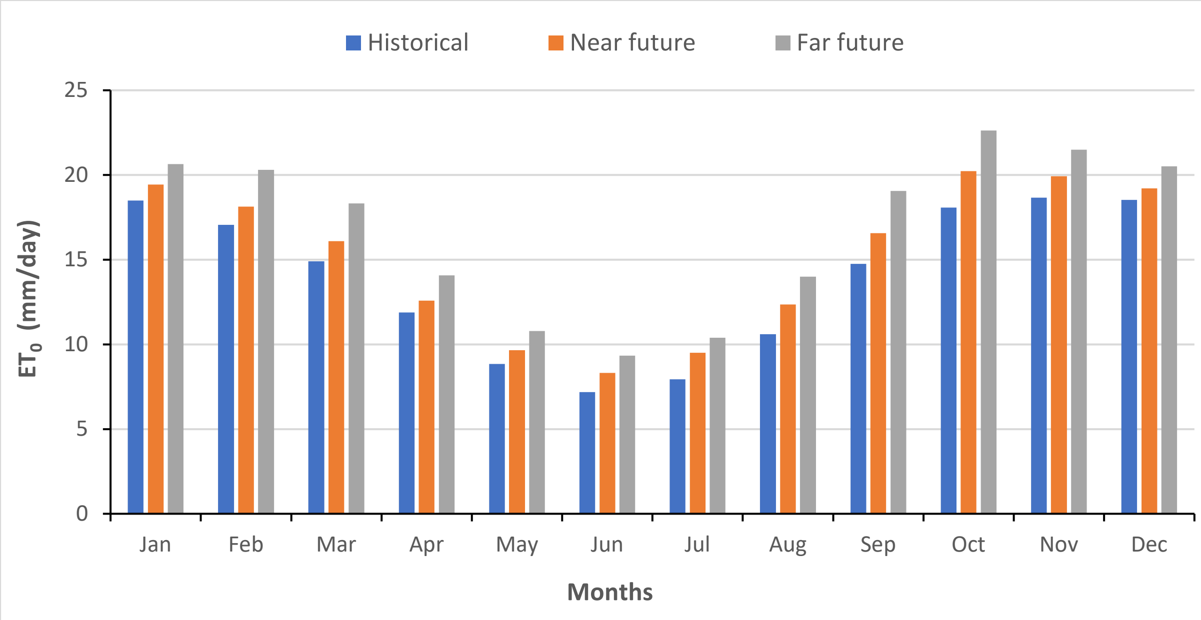


Figure 4.24: Simulated monthly reference evapotranspiration

### 4.5.4. Future crop water requirements in wet season (summer)

Figures 4.25 to 4.28 indicate the CWRs for four selected prioritised crops (groundnuts, maize, sweet potato, and tomato) in wet season for the three 30-year periods: 1993-2022 (historical), 2023-2052 (near future) and 2053-2082 (far future). From Figures 4.25 to 4.28, it can be observed that the water requirement for all crops during all periods where low at the initial stage of growth. This can be associated with low Kc values (0.40, 0.30, 0.50 and 0.60 for groundnuts, maize, sweet potato, and tomato, respectively) at the initial stages due to low canopy as the crops were still on their establishment phase with little ground cover, resulting in lower water requirements. As the crops grow, the amount of water required gradually increased in the development stage and peaked in the mid-season stage, which is the stage where the crop's maturity starts, and high amount of water is used, Kc values were also high at this stage reaching a maximum of 1.20 for maize and 1.15 for groundnuts, tomato, and sweet potato. The increase is compounded by crops growing periods (October to February for groundnuts and sweet potato, November to March for maize and September to January for tomato) which are dominated by summer months with high temperatures leading to high water requirement to compensate water lost through evapotranspiration. The CWRs then decreased when the crops reached full maturity and is ready for harvest.

The results show a general increase in water requirements for all crops from the historical period to near future and far future. The total estimated seasonal water requirement for groundnuts increased from 1873.05 mm at historical period to 2070.94 mm in near and 2282.26 mm in far future, for maize, water requirement increased from 1829.53 mm to

1952.62 and 2115.73 mm in historical period, near future and far future, respectively. For sweet potato, total water requirement was 2582.57 mm in the historical period and increased to 2716.50 and 2962.84 mm in near future and far future, respectively, and for tomato water increased from 2265.82 mm to 2534.13 mm and 2772.23 mm in historical period, near future and far future respectively.

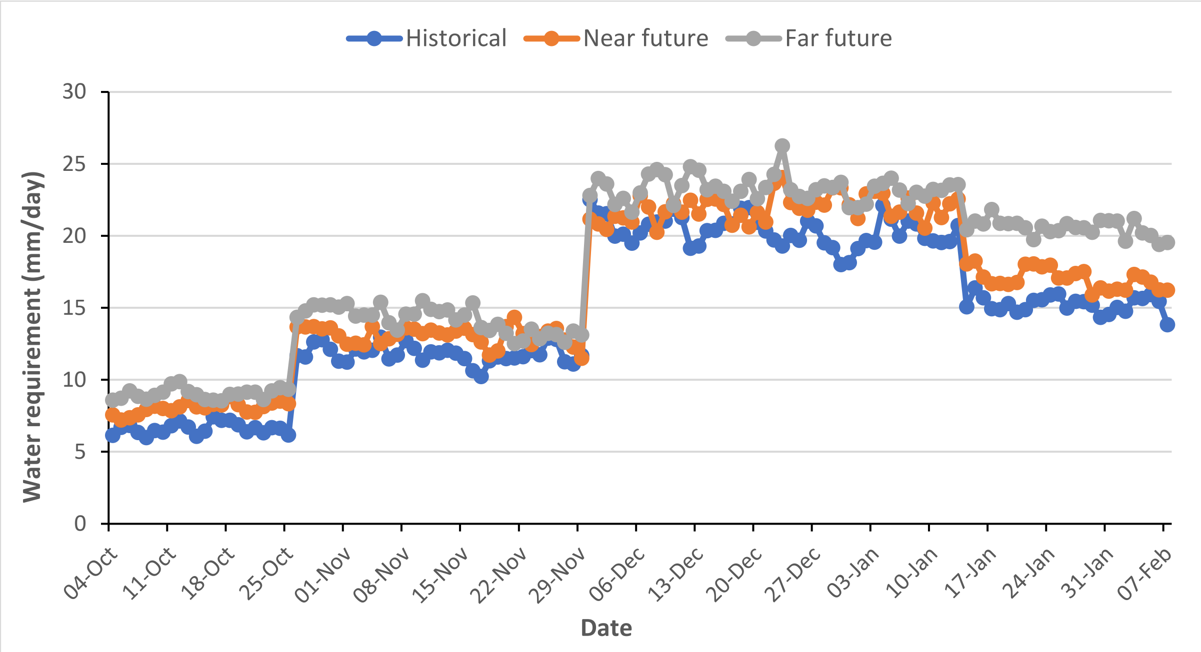


Figure 4.25: Estimated water requirement for groundnuts for wet season

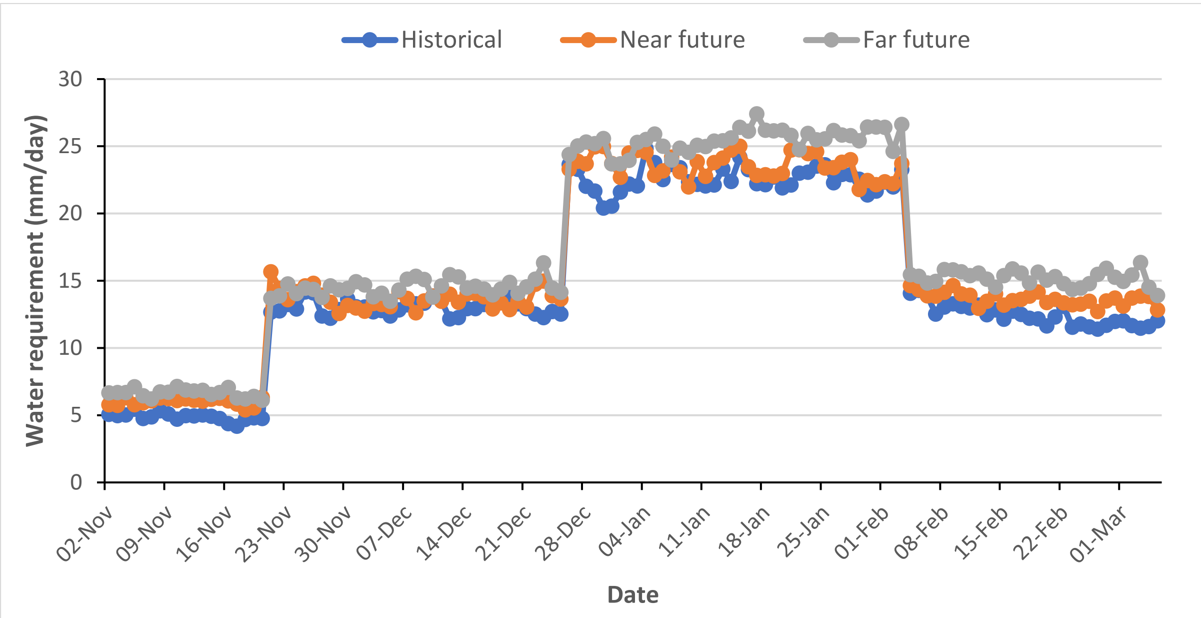


Figure 4.26: Estimated water requirement for maize for wet season

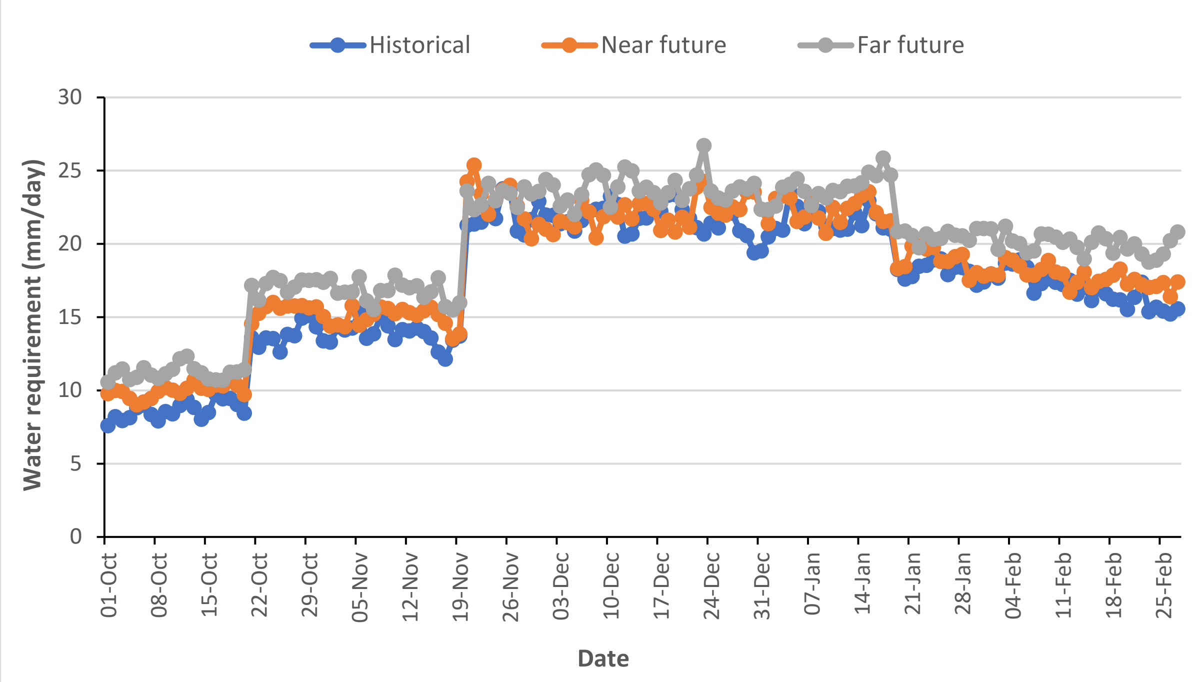


Figure 4.27: Estimated water requirement for sweet potato for wet season

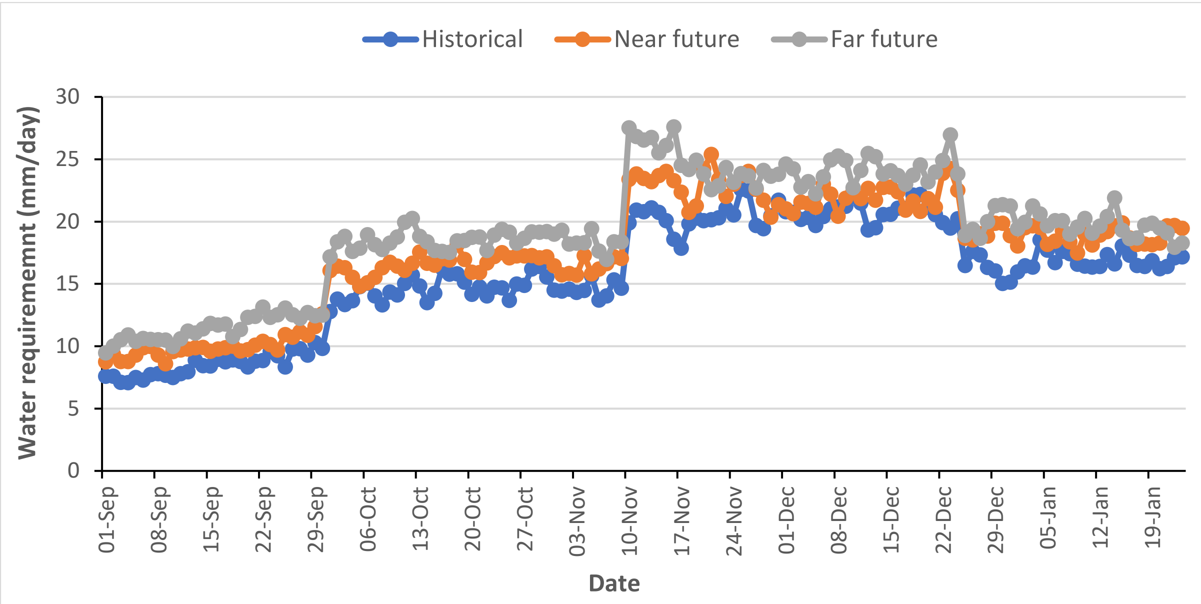


Figure 4.28: Estimated water requirements for tomato for wet season

#### 4.5.5. Comparison of future crop water requirements and inflows in wet season (summer)

Figures 4.29 to 4.32 show the comparison of projected average crop water requirements and inflows for groundnuts, maize, tomato, and sweet potato in near future and far future for the wet season. This was conducted to find out if future inflows will be able to meet the CWRs. Based on the results, there will be a constant increase in irrigation water requirements for near future and far future while inflows remain low in most months of the growing seasons for all crops except in February, March and January which recorded high inflows than CWRs for groundnuts and maize, and tomato respectively. However, this may be possibly because the crops were at full maturity stage where very little water is used since, they are ready for harvest. Moreover, irrigation water requirements for maize are much higher than inflows as compared to other crops, this can be associated with high area under irrigation for maize as farmers prefer cultivating this crop in larger quantities during summer. Groundnuts are also a preferred summer crop after maize with estimated high IWRs. A comparison of inflows and crop water requirements showed that in near future, water requirements for maize, tomato, groundnuts, and sweet potato will exceed inflows by 49.54, 10.05, 9.43, and 9.14%, respectively, and in far future, water requirements will be higher than inflows by 66.08, 26.9, 27.15, and 37.22%, for maize, tomato, groundnuts, and sweet potato, respectively.

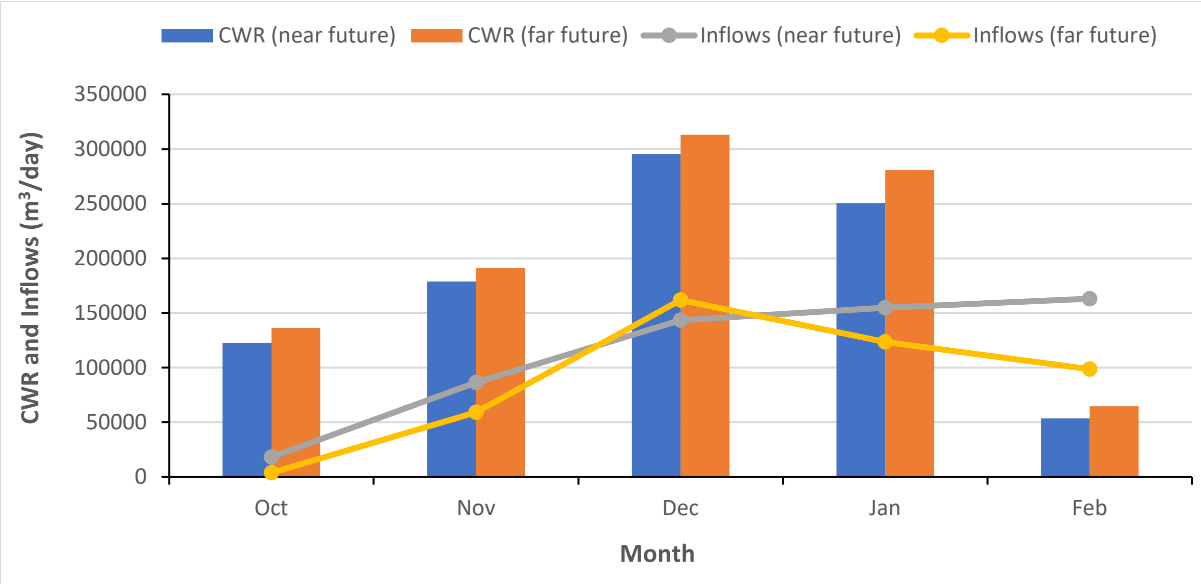


Figure 4.29: Comparison of average CWRs for groundnuts and inflows for wet season

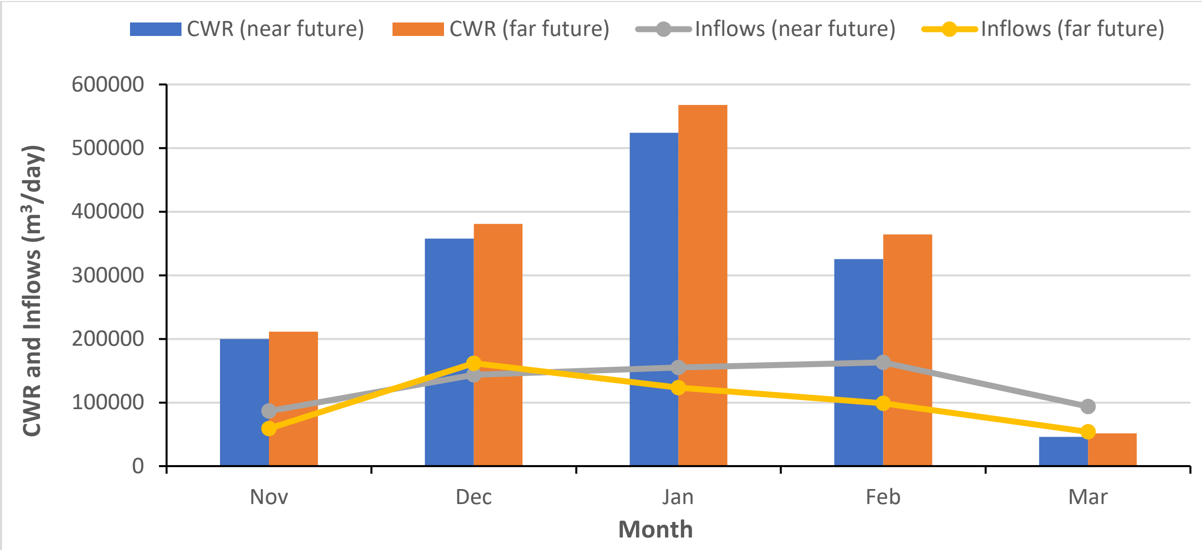


Figure 4.30: Comparison of average CWRs for maize and inflows for wet season

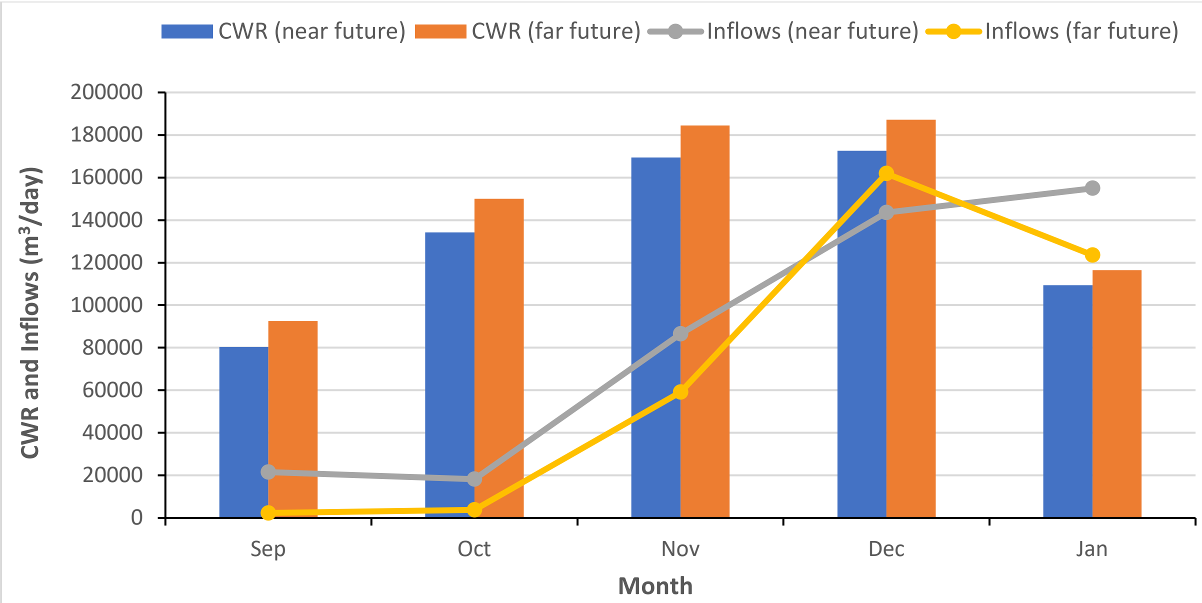


Figure 4.31: Comparison of average CWRs for tomato and inflows for wet season

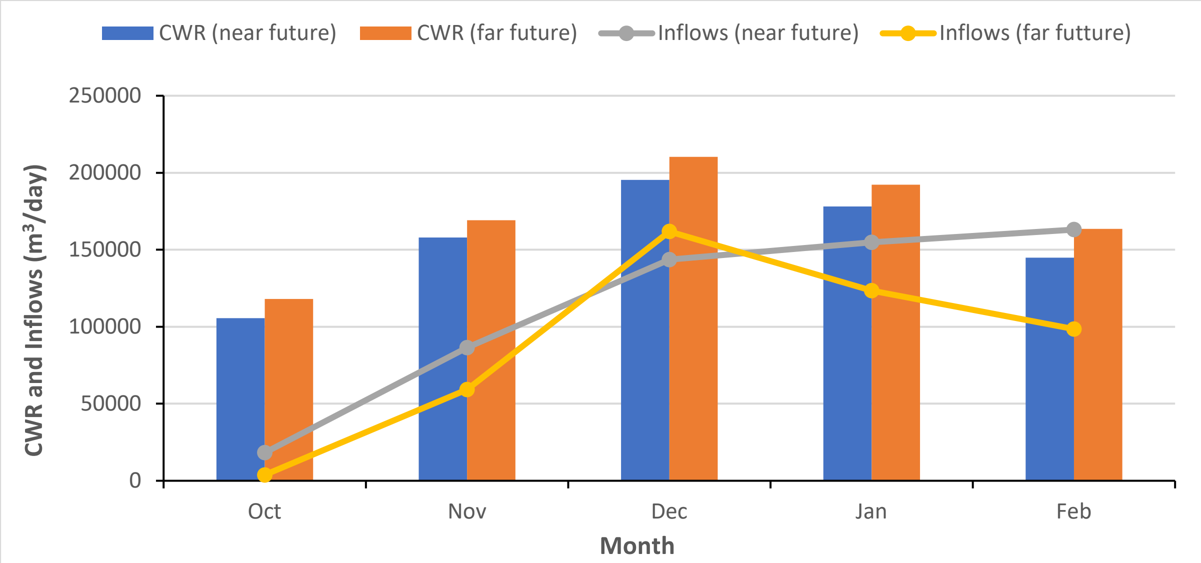


Figure 4.32: Comparison of average CWRs for sweet potato and inflows for wet season

#### 4.5.6. Future crop water requirements in dry season (winter)

Figure 4.33 to 4.35 present the CWRs for maize, tomato, and sweet potato in dry season for three periods: historical (1993-2022), near future (2023-2052) and far future (2023-2082). Just like in summer season, the CWRs for all crops in all periods were different at each growing stage due to different values in the crop's coefficient curve. Estimated CWRs were low at the initial stage of growth, increased into the development and mid-season stage then decreased when the crop reached full maturity. However, for tomato and sweet potato water requirements did not decrease from the mid-season stage to full maturity stage. Based on the results, there is a general increase in water requirements for all crops from historical period to near future and far future. The total estimated seasonal water requirement increased respectively from historical period to near future and far future by 914.83 to 1020.42 and 1136.58, 1220.7 to 1321.9 and 1484.63, and 1434.71 to 1577.72 and 1787.43 mm for maize, tomato, and sweet potato, respectively.

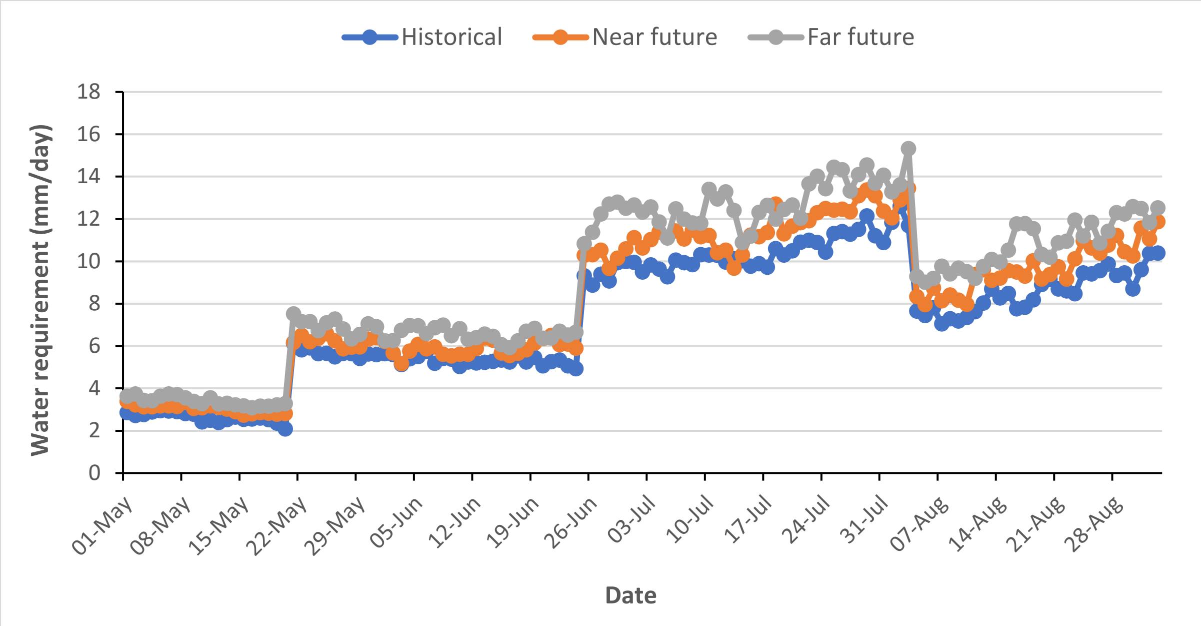


Figure 4.33: Estimated water requirements for maize for dry season

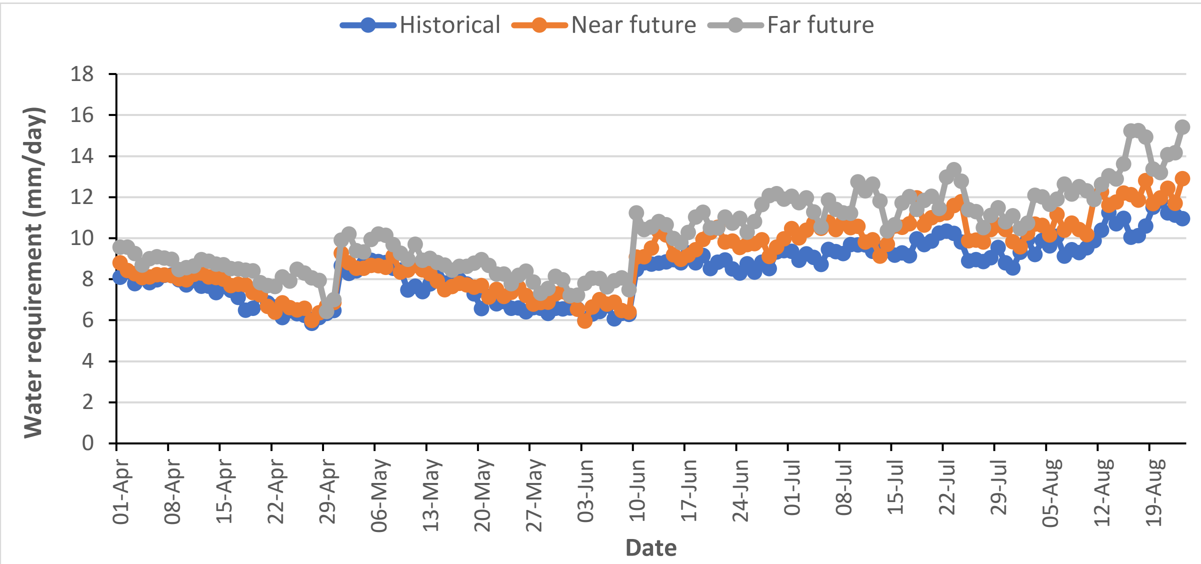


Figure 4.34: Estimated water requirements for tomato for dry season

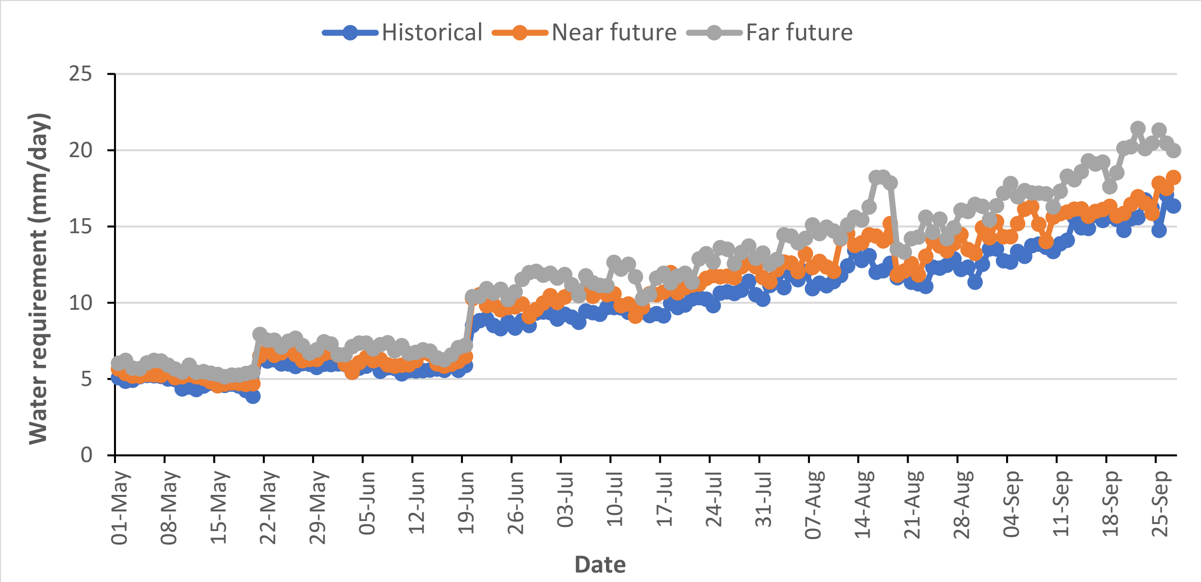


Figure 4.35: Estimated water requirements for sweet potato for dry season

### 4.5.7. Comparison of future crop water requirements and inflows in dry season (winter)

Figures 4.36 to 4.38 show the comparison of projected CWRs and inflows for maize, tomato, and sweet potato in near future and far future for the dry season. Based on the results, water requirements for sweet potato were much higher than inflows in contrast to maize and tomato, this can be because farmers prioritise cultivating sweet potato in large quantities during winter as the as they believe it can survive in water stress conditions. Maize and tomato are the farmer's least preferred crops during winter. Projected inflows are too low to meet the water requirements during most months of the growing season in both future periods except for maize which had lower water requirements than inflows. In the near future, the estimated water requirements for sweet potato and tomato will exceed inflows by 71.12% and 29.87%, respectively, but will be lower than inflows by 62% for maize, and in far future, water requirements for sweet potato, tomato and maize will be higher than inflows by 89.42, 62.30, and 25.87%, respectively.

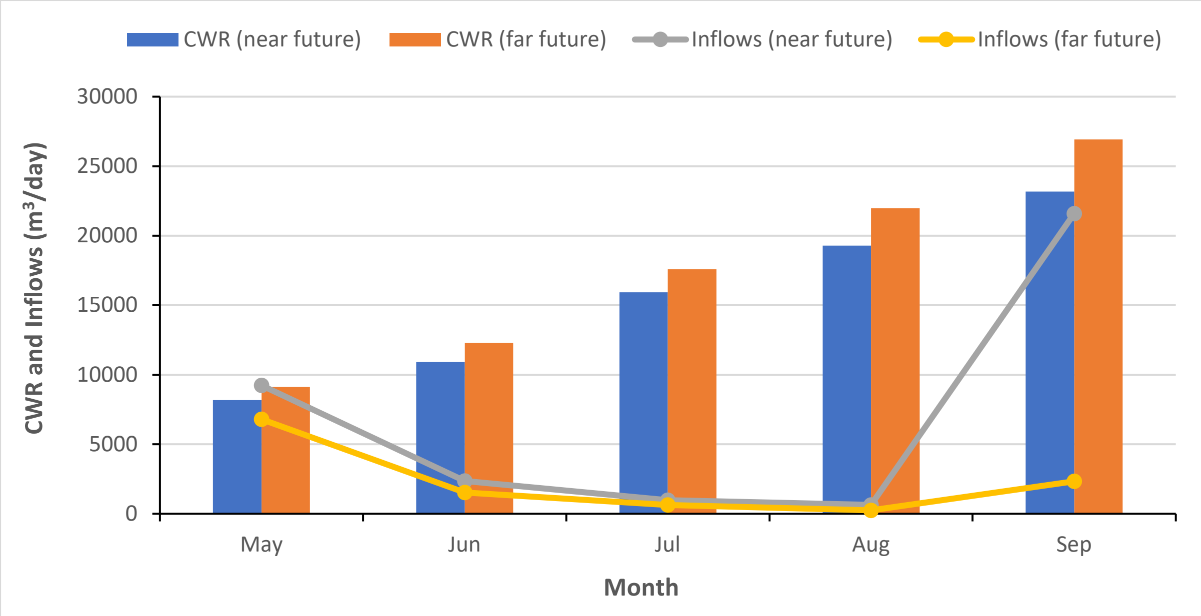


Figure 4.36: Comparison of average CWRs for sweet potato and inflows for dry season

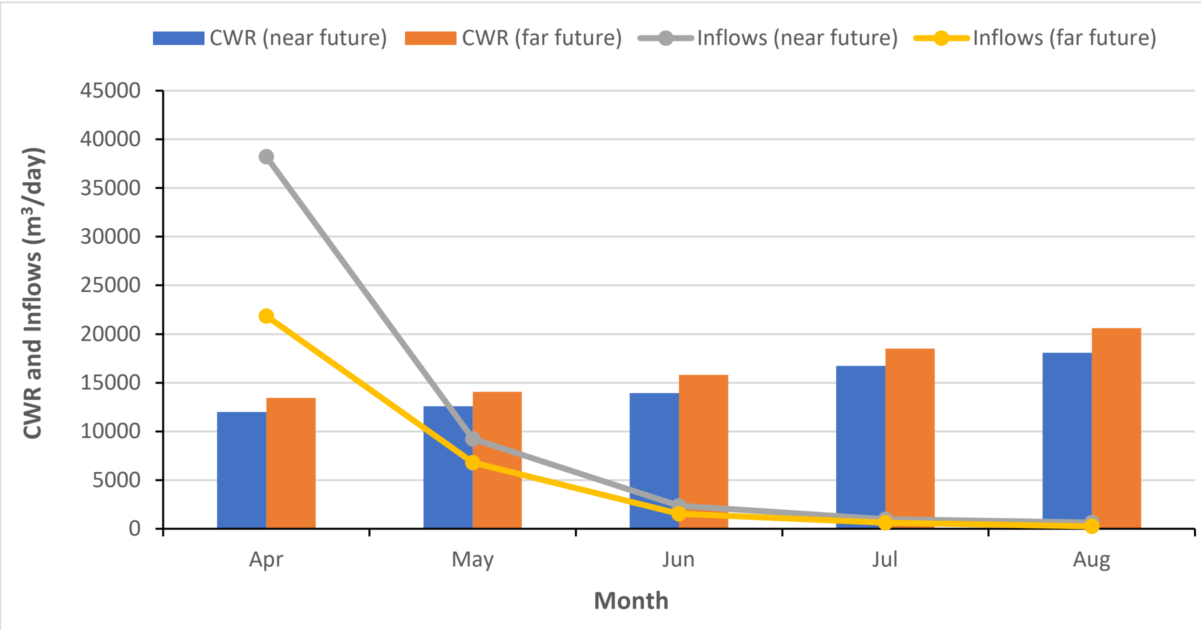


Figure 4.37: Comparison of average CWRs for tomato and inflows for dry season

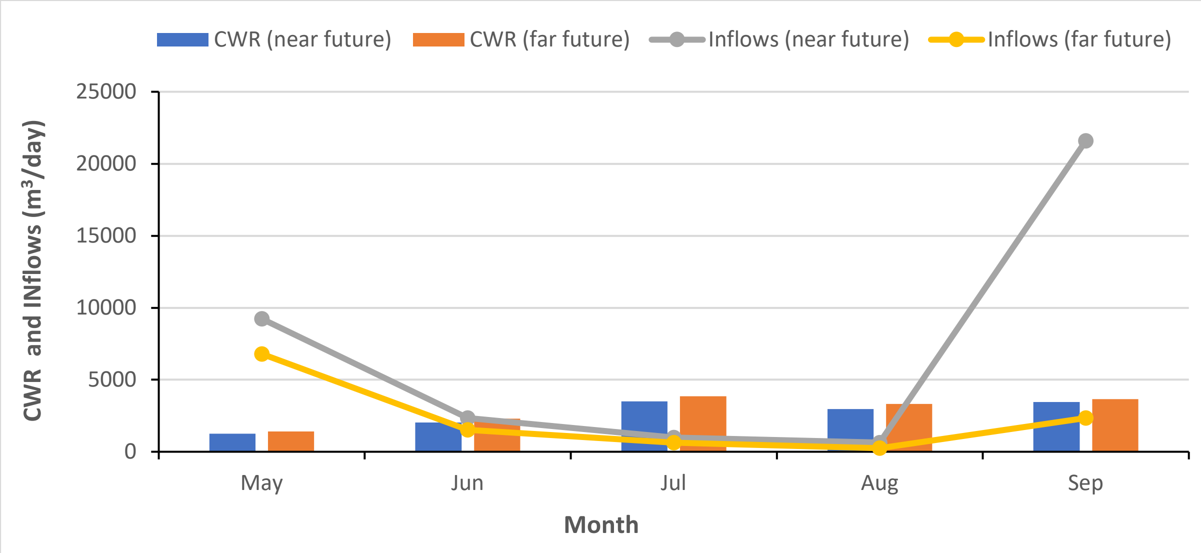


Figure 4.38: Comparison of average CWRs for maize and inflows for dry season

### 4.6. Summary

This chapter presents the results of historic rainfall and temperature trends for the period 1987-2009 stations 299303, Mphephu, Jouberstroom and Veermedling. Trends analysis for rainfall and temperature for a 30-year period: 1993-2022 (historical), 2023-2053 (near future), and 2053-2082 (far future) for CCAM station p299301 are also presented and have shown high variabilities in rainfall and temperature throughout the years under changing climatic conditions. Trends showed that rainfall will increase in near future, but high intensity of rainfall decrease was projected in far future, as well as increases in maximum and minimum temperatures. This will necessitate a greater reliance on early warning systems to prepare farmers, communities, policymakers, and other stakeholders for the likelihood of a climate shock.

The SWAT hydrological model used in the study showed a good agreement between the simulated and observed streamflow in the study area quaternary catchments. The projected impacts of climate change on inflows into the Raliphaswa irrigation weir showed a decrease in inflows in near future and far future which can be associated with expected decrease in rainfall and high temperatures, together with the dry and arid conditions of the area. The estimated increase in crop water requirements in both future and far future scenarios will put more pressure on the already limited water available for irrigation. A decrease in inflows coupled with a decrease of rainfall in far future and increases in maximum and minimum temperatures in near future and far future will highly reduce crop productivity. This is expected to exacerbate the existing problem of agricultural water deficit in the study area. Farmers opt to reduce the number of acres cultivated or some do not plant at all during periods of deficits.

# CHAPTER 5: CONCLUSION AND RECOMMENDATIONS

## 5.1. Conclusion

The present study assessed the impacts of climate change on current and future water resources availability and agriculture in the study area. Several methodologies were employed to assess the impacts of climate change on water resources availability for agriculture, paying particular attention on whether inflows into Raliphswa irrigation weir will be able to meet future crop water requirements in Raliphaswa irrigation scheme.

Rainfall data analysis has shown high variability in rainfall patterns for current years (1993-2022) and future periods 2023-2052 (near future) and 2023-2082 (far future) with trends showing increase and decrease in rainfall in near future and far future, respectively. rainfall is projected to increase by 5.7% in near future and decrease by 15.7% in far future relative to the baseline period. Analysis of temperature data showed increasing trends in maximum and minimum temperature in both future periods. Maximum temperature will respectively increase by 1 °C and 4 °C in near future and far future, on the other hand, minimum temperature will increase by 1.4 °C and 3.4 °C in near future and far future, respectively, relative to the baseline period. The decrease and high variability in rainfall accompanied by high temperatures and the semi-arid nature of the study area are expected to increase the impacts of climate change on water resources availability for agriculture.

The SWAT hydrological model was used to assess the impacts of climate change on water resources availability. The results showed that SWAT model performs well in a semi-arid area like Nzhelele. The model performance was evaluated based on evaluation criteria Coefficient of determination ($R^2$), Nash-Sutcliffe efficiency (NSE), percent bias (PBIAS) and ratio of the root mean square error to the standard deviation of measured data (RSR). The model showed good performance statistics of $R^2$ of 0.71, NSE of 0.56, PBIAS of +0.6% and RSR of 0.66 after calibration and validation. The availability of water in the study area was assessed for near future and far future based on inflows into the irrigation weir. Analysis of climate change impacts water availability showed a general decrease in inflows in all months in all scenarios. Inflows were projected to decrease by 28.7% and 48% in near future and far future.

The results in this study have indicated an increase in CWRs for both growing seasons in all future scenarios. Since the irrigation schemes receives irrigation water by a means of a weir which is fed by Mutshedzi Dam and with future projections showing a possible decrease in mean rainfall in the next few years (Maponya et al., 2013), inflows into the irrigation weir will also decrease which means little or no water will be available to meet the increased crop water needs. A comparison of projected inflows and estimated crop water requirements indicated that in wet season (summer), water requirements for maize, tomato, groundnuts, and sweet potato in near future will exceeds inflows by 49.54, 10.05, 9.43, and 9.14%, respectively, and in far future, water requirements will be higher than inflows by 66.08, 26.9, 27.15, and 37.22%, for maize, tomato, groundnuts, and sweet potato respectively, while in dry season (winter), the estimated water requirements for sweet potato and tomato in near future will exceed inflows by 71.12% and 29.87%, respectively, but will be lower than inflows by 62% for maize, and in far future, water requirements for sweet potato, tomato and maize will be higher than inflows by 89.42, 62.30, and 25.87%, respectively.

Water shortages have already been identified as a major threat to a successful farm productivity. The increase in crop water requirements will put more pressure on the already limited water resources. The inability of irrigation water to meet future CWRs will decrease the crop yield which will reduce food productivity thereby threatening food security. Furthermore, income generation is also threatened as farmers also sell their crops, as well as employment for farm labours. Furthermore, increased crop water requirements will limit the ability of farmers to increase the size of their irrigated crop land along with their cropping pattens.

The key finding of this study is that there is evidence that climate in Nzhelele area is changing and will continue to change in the future. Thus, water availability and crop water requirements are sensitive to this change. The results of this study will therefore significantly advance knowledge of the implications of climate change on the water availability for agriculture both inside Nzhelele area community and throughout the country.

The findings of this are supported by previous studies which have also shown a possible increase in future crop water requirements in different parts of the world under the changing climate. Sayari et al. (2011) simulated the crop water use for sugar beet, cotton, been, and chickpea for three time periods (2010-2039, 2040-2069 and 2070-2099) under the changing climatic conditions in northeast of Iran (Kashafrood basin). The current study showed an increase in seasonal crop water use with an increase in projected temperature under climate change conditions. Odiyo et al. (2020) estimated the crop water requirements for maize, banana, and tomato for the 3, 10-year periods (2010-2019, 2050-2059 and 2090-2099) in the Luvuvhu River Catchment, Limpopo Province under the impacts of climate change. This study found that there will be a constant increase in crop water requirements for both near future and far future scenarios which will be influenced by expected increases in temperature and a decrease in rainfall. Ngoc and Khanh (2021) Calculated the rice crop water demand for the year 2020 in Giang province (Vietnam) under three seasonal schedules: Winter-

Spring, Summer-Autunm, and Autumn-Winter. According to the results, water demand in the Summer-Autumn season was highest due to high temperatures, followed by Winter-Spring season and the lowest was reported in Autumn-Winter season which is a rainy season in the study area.

### 5.2. Recommendations

The recommendations of the study are as follows:

- The findings of the study have indicated that the crop waster requirements will continue to increase in the future under the changing climate conditions while inflows will be unable to meet these requirements. Therefore, raising awareness about climate change will help farmers understand how these changes will affect their crop productions and what actions can they take to minimise the effects of climate change.
- Climate change adaption measures to minimize the impact of climate change on irrigation water availability and crop production should be highly promoted in Raliphaswa irrigation scheme. This includes encouraging farmers to adopt climate-smart agriculture technologies, which can be accomplished through developing and supporting an adaptation-friendly legislative environment.

- The government should adopt national policies that encourage research and development programs that encourage the use of innovative technology and practices that can help to relieve climate change impacts on agricultural water availability. These policies must enhance irrigation, increase crop, and water productivity.

# REFERENCES

ABBASPOUR, K. C., FARAMARZI, M., GHASEMI, S. S. & YANG, H. 2009. Assessing the impact of climate change on water resources in Iran. *Water Resour. Res.,* 45.

ABBASPOUR, K. C., YANG, J., MAXIMOV, I., SIBER, R., BOGNER, K., MIELEITNER, J., ZOBRIST, J. & SRINIVASAN, R. 2007. Modelling hydrology and water quality in the pre-alpine/alpine Thur watershed using SWAT. *Journal of Hydrology,* 333**,** 413-430.

ABBOTT, M., BATHURST, J., CONNELL, P. & RASMUSSEN, J. 1986. An introduction to the European hydrologic system-system hydrologue European, SHE, 1: history of a physically-based, distributed modeling system. *J. Hydrol,* 87**,** 45-59.

ABERA ABDI, D. & AYENEW, T. 2021. Evaluation of the WEAP model in simulating subbasin hydrology in the Central Rift Valley basin, Ethiopia. *Ecological Processes,* 10**,** 1-14.

ABRAHAM, T. & MULUNEH, A. 2022. Quantifying Impacts of Future Climate on the Crop Water Requirement, Growth Period, and Drought on the Agricultural Watershed, in Ethiopia. *Air, Soil and Water Research,* 15**,** 1-15.

ABRAMS, M., CRIPPEN, R. & FUJISADA, H. 2020. ASTER Global Digital Elevation Model (GDEM) and ASTER Global Water Body Dataset (ASTWBD). *Remote Sensing,* 12**,** 1156.

ADOM, R. K., SIMATELE, M. D. & REID, M. 2022. Addressing the challenges of water-energy-food nexus programme in the context of sustainable development and climate change in South Africa. *Journal of Water and Climate Change,* 13**,** 2761-2779.

AFSHAR, N. R. & SUHAIMI, D. N. 2018. Climate change impact on water resources availability in Kuching Sarawak. *MCRJ special issue,* 5.

AHMADAALI, J., BARANI, G.-A., QADERI, K. & HESSARI, B. 2018. Analysis of the effects of water management strategies and climate change on the environmental and agricultural sustainability of Urmia Lake Basin, Iran. *Water,* 10**,** 160.

AHMADIPOUR, A., SHAIBANI, P. & MOSTAFAVI, S. A. 2019. Assessment of empirical methods for estimating potential evapotranspiration in Zabol Synoptic Station by REF-ET model. *Medbiotech Journal,* 3**,** 1-4.

AKANBI, R., DAVIS, N. & NDARANA, T. 2020. Climate change and maize production in the Vaal catchment of South Africa: assessment of farmers' awareness, perceptions and adaptation strategies. *Climate Research,* 82.

AKOKO, G., LE, T., GOMI, T. & KATO, T. 2021. A Review of SWAT Model Application in Africa. *Water,* 13**,** 1313.

AKPOR, O. B. & BOAKYE, M. K. 2011. Impacts of Climate Change on Water Resources in Africa. *African Journal of Science,Technology, innovation and development,* 3**,** 83-98.

AKRAM, N. 2012. Is climate change hindering economic growth of Asian economies? *Asia-Pacific Development Journal* 19.

ALCAMO, J., MORENO, J. M., NOVÁKY, B., BINDI, M., COROBOV, R., DEVOY, R. J. N., GIANNAKOPOULOS, C., MARTIN, E., OLESEN, J. E. & SHVIDENKO, A. 2007. Europe. Climate Change 2007: Impacts, Adaptation and Vulnerability. *Contribution of Working Group II to the Fourth Assessment Report of the Intergovernmental Panel on Climate Change. Cambridge University Press, Cambridge, UK***,** 541-580.

ALLEN, R. G., PEREIRA, L. S., RAES, D. & SMITH, M. 1998. Crop evapotranspiration-Guidelines for computing crop water requirements-FAO Irrigation and drainage paper 56. *Fao, Rome,* 300**,** D05109.

ALTALIB, A. A., MAHMOOD, M. T. & AL-OGAIDI, A. A. 2021. Mapping Reference Evapotranspiration for Iraq Using FAO-Penman-Monteith Method. *Agricultural Engineering International: CIGR Journal,* 23.

AMIN, A. & NURU, N. 2020. Evaluation of the Performance of SWAT Model to Simulate Stream Flow of Mojo River Watershed: In the Upper Awash River Basin, in Ethiopia. *Hydrology,* 8**,** 7.

AMPOSAH-DACOSTA, F. & MATHADA, H. 2017. Study of sand mining and related environmental problems along the Nzhelele River in Limpopo Province of South Africa. *Mine Water and Circular Economy, Finland*.

ANDERSSON, L., SAMUELSSON, P. & KJELLSTRO, M. E. 2011. Assessment of climate change impact on water resources in the Pungwe river basin. *Tellus A: Dynamic Meteorology and Oceanography,* 63**,** 138-157.

ANDRADE, C. 2019. The P Value and Statistical Significance: Misunderstandings, Explanations, Challenges, and Alternatives. *Indian J Psychol Med,* 41**,** 210-215.

ANG, R. & OEURNG, C. 2018. Simulating streamflow in an ungauged catchment of Tonlesap Lake Basin in Cambodia using Soil and Water Assessment Tool (SWAT) model. *Water Science,* 32**,** 89-101.

AQNOUY, M., EL MESSARI, J. E. S., ISMAIL, H., BOUADILA, A., MORENO NAVARRO, J. G., LOUBNA, B. & MANSOUR, M. R. A. 2019. Assessment of the SWAT Model and the Parameters Affecting the Flow Simulation in the Watershed of Oued Laou (Northern Morocco). *Journal of Ecological Engineering,* 20.

ARKU, A. Y., MUSA, S. M. & MOFOKE, A. L. E. 2012. Determination of water requirement and irrigation timing for Amaranthus hybridus in Maiduguri metropolis, north-eastern Nigeria. *WIT Transactions on Ecology and The Environment,* 168.

ARNELL, N. W., HALLIDAY, S. J., BATTARBEE, R. W., SKEFFINGTON, R. A. & WADE, A. J. 2015. The implications of climate change for the water environment in England. *Progress in Physical Geography,* 39**,** 93–120.

ARNOLD, J. G., MORIASI, D. N., GASSMAN, P. W., ABBASPOUR, K. C., WHITE, M. J., SRINIVASAN, R., SANTHI, C., HARMEL, R., VAN GRIENSVEN, A. & VAN LIEW, M. W. 2012. SWAT: Model use, calibration, and validation. *Transactions of the ASABE,* 55**,** 1491-1508.

ARREY, I., ODIYO, J. O., MAKUNGO, R. & KATAKA, M. 2019. Vadose zone infiltration and its implication for groundwater contamination risk assessment in Siloam village, Limpopo province, South Africa. *Jàmbá: Journal of Disaster Risk Studies,* 11**,** 1-9.

ASHOFTEH, P.-S., RAJAEE, T. & GOLFAM, P. 2017. Assessment of Water Resources Development Projects under Conditions of Climate Change Using Efficiency Indexes (EIs). *Water Resources Management,* 31**,** 3723-3744.

ASSENG, S., EWERT, F., MARTRE, P., RÖTTER, R. P., LOBELL, D. B., CAMMARANO, D., KIMBALL, B. A., OTTMAN, M. J., WALL, G. W., WHITE, J. W., REYNOLDS, M. P., ALDERMAN, P. D., PRASAD, P. V. V., AGGARWAL, P. K., ANOTHAI, J., BASSO, B., BIERNATH, C., CHALLINOR, A. J., DE SANCTIS, G., DOLTRA, J., FERERES, E., GARCIA-VILA, M., GAYLER, S., HOOGENBOOM, G., HUNT, L. A., IZAURRALDE, R. C., JABLOUN, M., JONES, C. D., KERSEBAUM, K. C., KOEHLER, A. K., MÜLLER, C., NARESH KUMAR, S., NENDEL, C., O'LEARY, G., OLESEN, J. E., PALOSUO, T., PRIESACK, E., EYSHI REZAEI, E., RUANE, A. C., SEMENOV, M. A., SHCHERBAK, I., STÖCKLE, C., STRATONOVITCH, P., STRECK, T., SUPIT, I., TAO, F., THORBURN, P. J., WAHA, K., WANG, E., WALLACH, D., WOLF, J., ZHAO, Z. & ZHU, Y. 2015. Rising temperatures reduce global wheat production. *Nature Climate Change,* 5**,** 143-147.

AWAL, R., RAHMAN, A., FARES, A. & HABIBI, H. 2022. Calibration and Evaluation of Empirical Methods to Estimate Reference Crop Evapotranspiration in West Texas. *Water,* 14**,** 3032.

AYIVI, F. & JHA, M. K. 2018. Original ResearchArticle Estimation ofwaterbalanceandwateryieldintheReedyFork-Buffalo CreekWatershedinNorthCarolinausingSWAT. *International SoilandWaterConservationResearch,* 6**,** 203–213.

AYYANAGOWDAR, M., POLISGOWADAR, B., NEMICHANDRAPPA, M., RAVI, M., LATA, H. & RAMESH, G. 2020. Estimation of crop water requirement and irrigation scheduling of baby corn using CROPWAT model. *Journal of Pharmacognosy and Phytochemistry,* 9**,** 1944-1949.

BAUER, S. & SCHOLZ, I. 2010. Adaptation to climate change in Southern Africa: New boundaries for sustainable development? *Climate and development,* 2**,** 83–93.

BELLO, Q. 2020. *A Literature Review of Multi-modeling in Hydrology*.

BENHIN, J. K. A. 2008. South African crop farming and climate change: An economic assessment of impacts *Global Environmental Change,* 18**,** 666–678.

BERAN, A., HANEL, M., NESLÁDKOVÁ, M. & VIZINA, A. 2016 Increasing water resources availability under climate change. *Procedia Engineering,* 162 448 – 454.

BERGSTRÖM, S. 1992. The HBV model: its structure and applications. Norrkoping: Swedish Meteorological and Hydrological Institute.

BERGSTRÖM, S. & FORSMAN, A. 1973. Development of a conceptual deterministic rainfall-runoff model. *Nord Hydrol* 4**,** 174–190.

BLANEY, H. F. & CRIDDLE, W. D. 1950. Determining water requirements in irrigated areas from climatological and irrigation data. Soil conservation service technical paper 96, Soil conservation service. US Department of Agriculture, Washington. 44.

BLIGNAUT, J., UECKERMANN, L. & ARONSON, J. 2009. Agriculture production's sensitivity to changes in climate in South Africa. *South African Journal of Science,* 105.

BOTAI, C. M., BOTAI, J. O. & ADEOLA, A. M. 2018. Spatial distribution of temporal precipitation contrasts in South Africa. *S Afr J Sci,* 114**,** 1-9.

BUI, M. T., LU, J. & NIE, L. 2020. A Review of Hydrological Models Applied in the Permafrost-Dominated Arctic Region. *Geosciences,* 10**,** 401.

BUSARI, O. 2008. Groundwater in the Limpopo Basin: occurrence, use and impact. *Environment, development and sustainability,* 10**,** 943-957.

CAESAR, J., PALIN, E., LIDDCOAT, S., LOWE, J., BURKE, E., PARDAENS, A., SANDERSON, M. & KANAHA, R. 2012. Response of the HadGEM2 Earth System Model to Future Greenhouse Gas Emissions Pathways to the Year 2300*. *journal of Climate*.

CAI, X., MAGIDI, J., NHAMO, L. & VAN KOPPEN, B. 2017. *Mapping irrigated areas in the Limpopo Province, South Africa*, International Water Management Institute (IWMI).

CALZADILLA, A., ZHU, T., REHDANZ, K., TOL, R. S. J. & RINGLER, C. 2014. Climate change and agriculture: Impacts and adaptation options in South Africa. *Water Resources and Economics,* 5**,** 24-48.

CAMMARANO, D., VALDIVIA, R., BELETSE, Y. G., DURAND, W., CRESPO, O., TESFUHUNEY, W., JONES, M., WALKER, S., MPUISANG, T., NHEMACHENA, C., RUANE, A., MUTTER, C., ROSENZWEIG, C. & ANTLE, J. 2020. Integrated assessment of climate change impacts on crop productivity and income of commercial maize farms in northeast South Africa. *Food Security,* 12.

CARDOSO DE SALIS, H. H., MONTEIRO DA COSTA, A., MOREIRA VIANNA, J. H., AZENETH SCHULER, M., KÜNNE, A., SANCHES FERNANDES, L. F. & LEAL PACHECO, F. A. 2019. Hydrologic modeling for sustainable water resources management in urbanized karst areas. *International Journal of Environmental Research and Public Health,* 16**,** 2542.

CHATURVEDI, R. K., JOSHI, J., JAYARAMAN, M., BALA, G. & RAVINDRANATH, N. 2012. Multi-model climate change projections for India under representative concentration pathways. *Current Science***,** 791-802.

CHELLANEY, B. 2012. Asia's worsening water crisis Survival *Survival,* 54**,** 143–156.

CHEN, J., BRISSETTE, F. P., POULIN, A. & LECONTE, R. 2011. Overall uncertainty study of the hydrological impacts of climate change for a Canadian watershed. *Water Resources Research,* 47.

CHESHMBERAH, F. & ZOLFAGHARI, A. A. 2019. The Effect of Climate Change on Future Reference Evapotranspiration in Different Climatic Zones of Iran. *Pure and Applied Geophysics,* 176**,** 3649-3664.

CHIKOSI, E. S., MUGAMBIWA, S. S., TIRIVANGASI, H. M. & RANKOANA, S. A. 2019. Climate change and variability perceptions in Ga-Dikgale community in Limpopo Province, South Africa. *International Journal of Climate Change Strategies and Management,* 11**,** 392-405.

CHORDIA, J., PANIKKAR, U. R., SRIVASTAV, R. & SHAIK, R. U. 2022. Uncertainties in Prediction of Streamflows Using SWAT Model—Role of Remote Sensing and Precipitation Sources. *Remote Sensing,* 14**,** 5385.

CHORUMA, D. J., AKAMAGWUNA, F. C. & ODUME, N. O. 2022. Simulating the Impacts of Climate Change on Maize Yields Using EPIC: A Case Study in the Eastern Cape Province of South Africa. *Agriculture,* 12**,** 794.

CLARK, M. P., WILBY, R. L., GUTMANN, E. D., VANO, J. A., GANGOPADHYAY, S., WOOD, A. W., FOWLER, H. J., PRUDHOMME, C., ARNOLD, J. R. & BREKKE, L. D. 2016. Characterizing uncertainty of the hydrologic impacts of climate change. *Current Climate Change Reports,* 2**,** 55-64.

CONWAY, D., VAN GARDEREN, E. A., DERYNG, D., DORLING, S., KRUEGER, T., LANDMAN, W., LANKFORD, B., LEBEK, K., OSBORN, T. & RINGLER, C. 2015. Climate and southern Africa's water–energy–food nexus. *Nature Climate Change,* 5**,** 837-846.

CORON, L., ANDRÉASSIAN, V., PERRIN, C., BOURQUI, M. & HENDRICKX, F. 2014. On the lack of robustness of hydrologic models regarding water balance simulation: a diagnostic approach applied to three models of increasing complexity on 20 mountainous catchments. *Hydrology and Earth System Sciences,* 18**,** 727-746.

COULIBALY, N., COULIBALY, T. J. H., MPAKAMA, Z. & SAVANÉ, I. 2018. The Impact of Climate Change on Water Resource Availability in a Trans-Boundary Basin in West Africa: The Case of Sassandra. *Hydrology,* 5.

CRISTEA, N. C., KAMPF, S. K. & BURGES, S. J. 2013. Linear models for estimating annual and growing season reference evapotranspiration using averages of weather variables. *International journal of climatology,* 33**,** 376-387.

CULLIS, J. D. S., HORN, A., ROSSOUW, N., FISHER-JEFFES, L., KUNNEKE, M. M. & HOFFMAN, W. 2019. Urbanisation, climate change and its impact on water quality and economic risks in a water scarce and rapidly urbanising catchment: case study of the Berg River Catchment. *H2Open Journal,* 2.

DAFF 2017. A pofile of the South African tomato market value chain. South Africa : Department of Agricuiture, Foresty and Fisheries.

DALLAS, H. F. & RIVERS-MOORE, N. 2014. Ecological consequences of global climate change for freshwater ecosystems in South Africa. *South African Journal of Science,* 110**,** 11.

DANIYA, T., GEETHA, M., KUMAR, B. S. & CRISTIN, R. 2020. Least square estimation of parameters for linear regression. *International Journal of Control and Automation,* 13**,** 447-452.

DARON, J. D. 2014. Regional Climate Messages: Southern Africa”. Scientific report from the CARIAA Adaptation at Scale in Semi-Arid Regions (ASSAR) Project, December 2014.

DAUDA, K. A. & OLAYAKI-LUQMAN, M. 2016. Determination of crop coefficients of three varieties of tomatoes. *International Journal of Research in Science and Engineering Technology,* 1.

DEA 2010. National Climate Change Response Green Paper. South Africa : Department of Environmental Affairs.

DEA 2013. Long-Term Adaptation Scenarios Flagship Research Programme (LTAS) for South Africa. Climate Trends and Scenarios for South Africa. Pretoria, South Africa.

DEDET 2016. Limpopo Climate Change Response Strategy. South Africa : Department of Economic Development, Environment & Tourism

DENNIS, I. & DENNIS, R. 2012. Climate change vulnerability index for South African aquifers. *Water SA,* 38.

DESMAE, H. & SONES, H. 2017. Groundnut cropping guide.

DEVI, G., BIGGANAHALLI PUTTASWAMIGOWDA, G. & DWARAKISH, G. S. 2015. A Review on Hydrological Models. *Aquatic Procedia,* 4**,** 1001-1007.

DIAS, A., DHAWDE, R., SURVE, N., WEINBERG, A., BIRDI, T. & MISTRY, N. 2015. Impact of climate change on water availability and quality in the state of Maharashtra in Western India. *Asian Jr. of Microbiol. Biotech. Env. Sc. ,* 17**,** 1071-1081.

DIDARI, S. & AHMADI, S. H. 2019. Calibration and evaluation of the FAO56-Penman-Monteith, FAO24-radiation, and Priestly-Taylor reference evapotranspiration models using the spatially measured solar radiation across a large arid and semi-arid area in southern Iran. *Theoretical and Applied Climatology,* 136**,** 441-455.

DJAMAN, K., O'NEILL, M., DIOP, L., BODIAN, A., ALLEN, S., KOUDAHE, K. & LOMBARD, K. 2019. Evaluation of the Penman-Monteith and other 34 reference evapotranspiration equations under limited data in a semiarid dry climate. *Theoretical and Applied Climatology,* 137**,** 729-743.

DONNENFELD, Z., CROOKES, C. & HEDDEN, S. 2018. A delicate balance: Water scarcity in South Africa. *ISS Southern Africa Report,* 2018**,** 1-24.

DOORENBOS, J. & PRUITT, W. 1977. Crop water requirements. FAO irrigation and drainage paper 24. *Land and Water Development Division, FAO, Rome,* 144.

DOSIO, A., JONES, R. G., JACK, C., LENNARD, C., NIKULIN, G. & HEWITSON, B. 2019. What can we know about future precipitation in Africa? Robustness, significance and added value of projections from a large ensemble of regional climate models. *Climate Dynamics,* 53**,** 5833-5858.

DOSIO, A., PANITZ, H.-J., SCHUBERT-FRISIUS, M. & LÜTHI, D. 2015. Dynamical downscaling of CMIP5 global circulation models over CORDEX-Africa with COSMO-CLM: evaluation over the present climate and analysis of the added value. *Climate Dynamics,* 44**,** 2637-2661.

DU PLESSIS, C., IRURAH, D. K. & SCHOLES, R. J. 2003. The built environment and climate change in South Africa *BUILDING RESEARCH & INFORMATION,* 31**,** 240–256.

DURÃES, M. F., DE MELLO, C. R. & NAGHETTINI, M. 2011. Applicability of the Swat Model for Hydrologic Simulation in Paraopeba River Basin. *Cerne, Lavras,* 17**,** 481-488.

DURAN-ENCALADA, J. A., PAUCAR-CACERES, A., BANDALA, E. R. & WRIGHT, G. H. 2017. The impact of global climate change on water quantity and quality: A system dynamics approach to the US–Mexican transborder region. *European Journal of Operational Research 256* 256**,** 567–581.

DWARAKISH, G. & GANASRI, B. 2015. Impact of land use change on hydrological systems: A review of current modeling approaches. *Cogent Geoscience,* 1**,** 1115691.

EARLE, A., GOLDIN, J., MACHIRIDZA, R., MALZBENDER, D., MANZUNGU, E. & MPHO, T. 2006. *Indigenous and institutional profile: Limpopo river basin*, International Water Management Institute.

EDOKPAYI, J. N., ODIYO, J. O., POPOOLA, E. O. & MSAGATI, T. A. 2018. Evaluation of microbiological and physicochemical parameters of alternative source of drinking water: a case study of nzhelele river, South Africa. *The open microbiology journal,* 12**,** 18.

EDOSSA, D. C., WOYESSA, Y. E. & WELDERUFAEL, W. A. 2014. Analysis of droughts in the central region of South Africa and their association with SST anomalies. *International Journal of Atmospheric Sciences,* 2014.

EL CHAMI, D. & EL MOUJABBER, M. 2016. Drought, climate change and sustainability of water in agriculture: A roadmap towards the NWRS2. *South African Journal of Science,* 112.

EL HARRAKI, W., OUAZAR, D., BOUZIANE, A., EL HARRAKI, I. & HASNAOUI, D. 2021. Streamflow Prediction Upstream of a Dam Using SWAT and Assessment of the Impact of Land Use Spatial Resolution on Model Performance. *Environmental Processes,* 8**,** 1165-1186.

ELBELTAGI, A., DENG, J., WANG, K., MALIK, A. & MAROUFPOOR, S. 2020. Modeling long-term dynamics of crop evapotranspiration using deep learning in a semi-arid environment. *Agricultural Water Management,* 241**,** 106334.

ELUM, Z. A., MODISE, D. M. & MARR, A. 2017. Farmer's perception of climate change and responsive strategies in three selected provinces of South Africa. *Climate Risk Management,* 16**,** 246-257.

EMANUEL, W. R. & JANETOS, A. C. 2013. Implications of Representative Concentration Pathway 4.5 Methane Emissions to Stabilize Radiative Forcing. *U.S. Department of Energy*.

ENDRIS, H. S., OMONDI, P., JAIN, S., LENNARD, C., HEWITSON, B., CHANG'A, L., AWANGE, J. L., DOSIO, A., KETIEM, P. & NIKULIN, G. 2013. Assessment of the performance of CORDEX regional climate models in simulating East African rainfall. *Journal of Climate,* 26**,** 8453-8475.

ENGELBRECHT, F. 2019. Green Book-Detailed Projectionsof future Climate Change over South Africa. *Technical report, Pretoria: CSIR*.

ENGELBRECHT, F., ADEGOKE, J., BOPAPE, M.-J., NAIDOO, M., GARLAND, R., THATCHER, M., MCGREGOR, J., KATZFEY, J., WERNER, M., ICHOKU, C. & GATEBE, C. 2015. Projections of rapidly rising surface temperatures over Africa under low mitigation. *Environ. Res. Lett,* 10.

ENGELBRECHT, F. A., LANDMAN, W. A., ENGELBRECHT, C. J., LANDMAN, S., BOPAPE, M. M., ROUX, B., MCGREGOR, J. L. & THATCHER, M. 2011. Multi-scale climate modelling over Southern Africa using a variable-resolution global model. *Water SA,* 37**,** 647-658.

ENGELBRECHT, F. A., MCGREGOR, J. L. & ENGELBRECHT, C. J. 2009. Dynamics of the Conformal-Cubic Atmospheric Model projected climate-change signal over southern Africa. *International Journal of Climatology: A Journal of the Royal Meteorological Society,* 29**,** 1013-1033.

ESTRELA, T., PÉREZ-MARTIN, M. A. & VARGAS, E. 2012. Impacts of climate change on water resources in Spain. *Hydrological Sciences Journal* 57**,** 1154-1167.

ESTRELA, T. & SANCHO, T. A. 2016. Drought management policies in Spain and the European Union: from traditional emergency actions to Drought Management Plans. *Water Policy,* 18**,** 153–176.

EZE, E., GIRMA, A., ZENEBE, A., KOUROUMA, J. M. & ZENEBE, G. 2020. Exploring the possibilities of remote yield estimation using crop water requirements for area yield index insurance in a data-scarce dryland. *Journal of Arid Environments,* 183**,** 104261.

FAO 2016. AQUASTAT Country Profile – South Africa. Food and Agriculture Organization of the United Nations (FAO). Rome, Italy.

FARAMARZI, M., ABBASPOUR, K. C., VAGHEFI, S. A., FARZANEH, M. R., ZEHNDER, A. J. B., SRINIVASAN, R. & YANG, H. 2013. Modeling impacts of climate change on freshwater availability in Africa. *Journal of Hydrology,* 480**,** 85-101.

FARIAS, V. D. D. S., COSTA, D. L. P., PINTO, J. V. D. N., SOUZA, P. J. D. O. P. D., SOUZA, E. B. D. & ORTEGA-FARIAS, S. 2020. Calibration of reference evapotranspiration models in Pará. *Acta Scientiarum. Agronomy,* 42.

FERREIRA, L. B., CUNHA, F. F., SILVA, G. H., CAMPOS, F. B., DIAS, S. H. & SANTOS, J. E. 2021. Generalizability of machine learning models and empirical equations for the estimation of reference evapotranspiration from temperature in a semiarid region. *Anais da Academia Brasileira de Ciências,* 93.

FOLEY, A. M. 2010. Uncertainty in regional climate modelling: A review. *Progress in Physical Geography,* 34**,** 647-670.

FOWLER, K. J., PEEL, M. C., WESTERN, A. W., ZHANG, L. & PETERSON, T. J. 2016. Simulating runoff under changing climatic conditions: Revisiting an apparent deficiency of conceptual rainfall-runoff models. *Water Resources Research,* 52**,** 1820-1846.

GAFUROV, Z., ELTAZAROV, S., AKRAMOV, B., YULDASHEV, T., DJUMABOEV, K. & ANARBEKOV, O. 2018. Modifying Hargreaves-Samani Equation for Estimating Reference Evapotranspiration in Dryland Regions of Amudarya River Basin. *Agricultural Sciences,* 09**,** 1354-1368.

GAN, T. Y., ITO, M., HÜLSMANN, S., QIN, X., LU, X. X., LIONG, S. Y., RUTSCHMAN, P., DISSE, M. & KOIVUSALO, H. 2016. Possible climate change/variability and human impacts, vulnerability of drought-prone regions, water resources and capacity building for Africa. *Hydrological Sciences Journal,* 61**,** 1209-1226.

GAO, F., FENG, G., OUYANG, Y., WANG, H., FISHER, D., ADELI, A. & JENKINS, J. 2017. Evaluation of reference evapotranspiration methods in arid, semiarid, and humid regions. *JAWRA Journal of the American Water Resources Association,* 53**,** 791-808.

GAO, X., SCHLOSSER, C. S., FANT, C. & STRZEPEK, K. 2018. The impact of climate change policy on the risk of water stress in southern and eastern Asia. *Environ. Res. Lett. ,* 13.

GARETH, J., DANIELA, W., TREVOR, H. & ROBERT, T. 2013. *An introduction to statistical learning: with applications in R*, Spinger.

GASSMAN, P., REYES, M., GREEN, C. & ARNOLD, J. 2007. Soil and Water Assessment Tool: Historical Development, Applications, and Future Research Directions, The. *Transactions of the ASABE,* 50.

GASSMAN, P. W., SADEGHI, A. M. & SRINIVASAN, R. 2014. Applications of the SWAT model special section: overview and insights. *Journal of Environmental Quality,* 43**,** 1-8.

GAYATHRI, K. D., GANASRI, B. P. & DWARAKISH, G. S. 2015. INTERNATIONAL CONFERENCE ON WATER RESOURCES, COASTAL AND OCEAN ENGINEERING (ICWRCOE 2015): A Review on Hydrological Models. *Aquatic Procedia* 4**,** 1001 – 1007.

GBETIBOUO, G. A., RINGLER, C. & HASSAN, R. 2010. Vulnerability of the South African farming sector to climate change and variability: An indicator approach Glwadys. *Natural Resources Forum,* 34.

GIORGI, F., JONES, C. & ASRAR, G. R. 2009. Addressing climate information needs at the regional level: the CORDEX framework. *World Meteorological Organization (WMO) Bulletin,* 58**,** 175.

GRIMALDI, S., SCHUMANN, G. P., SHOKRI, A., WALKER, J. & PAUWELS, V. 2019. Challenges, opportunities, and pitfalls for global coupled hydrologic-hydraulic modeling of floods. *Water Resources Research,* 55**,** 5277-5300.

GROSSMAN, M. R. 2018. Climate Change and the Individual. *The american journal of comparative law,* 66.

GUO, L., ZHOU, H., XIA, Z. & HUANG, F. 2016. Evolution, opportunity and challenges of transboundary water and energy problems in Central Asia. *Springer Plus,* 5.

GUUG, S. S., ABDUL-GANIYU, S. & KASEI, R. A. 2020. Application of SWAT hydrological model for assessing water availability at the Sherigu catchment of Ghana and Southern Burkina Faso. *HydroResearch,* 3**,** 124-133.

GYAMFI, C., NDAMBUKI, J. M. & SALIM, R. W. 2016. Hydrological Responses to Land Use/Cover Changes in the Olifants Basin, South Africa. *Water,* 588.

HAGEMANN, S., CHEN, C., CLARK, D. B., FOLWELL, S., GOSLING, S. N., HADDELAND, I., HANASAKI, N., HEINKE, J., LUDWIG, F., VOSS, F. & WILTSHIRE, A. J. 2013. Climate change impact on available water resources obtained using multiple global climate and hydrology models. *Earth Syst. Dynam,* 4**,** 129–144.

HANEL, M., RAKOVEC, O., MARKONIS, Y., MÁCA, P., SAMANIEGO, L., KYSELÝ, J. & KUMAR, R. 2018. Revisiting the recent European droughts from a long-term perspective. *scientific reports,* 8.

HARGREAVES, G. H. & SAMANI, Z. A. 1985. Reference crop evapotranspiration from temperature. *Applied engineering in agriculture,* 1**,** 96-99.

HERNÁNDEZ-DÍAZ, L., LAPRISE, R., SUSHAMA, L., MARTYNOV, A., WINGER, K. & DUGAS, B. 2013. Climate simulation over CORDEX Africa domain using the fifth-generation Canadian Regional Climate Model (CRCM5). *Climate Dynamics,* 40**,** 1415-1433.

HERRFAHRDT-PÄHLE, E. 2010. South African water governance between administrative and hydrological boundaries. *Climate and Development,* 2**,** 111-127.

HEYDARI, M. M., TAJAMOLI, A., GHOREISHI, S. H., DARBE-ESFAHANI, M. K. & GILASI, H. 2015. Evaluation and calibration of Blaney–Criddle equation for estimating reference evapotranspiration in semiarid and arid regions. *Environmental Earth Sciences,* 74**,** 4053-4063.

HEYI, E. A., DINKA, M. O. & MAMO, G. 2022. Assessing the impact of climate change on water resources of upper Awash River sub-basin, Ethiopia. *Journal of Water and Land Development***,** 232-244-232-244.

HIJIOKA, Y., LIN, E., PEREIRA, J. J., CORLETT, R. T., CUI, X., INSAROV, G. E., LASCO, R. D., LINDGREN, E. & SURJAN, A. 2014. Asia. In: Climate Change 2014: Impacts, Adaptation, and Vulnerability. Part B: Regional Aspects. Contribution of Working Group II to the Fifth Assessment Report of the Intergovernmental Panel on Climate Change. *Cambridge University Press, Cambridge, United Kingdom and New York, NY, USA*, 1327-1370.

HUANG, S., EISNER, S., MAGNUSSON, J. O., LUSSANA, C., YANG, X. & BELDRING, S. 2019. Improvements of the spatially distributed hydrological modelling using the HBV model at 1 km resolution for Norway. *Journal of hydrology,* 577, 123585.

IKEGWUOHA, D. C. & DINKA, M. O. 2020. Drought prediction in the Lepelle River basin, South Africa under general circulation model simulations. *Journal of Water and Land Development*.

IKHWALI, M. F. & PAWATTANA, C. 2022. Assessment of hydrologic variations under climate change scenarios using fully-distributed hydrological model in Huai Luang Watershed, Thailand. *Engineering and Applied Science Research,* 49, 470-484.

IKUDAYISI, A., CALITZ, A., NASR, M. & ABEJIDE, S. 2022. Modelling of Reference Evapotranspiration Parameters in South Africa Using Fuzzy Inference Systems. *Engineering Advances,* 2, 147-155.

IPCC 2013. Climate Change 2013: The Physical Science Basis. Contribution of Working Group I to the Fifth Assessment Report of the Intergovernmental

Panel on Climate Change [Stocker, T.F., D. Qin, G.-K. Plattner, M. Tignor, S.K. Allen, J. Boschung, A. Nauels, Y. Xia, V. Bex and P.M. Midgley (eds.)]. *Cambridge University Press, Cambridge, United Kingdom and New York, NY, USA.*, 1535

IPCC 2014. Climate Change 2014: Synthesis Report. Contribution of Working Groups I, II and III to the Fifth Assessment Report of the

Intergovernmental Panel on Climate Change [Core Writing Team, R.K. Pachauri and L.A. Meyer (eds.)]. IPCC, Geneva, Switzerland. 151.

IRMAK, S. & HAMAN, D. Z. 2003. Evapotranspiration: potential or reference. *IFAS Extension, ABE,* 343, 1-3.

ISHIZAKI, Y., SHIOGAMA, H., EMORI, S., YOKOHATA, T., NOZAWA, T., OGURA, T., ABE, M. & TAKAHASHI, K. 2012. Temperature scaling pattern dependence on representative concentration pathway emission scenarios. *Climatic Change* 112, 535–546.

ISLAM, Z. 2011. A review on physically based hydrologic modeling. *University of Alberta: Edmonton, AB, Canada*.

JAYAKRISHNAN, R., SRINIVASAN, R., SANTHI, C. & ARNOLD, J. 2005. Advances in the application of the SWAT model for water resources management. *Hydrological Processes: An International Journal,* 19, 749-762.

JUANA, J. S., MANGADI , K. T. & STRZEPEK, K. M. 2012. The socio-economic impacts of climate change on water resources in South Africa. *Water International,* 37, 265–278.

JURY, M. R. 2013. Climate trends in southern Africa. *S Afr J Sci,* 109.

KAEWMESR, P. & VARNAKOVIDA, P. 2018. Rainfall trend by linear regression analysis over Indochina Peninsula during 1981-2017 (37 Years). *GEOMATE Journal,* 15, 206-213.

KALOGNOMOU, E.-A., LENNARD, C., SHONGWE, M., PINTO, I., FAVRE, A., KENT, M., HEWITSON, B., DOSIO, A., NIKULIN, G. & PANITZ, H.-J. 2013. A diagnostic evaluation of precipitation in CORDEX models over southern Africa. *Journal of climate,* 26, 9477-9506.

KARIM, M. D. R., NOOR, M., DEPIO, S. A. & BHUVANA, N. 2017. POVERTY, CLIMATE CHANGE CHALLENGES AND COPING STRATEGIES OF SMALL SCALE FARM HOUSEHOLD. *Int. J. Agr. Ext. ,* 5, 87-96.

KAWASE, H., NAGASHIMA, T., SUDO, K. & NOZAWA, T. 2011. Future changes in tropospheric ozone under Representative Concentration Pathways (RCPs). *Geophysical Research Letters,* 38.

KHALIL, A., RITTIMA, A. & PHANKAMOLSIL, Y. 2018. The projected changes in water status of the Mae Klong Basin, Thailand, using WEAP model. *Paddy and Water Environment,* 16, 439-455.

KIM, J., WALISER, D. A., MATTMANN, C. A., GOODALE, C. E., HART, A. F., ZIMDARS, P. A., CRICHTON, D. J., JONES, C., NIKULIN, G., HEWITSON, B., JACK, C., LENNARD, C. & FAVRE, A. 2013.

Evaluation of the CORDEX-Africa multi-RCM hindcast: systematic model errors. *Climate Dynamics,* 42**,** 1189–1202.

KOBULIEV, M., LIU, T., KOBULIEV, Z., CHEN, X., GULAKHMADOV, A. & BAO, A. 2021. Effect of future climate change on the water footprint of major crops in southern Tajikistan. *Regional Sustainability,* 2**,** 60-72.

KOM, Z., NETHENGWE, N. S., MPANDELI, S. & CHIKOORE, H. 2020. Climate Change Grounded on Empirical Evidence as Compared with the Perceptions of Smallholder Farmers in Vhembe District, South Africa. *Journal of Asian and African Studies,* 55**,** 683-698.

KUMAR, N., TISCHBEIN, B., KUSCHE, J., LAUX, P., BEG, M. K. & BOGARDI, J. J. 2017. Impact of climate change on water resources of upper Kharun catchment in Chhattisgarh, India. *Journal of Hydrology: Regional Studies* 13**,** 189–207.

KUNDZEWICZ, Z. W., KRYSANOVA, V., BENESTAD, R. E., HOV, Ø., PINIEWSKI, M. & OTTO, I. M. 2018. Uncertainty in climate change impacts on water resources. *Environmental Science & Policy,* 79**,** 1-8.

KUSANGAYA, S., WARBURTON, M. L., ARCHER VAN GARDEREN, E. & JEWITT, G. P. W. 2014. Impacts of climate change on water resources in southern Africa: A review. *Physics and Chemistry of the Earth* 67–69**,** 47–54.

KWAK, S. 2023. Are Only p-Values Less Than 0.05 Significant? A p-Value Greater Than 0.05 Is Also Significant! *J Lipid Atheroscler,* 12**,** 89-95.

KWAKYE, S. O. & BÁRDOSSY, A. 2020. Hydrological modelling in data-scarce catchments: Black Volta basin in West Africa. *SN Applied Sciences,* 2**,** 1-19.

KWEKU, D. W., BISMARK, O., MAXWELL, A., DESMOND, K. A., DANSO, K. B., OTI-MENSAH, E. A., QUACHIE, A. T. & ADORMAA, B. B. 2017. Greenhouse effect: Greenhouse gases and their impact on global warming. *Journal of Scientific Research and Reports***,** 1-9.

LANDMAN, S., ENGELBRECHT, F. A., ENGELBRECHT, C. J., DYSON, L. L. & LANDMAN, W. A. 2012. A short-range weather prediction system for South Africa based on a multi-model approach. *Water SA* 38.

LANDMAN, W. A., ENGELBRECHT, F., HEWITSON, B., MALHERBE, J. & VAN DER MERWE, J. 2018. Towards bridging the gap between climate change projections and maize producers in South Africa. *Theor Appl Climatol* 132**,** 1153–1163.

LANKAO, P. R. 2010. Water in Mexico City: what will climate change bring to its history of water-related hazards and vulnerabilities? *International Institute for Environment and Development (IIED),* 22**,** 157–178.

LATIF, M. & JAVED, S. 1998. Application of Hargreaves Method for Estimation of Crop Water Requirements. *Rural and Environment Engineering,* 2**,** 43-54.

LEDA 2019. Specialist climate change assessment report for the proposed Musina-Makhado Special Economic Zone (SOC) Limited Limpopo Economic Development Agency.

LEIPPRAND, A., DWORAK, T., BENZLE, M., BERGLUND, M., KADNER, S., HATTERMANN, F., POST, J. & KRYSANOVA, V. 2008. Impacts of climate change on water resources – adaption strategies for Europe. *Environmental research of the federal ministry of the environment, nature conservation and nuclear safety. Research Report 205 21 200*.

LENHART, T. E., ECKHARDT, K., FOHRER, N. & FREDE, H.-G. 2002. Comparison of two different approaches of sensitivity analysis. *Physics and Chemistry of The Earth,* 27**,** 645-654.

LIN, P., HE, Z., DU, J., CHEN, L., ZHU, X. & LI, J. 2018. Impacts of climate change on reference evapotranspiration in the Qilian Mountains of China: Historical trends and projected changes. *International Journal of Climatology,* 38**,** 2980-2993.

LINDSTRÖM, G., JOHANSSON, B., PERSSON, M., GARDELIN, M. & BERGSTRÖM, S. 1997. Development and test of the distributed HBV-96 hydrological model. *Journal of hydrology,* 201**,** 272-288.

LIU, Q., WU, Z., CUI, N., ZHANG, W., WANG, Y., HU, X., GONG, D. & ZHENG, S. 2022. Genetic Algorithm-Optimized Extreme Learning Machine Model for Estimating Daily Reference Evapotranspiration in Southwest China. *Atmosphere,* 13**,** 971.

LUHUNGA, P. M., BOTAI, J. O. & KAHIMBA, F. 2016. Evaluation of the performance of CORDEX regional climate models in simulating present climate conditions of Tanzania.

LUMSDEN, T., G. 2009. Evaluation of potential changes in hydrologically relevant statistics of rainfall in Southern Africa under conditions of climate change. *Water Sa,* 35.

MABHAUDHI, T., CHIBARABADA, T. P., CHIMONYO, V. G. P. & THEMBINKOSI MODI, A. T. 2018. Modelling climate change impact: A case of bambara groundnut (Vignasubterranea). *Physics and Chemistry of the Earth*.

MACALISTER, C. & SUBRAMANYAM, N. 2018. Climate change and adaptive water management: innovative solutions from the global South. *Water International,* 43**,** 133–144

MACHAKAIRE, A. T. B., STEYN, J. M. & FRANKE, A. C. 2021. Assessing evapotranspiration and crop coefficients of potato in a semi-arid climate using Eddy Covariance techniques. *Agricultural Water Management,* 255**,** 107029.

MADHUSOODHANAN, C. G., SREEJA, K. G. & ELDHO, T. I. 2016. Climate change impact assessments on the water resources of India under extensive human interventions. *Ambio* 45**,** 725–741.

MAGAÑA, V., ZERMEÑO, D. & NERI, C. 2012. Climate change scenarios and potential impacts on water availability in northern Mexico. *Clim Res,* 51**,** 171–184.

MAGWEDE, K., VAN WYK, B.-E. & VAN WYK, A. 2019. An inventory of Vhavenḓa useful plants. *South African Journal of Botany,* 122**,** 57-89.

MAKUNGO, R., ODIYO, J., NDIRITU, J. & MWAKA, B. 2010. Rainfall–runoff modelling approach for ungauged catchments: A case study of Nzhelele River sub-quaternary catchment. *Physics and Chemistry of the Earth, Parts a/b/c,* 35**,** 596-607.

MALAMATARIS, D., KOLOKYTHA, E. & LOUKAS, A. 2020. Integrated hydrological modelling of surface water and groundwater under climate change: the case of the Mygdonia basin in Greece. *Journal of Water and Climate Change,* 11**,** 1429-1454.

MALHERBE, J., ENGELBRECHT , F. A. & LANDMAN, W. A. 2013. Projected changes in tropical cyclone climatology and landfall in the Southwest Indian Ocean region under enhanced anthropogenic forcing. *Climate Dynamics,* 40**,** 2867–2886.

MALSY, M., AUS DER BEEK, T., EISNER, S. & FLORKE, M. 2012. Climate change impacts on Central Asian water resources. *Adv. Geosci.,* 32**,** 77–83.

MALULEKE, W. & MOKWENA, R. J. 2017. The effect of climate change on rural livestock farming: case stufy of Giyani policing area, republic of South Africa. *S. Afr. J. Agric. Ext,* 45**,** 26 – 40

MANGO, L. M., MELESSE, A. M., MCCLAIN, M. E., GANN, D. & SETEGN, S. G. 2011. Land use and climate change impacts on the hydrology of the upper Mara River Basin, Kenya: results of a modeling study to support better resource management. *Hydrol. Earth Syst. Sci. ,* 15**,** 2245–2258

MAPHELA, B. & CLOETE, F. 2019. Johannesburg's implementation of the National Water Act, 1998 in Soweto, South Africa. *Development Southern Africa***,** 1-18.

MAPONYA, P. 2012. Climate Change and Agricultural Production in Limpopo Province: Impact and Adaptation Options [doctral dissertation]. University of South Africa. 240.

MAPONYA, P. & MPANDELI, S. 2012a. Climate Change and Agricultural Production in South Africa: Impacts and Adaptation options. *Journal of Agricultural Science,* 4.

MAPONYA, P. & MPANDELI, S. 2012b. Impact of drought on food scarcity in Limpopo province, South Africa. *African Journal of Agricultural Research,* 7**,** 5270-5277.

MAPONYA, P. & MPANDELI, S. 2015. Climate Change Status in the Mutale Local Municipality : A Case Study of the Smallholder Farmers in Vhembe District, Limpopo Province. *Journal of human ecology,* 52**,** 1-8

MAPONYA, P., MPANDELI, S. & ODUNIYI, S. 2013. Climate Change Awareness in Mpumalanga Province, South Africa. *Journal of Agricultural Science,* 5.

MAPONYA, P. I. & MPANDELI, S. N. 2016. DROUGHT AND FOOD SCARCITY IN LIMPOPO PROVINCE, SOUTH AFRICA. *2nd World Irrigation Forum, Chiang Mai, Thailand*.

MARTINEZ, S., KRALISCH, S., ESCOLERO, O. & PEREVOCHTCHIKOVA, M. 2015. Vulnerability of Mexico City's water supply sources in the context of climate change. *Journal of Water and Climate Change* 6**,** 518–533.

MASIA, S., TRABUCCO, A., SPANO, D., SNYDER, R. L., SUŠNIK, J. & MARRAS, S. 2021. A modelling platform for climate change impact on local and regional crop water requirements. *Agricultural Water Management,* 255**,** 107005.

MASUI, T., MATSUMOTO, K., HIJIOKA, Y., KINOSHITA, T., NOZAWA, T., ISHIWATARI, S., KATO, E., SHUKLA, P. R., YAMAGATA, Y. & KAINUMA, M. 2011. An emission pathway for stabilization at 6 Wm−2 radiative forcing. *Climatic Change* 109**,** 59–76.

MATCHAYA, G., NHAMO, L., NHLENGETHWA, S. & NHEMACHENA, C. 2019. An Overview of Water Markets in Southern Africa: An Option for Water Management in Times of Scarcity. *Water,* 11**,** 1006.

MATJI, O. 2015. The impact of climate change on agricultural crop distribution in South Africa [Masters dissertation]. University of Witwatersrand, South Africa.

MBOKODO, I., BOPAPE, M.-J., CHIKOORE, H., ENGELBRECHT, F. & NETHENGWE, N. 2020. Article Heatwaves in the FutureWarmer Climate of SouthAfrica. *Atmosphere* 11.

MDODA, L. 2020. Climate Change Effects on Agricultural Productivity in the Smallholder Farming Systems of the Eastern Cape Province, South Africa. *Journal of human ecology,* 70.

MEBRAHTU, Y. 2021. Estimation of Crop Water Requirement Using CROPWAT Model for Onion and Tomato, A Case Study of Raya Azebo District, Ethiopia. *Journal of Biology, Agriculture and Healthcare,* 11.

MEBRAHTU, Y., MEHARI, H., NURGA, Y. & TAMIRU, H. 2021. Estimation of Crop Water Requirement using CROPWAT Model for Maize, A Case Study of Raya Azebo District, Ethiopia. *Journal of Resources Development and Managemen,* 74.

MENDELSOHN, R. 2014. The Impact of Climate Change on Agriculture in Asia *Journal of Integrative Agriculture,* 13**,** 660-665.

MENGISTU, A. G., VAN RENSBURG, L. D. & WOYESSA, Y. E. 2019. Techniques for calibration and validation of SWAT model in data scarce arid and semi-arid catchments in South Africa. *Journal of Hydrology: Regional Studies,* 25**,** 100621.

MERZ, R., PARAJKA, J. & BLÖSCHL, G. 2011. Time stability of catchment model parameters: Implications for climate impact analyses. *Water resources research,* 47.

METEOBLUE 2014. climate Nzelele Limpopo, South Africa. *[online] available at: https://www.meteoblue.com/en/weather/historyclimate/climatemodelled/nzhelele_south-africa_968616*.

MIMI, Z., A. & JAMOUS, S. A. 2010. Climate change and agricultural water demand: Impacts and adaptations. *African Journal of Environmental Science and Technology* 4**,** 183-191.

MINVILLE, M., BRISSETTE, F. & LECONTE, R. 2008. Uncertainty of the impact of climate change on the hydrology of a nordic watershed. *Journal of Hydrology,* 358 70– 83.

MIRDASHTVAN, M., NAJAFINEJAD, A., MALEKIAN, A. & SA'DODDIN, A. 2018. Downscaling the contribution to uncertainty in climate-change assessments: representative concentration pathway (RCP) scenarios for the South Alborz Range, Iran. *Meteorol. Appl. ,* 25**,** 414–422

MIZYED, N. 2009. Impacts of Climate Change on Water Resources Availability and Agricultural Water Demand in theWest Bank. *Water Resour Manage* 23**,** 2015–2029.

MOELETSI, M. E., WALKER, S. & HAMANDAWANA, H. 2013. Comparison of the Hargreaves and Samani equation and the Thornthwaite equation for estimating dekadal evapotranspiration in the Free State Province, South Africa. *Physics and Chemistry of the Earth, Parts A/B/C,* 66**,** 4-15.

MOLOBELA, I. P. & SINHA, P. 2011. Management of water resources in South Africa: A review. *African Journal of Environmental Science and Technology* 5**,** 993-1002.

MONTECELOS-ZAMORA, Y., CAVAZOS, T., KRETZSCHMAR, T., VIVONI, E. R., CORZO, G. & MOLINA-NAVARRO, E. 2018. Hydrological modeling of climate change impacts in a tropical river basin: A case study of the Cauto river, Cuba. *Water,* 10**,** 1135.

MORIASI, D. N., ARNOLD, J. G., LIEW, M., BINGNER, R. L., HARMEL, R. D. & VEITH, T. L. 2007. Model Evaluation Guidelines for Systematic Quantification of Accuracy in Watershed Simulations. *Transactions of the ASABE,* 50**,** 885-900.

MOUSSA, R. & BOCQUILLON, C. 2000. Approximation zones of the Saint-Venant equations f flood routing with overbank flow. *Hydrology and Earth System Sciences,* 4**,** 251-260.

MPANDELI, N. S. & MAPONYA, P. I. 2013. Coping with climate variability in Limpopo Province, South Africa. *Peak Journal of Agricultural Sciences,* 1**,** 54-64.

MPANDELI, S. 2014a. Evaluation of Crop Production Practices by Farmers in Tshakhuma, Tshiombo and Rabali Areas in Limpopo Province of South Africa. *Journal of Agricultural Science,* 6.

MPANDELI, S. 2014b. Managing Climate Risks Using Seasonal Forecast Information in Vhembe District In Limpopo Province, South Africa. *journal of Sustainable Development,* 7.

MPANDELI, S., NAIDOO, D., MABHAUDHI, T., NHEMACHENA, C., NHAMO, L., LIPHADZI, S., HLAHLA, S. & MODI, A. T. 2018. Climate change adaptation through the water-energy-food nexus in southern Africa. *International journal of environmental research and public health,* 15**,** 2306.

MQADI, L. 2007. *Production function analysis of the sensitivity of maize production to climate change in South Africa (Doctoral dissertation, University of Pretoria).*

MUKHELI, A. 2018. Investigation of factors influencing borehole yields in the Nzhelele-Makhado Area in Limpopo Province, South Africa [Masters dissertation]. University of Venda, South Africa. 139.

MUSAKWA, W., WANG, S., WEI, F., MALAPANE, O. L., THOMAS, M. M., MAVENGAHAMA, S., ZENG, H., WU, B., ZHAO, W. & NYATHI, N. A. 2020. Survey of community livelihoods and landscape change along the Nzhelele and Levuvhu river catchments in Limpopo Province, South Africa. *Land,* 9**,** 91.

MUSETHA, M. B. 2016. The Impact of Climate Change on Agricultural Crop Production In The Vhembe Disrict Municipality, Limpopo Province South Africa [Masters dissertation]. University of South Africa.

MUTAMBA, J. 2019. Water security: Is South Africa optimally pursuing its options. *Trans Ecol Environ,* 239**,** 47-54.

MZEZEWA, J., MISI, T. & VAN RENSBURG, L. D. 2010. Characterisation of rainfall at a semi-arid ecotope in the Limpopo Province (South Africa) and its implications for sustainable crop production. *Water SA* 36.

NAIK, P. K. 2016. Water crisis in Africa: myth or reality? . *International Journal of Water Resources Development*.

NAKICENOVIC, N., ALCAMO, J., DAVIS, G., DE VRIES, B., FENHANN, J., GAFFIN, S., GREGORY, K., GRUBLER, A., JUNG, T. Y. & KRAM, T. 2000. A special report of Working Group III of the Intergovernmental Panel on Climate Change. *Emissions Scenarios***,** 570.

NCOYINI-MANCIYA, Z., SAVAGE, M. J., STRYDOM, S. & CLULOW, A. D. 2022. Long-term reference evapotranspiration trend and causative factors analysis in the sugarbelt area of the midlands of KwaZulu-Natal, South Africa. *South African Journal of Plant and Soil,* 39**,** 204-212.

NCUBE, M. & TAIGBENU, A. E. 2014. Application of the SWAT model to assess the impact of land cover and land use on the hydrologic response in the Olifants Catchment.

NDHLEVE, S., NAKIN, M. & LONGO-MBENZA, B. 2017. Impacts of supplemental irrigation as a climate change adaptation strategy for maize production: a case of the Eastern Cape Province of South Africa. *Water SA,* 43**,** 222-228.

NENWIINI, S. & KABANDA, T. A. 2013. Trends and variability assessment of rainfall in Vhembe South Africa. *Journal of Human Ecology,* 42**,** 171-176.

NGAIRA, J. K. W. 2007. Impact of climate change on agriculture in Africa by 2030. *Scientific Research and Essays,* 2**,** 238-243.

NGOC, T. T. H. & KHANH, P. T. 2021. Water Demand Estimation for Rice in An Giang Province by Hargreaves Evapotranspiration Model. *Turkish Journal of Computer and Mathematics Education,* 12**,** 3034-3039.

NHAMO, L., MATCHAYA, G., MABHAUDHI, T., NHLENGETHWA, S., NHEMACHENA, S. & MPANDELI, S. 2019. Cereal Production Trends under Climate Change: Impacts and Adaptation Strategies in Southern Africa. *Agriculture,* 9.

NIKULIN, G., JONES, C., GIORGI, F., ASRAR, G., BÜCHNER, M., CEREZO-MOTA, R., CHRISTENSEN, O. B., DÉQUÉ, M., FERNANDEZ, J. & HÄNSLER, A. 2012. Precipitation climatology in an ensemble of CORDEX-Africa regional climate simulations. *Journal of Climate,* 25**,** 6057-6078.

NURSUGI, N. D. K. & WINDARI, E. H. 2014. HYDROLOGICAL MODELLING USING SWAT MODEL CASE STUDY CIMANUK WATERSHED.

OBIERO, J. P. O., HASSAN, M. A. & GUMBE, L. O. M. 2011. Modelling of Streamflow of a Catchment in Kenya. *Journal of Water Resource and Protection,* 3**,** 667-677.

ODIYO, J., MAKUNGO, R., NKUNA, T. R. & CHIKOORE, H. 2020. Hydrological modeling of climate change impacts for development of adaptation strategies: The case of Luvuvhu river catchement, Limpopo, South Africa. *Final Report to the Water Research Commission*.

ODIYO, J. O. & MAKUNGO, R. 2018. Chemical and microbial quality of groundwater in Siloam village, implications to human health and sources of contamination. *International journal of environmental research and public health,* 15**,** 317.

OGUNDEJI, A. A. & JORDAAN, H. 2017. A simulation study on the effect of climate change on crop water use and chill unit accumulation. *South African Journal of Science,* 113**,** 1-7.

OLABANJI, F. M., NDARANA, T. & DAVIS, N. 2020. Impact of Climate Change on Crop Production and Potential Adaptive Measures in the Olifants Catchment, South Africa. *Climate,* 9**,** 6.

OLABANJI, M. F., NDARANA, T. & DAVIS, N. 2021. Impact of Climate Change on Crop Production and Potential Adaptive Measures in the Olifants Catchment, South Africa. *Climate,* 9**,** 6.

OMOTAYO, A. O. 2018. Climate Change and Food Insecurity Dynamics in the Rural Limpopo Province of South Africa. *Journal of Economics and Behavioral Studies* 10**,** 22-32.

ONI, S. A., NESAMVUNI, A. E., ODHIAMBO, J. J. O. & DAGADA, M. C. 2012. The study of agricultural industry in the Limpopo Province (Executive Summary).

OTI, J. O., KABO-BAH, A. T. & OFOSU, E. 2020. Hydrologic response to climate change in the Densu River Basin in Ghana. *Heliyon,* 6**,** e04722.

OTTO, F., WOLSKI, P., LEHNER, F., TEBALDI, C., VAN OLDENBORGH, G. J., HOGESTEEGER, S., SINGH, R., HOLDEN, P., FUCKAR, N., ODOULAMI, R. & NEW, M. 2018. Anthropogenic influence on the drivers of the Western Cape drought 2015–2017. *Environmental Research Letters,* 13**,** 124010.

PAPADIMOS, D., DEMERTZI, K. & PAPAMICHAIL, D. 2022. Assessing Lake Response to Extreme Climate Change Using the Coupled MIKE SHE/MIKE 11 Model: Case Study of Lake Zazari in Greece. *Water,* 14**,** 921.

PAREKH, F., PRAMODCH, K. & PRAJAPATI, R. 2013. CLIMATE CHANGE IMPACTS ON CROP WATER REQUIREMENT FOR SUKHI RESERVOIR PROJECT. *International Journal of Innovative Research in Science, Engineering and Technology,* 2**,** 4685-4692.

PARK, J.-Y., PARK, M.-J., AHN, S.-R., PARK, G.-A., YI, J.-E., KIM, G.-S., SRINIVASAN, R. & KIM, S.-J. 2011. Assessment of future climate change impacts on water quantity and quality for a mountainous dam watershed using SWAT. *Transactions of the ASABE,* 54**,** 1725-1737.

PARRA, V., FUENTES-AGUILERA, P. & MUÑOZ, E. 2018. Identifying advantages and drawbacks of two hydrological models based on a sensitivity analysis: a study in two Chilean watersheds. *Hydrological Sciences Journal,* 63**,** 1831-1843.

PATHAK, H., PRAMANIK, P., KHANNA, M. & KUMAR, A. 2014. Climate change and water availability in Indian agriculture: Impacts and adaptation. *Indian Journal of Agricultural Sciences,* 84.

PAUL, P. K., ZHANG, Y., MA, N., MISHRA, A., PANIGRAHY, N. & SINGH, R. 2021. Selecting hydrological models for developing countries: Perspective of global, continental, and country scale models over catchment scale models. *Journal of Hydrology,* 600**,** 126561.

PAUWELS, V. R., DE LANNOY, G. J., HENDRICKS FRANSSEN, H.-J. & VEREECKEN, H. 2013. Simultaneous estimation of model state variables and observation and forecast biases using a two-stage hybrid Kalman filter. *Hydrology and earth system sciences,* 17**,** 3499-3521.

PECHLIVANIDIS, I., JACKSON, B., MCINTYRE, N. & WHEATER, H. 2011. Catchment scale hydrological modelling: a review of model types, calibration approaches and uncertainty analysis methods in the context of recent developments in technology and applications. *Global NEST journal,* 13**,** 193-214.

PEREIRA, L. 2017. Climate change impacts on agriculture across Africa. *Oxford Research Encyclopedia of Environmental Science*.

PEREIRA, L. S. & ALVES, I. 2005. CROP WATER REQUIR EMENTS. In D. Hillel (Ed.). *Encyclopedia of Soils in the Environment. Oxford: Elsevier.***,** 322-334.

PHOPHI, M. M., MAFONGOYA, P. & LOTTERING, S. 2020. Perceptions of Climate Change and Drivers of Insect Pest Outbreaks in Vegetable Crops in Limpopo Province of South Africa. *Climate* 8.

POONIA, R. C. & BHATNAGAR, V. 2022. Design of decision support system to identify crop water need. *Journal of Ambient Intelligence and Humanized Computing*.

POONIA, V., DAS, J. & GOYAL, M. K. 2021. Impact of climate change on crop water and irrigation requirements over eastern Himalayan region. *Stochastic Environmental Research and Risk Assessment,* 35**,** 1175-1188.

PRIESTLEY, C. H. B. & TAYLOR, R. J. 1972. On the assessment of surface heat flux and evapora- tion using large-scale parameters. . *Mon. Weather Rev,* 100**,** 81–92.

PRUDHOMME, C., GIUNTOLI, I., ROBINSON, E. L., CLARK, D. B., ARNELL, N. W., DANKERS, R., FEKETE, B. M., FRANSSEN, W., GERTEN, D., GOSLING, S. N., HAGEMANN, S., HANNAH, D. M., KIM, H., MASAKI, Y., SATOH, Y., STACKE, T., WADA, Y. & WISSER, D. 2013. Hydrological droughts in the 21st century, hotspots and uncertainties from a global multimodel ensemble experiment. *Proceedings of the National Academy of Sciences*.

QUERNER, E. P. & ZANEN, M. V. 2013. Modelling water quantity and quality using SWAT: a case study in the Limpopo River basin, South Africa. Wageningen.

RAHIMIKHOOB, A. & HOSSEINZADEH, M. 2014. Assessment of Blaney-Criddle Equation for Calculating Reference Evapotranspiration with NOAA/AVHRR Data. *Water Resources Management,* 28**,** 3365-3375.

RAHMAN, M. I. 2013. Climate change: A theoretical review. *Interdisciplinary Description of Complex Systems* 11**,** 1-13.

RAKSMEY ANG & OEURNG, C. 2018. Simulating streamflow in an ungauged catchment of Tonlesap LakeBasin in Cambodia using Soil and Water Assessment Tool (SWAT) model *Water Science 32 (2018)* 32**,** 89–101.

RAMARUMO, L. J. 2017. *Ethnobotanical survey of problem weeds, alien invasive plant species and their roles in Nzhelele, Makhado Local Municipality, Limpopo Province, South Africa (M.Sc. Thesis, University of Venda).*

RAMARUMO, L. J., MAROYI, A. & TSHISIKHAWE, M. P. 2019. Euphorbia pulvinata Marloth: A useful succulent plant species in Vhembe Biosphere Reserve, Limpopo Province, South Africa. *Indian Journal of Traditional Knowledge* 18**,** 122-126.

RAMTEKE, G., SINGH, R. & CHATTERJEE, C. 2020. Assessing Impacts of Conservation Measures on Watershed Hydrology Using MIKE SHE Model in the Face of Climate Change. *Water Resources Management,* 34**,** 4233-4252.

RATNA, R. C., YELLA, R. K., SATYANARAYANA, T. V. & YOGITHA, P. 2016. Estimation of Crop Water Requirement Using CROPWAT Software in Appapuram Channel Command under Krishna Western Delta. *International Journal of Agriculture Sciences,* 8**,** 1644-1649.

REBELO, A. J., HOLDEN, P. B., HALLOWES, J., EADY, B., CULLIS, J. D., ESLER, K. J. & NEW, M. G. 2022. The hydrological impacts of restoration: A modelling study of alien tree clearing in four mountain catchments in South Africa. *Journal of Hydrology,* 610**,** 127771.

REFSGAARD, J. & SØRENSEN, H. 1997. Water management of the Gabcikovo Scheme for balancing the interest of hydropower and environment. *Operational Water Management***,** 365-372.

REUNGSANG, P., KANWAR, R. S. & SRISUK, K. 2010. Application of SWAT Model in Simulating Stream Flow for the Chi River Subbasin II in Northeast Thailand. *Trends Research in Science and Technology,* 2**,** 23-28.

RIAHI, K., RAO, S., KREY, V., CHO, C., CHIRKOV, V., FISCHER, G., KINDERMANN, G., NAKICENOVIC, N. & RAFAJ, P. 2011. RCP 8.5—A scenario of comparatively high greenhouse gas emissions. *Climatic Change,* 109**,** 33.

RODNY, M., NOLZ, R., NOVÁK, V., HLAVACIKOVA, H., LOISKANDL, W. & HIMMELBAUER, M. 2016. Modified method of aerodynamic resistance calculation and its application to potential evapotranspiration estimation. *International Agrophysics,* 30.

ROJA, M., DEEPTHI, C. & DEVENDER REDDY, M. 2020. Estimation of Crop Water Requirement of Maize Crop Using FAO CROPWAT 8.0 Model. *Ind. J. Pure App. Biosci,* 8**,** 222-228.

ROTICH, S. & MULUNGU, D. 2017. Adaptation to climate change impacts on crop water requirements in Kikafu Catchment Tanzania. *Journal of Water and Climate Change,* 8**,** jwc2017058.

RUMMUKAINEN, M. 2010. State-of-the-art with regional climate models. *Climate Change,* 1.

SAFWAN, M., KARAM, A., ISTVÁN, T. & HARSÁNYI, E. 2019. Contemporary changes of greenhouse gases emission from the agricultural sector in the EU-27. *Geology, Ecology, and Landscapes*.

SANDU, M.-A. & VIRSTA, A. 2015. Applicability of MIKE SHE to simulate hydrology in Argesel River catchment. *Agriculture and Agricultural Science Procedia,* 6**,** 517-524.

SANTHI, C., SRINIVASAN, R., ARNOLD, J. G. & WILLIAMS, J. R. 2006. A modeling approach to evaluate the impacts of water quality management plans implemented in a watershed in Texas. *Environmental Modelling & Software* 21**,** 1141-1157.

SARUCHERA, D., ANSEEUW, W., FAROLFI, S. & OLWOCH, J. 2010. Silent dialogue? Combining land and water reforms in small-scale irrigation schemes in South Africa. *11th WaterNET/WARFSA/GWP-SA Symposium 2010, Victoria Falls***,** 27-29.

SAYARI, N., BANNAYAN, M., FARID, A., ALIZADEH, A. & KERMANI, M. R. H. 2011. Crop Water Consumption and Crop Yield Prediction under Climate Change Conditions at Northeast of Iran. *International Conference on Environmental and Computer Science,* 19.

SCHENK, N. J. & LENSINK, S. M. 2007. Communicating uncertainty in the IPCC's greenhouse gas emissions scenarios. *Climatic Change,* 82**,** 293-308.

SCHULZE, R. & WALKER, N. 2006. Maize yield estimation. *Water Research Commission, Pretoria, RSA, WRC Report,* 1489**,** 06.

SCHULZE, R. E. 2016. On Observations, Climate Challenges, the South African Agriculture Sector and Considerations for an Adaptation Handbook. *Handbook for Farmers, Officials and Other Stakeholders on Adaptation to Climate Change in the Agriculture Sector within South Africa. Section A: Agriculture and Climate Change in South Africa: Setting the Scene, Chapter A1*.

SEENU, N., CHETTY, R. K., SRINIVAS, T., KRISHNA, K. A. & SELOKAR, A. 2019. Reference Evapotranspiration Assessment Techniques for Estimating Crop Water Requirement. *International Journal of Recent Technology and Engineering (IJRTE,* 8.

SEJIAN, V., GAUGHAN, J., BAUMGARD, L. & PRASAD, C. 2015. Climate Change Impact on Livestock: Adaptation and Mitigation. *Springer India,* 37.

SELLAMI, H., BENABDALLAH, S., LA JEUNESSE, I. & VANCLOOSTER, M. 2016. Climate models and hydrological parameter uncertainties in climate change impacts on monthly runoff and daily flow duration curve of a Mediterranean catchment. *Hydrological sciences journal,* 61**,** 1415-1429.

SERDECZNY, O., ADAMS, S., BAARSCH, F., COUMOU, D., ROBINSON, A., HARE, W., SCHAEFFER, M. & PERRETTE, M. 2015. Climate change impacts in Sub-Saharan Africa: from physical changes to their social repercussions *Regional Environmental Change,* 15.

SHAH, I., T.M.V., S. & PAREKH, F. P. 2016. Estimation of crop water requirement and irrigation schedulling usinf CROPWAT. *ISH-Hydro 2016 International*.

SHAH, P. V., MISTRY, R. N., AMIN, J. B., PARMAR, A. M. & SHAIKH, M. R. A. 2015. IRRIGATION SCHEDULING USING CROPWAT. *International Journal of Advance Research in Engineering, Science & Technology(IJAREST),* 2.

SHANKA, A. S. & ARBA, Y. 2021. Evaluation of Maize Crop Water Requirement Under Changing Climate over Konso, Southern Ethiopia. *Environmental Analysis & Ecology Studies,* 8.

SHARMA, K. D. & GOSAIN, A. K. 2010. Application of Climate Information and Predictions in Water Sector: Capabilities. *Procedia Environmental Sciences,* 1**,** 120–129.

SHEW, A. M., TACK, J. B., NALLEY, L. L. & CHAMINUKA, P. 2020. Yield reduction under climate warming varies among wheat cultivars in South Africa. *Nature Communications,* 11**,** 4408.

SHIKWAMBANA, S., MALAZA, N. & SHALE, K. 2021. Impacts of Rainfall and Temperature Changes on Smallholder Agriculture in the Limpopo Province, South Africa. *Water,* 13**,** 2872.

SHRESTHA, J. 2019. P-Value: A true test of significance in agricultural research. *Available at SSRN 4592804*.

SHU, Y., LI, H. & LEI, Y. 2018. Modelling groundwater flow with MIKE SHE using conventional climate data and satellite data as model forcing in Haihe Plain, China. *Water,* 10**,** 1295.

SIPAYUNG, S. B., NURLATIFAH, A. & SISWANTO, B. 2018. Simulation and prediction the impact of climate change into water resources in Bengawan Solo watershed based on CCAM (Conformal Cubic Atmospheric Model) data. *Physics: Conf. Series* 1022.

SIRODOEV, I., COROBOV, R., SIRODOEV, G. & TROMBITSKY, I. 2022. Modelling Runoff within a Small River Basin under the Changing Climate: A Case Study of Using SWAT in the Bălțata River Basin (The Republic of Moldova). *Land,* 11**,** 167.

ŚLIWIŃSKI, D., KONIECZNA, A. & ROMAN, K. 2022. Geostatistical Resampling of LiDAR-Derived DEM in Wide Resolution Range for Modelling in SWAT: A Case Study of Zgłowiączka River (Poland). *Remote Sensing,* 14**,** 1281.

SOLEIMANIAN, E., AFSHAR, A. & MOLAJOU, A. 2022. A review on water simulation models for the WEF Nexus: development perspective. *Environmental Science and Pollution Research***,** 1-17.

SPINONI, J., BARBOSA, P., BUCCHIGNANI, E., CASSANO, J., CAVAZOS, T., CHRISTENSEN, J., CHRISTENSEN, O., COPPOLA, E., EVANS, J. & GEYER, B. 2020. Future global meteorological drought hot spots: A study based on CORDEX Data. *Journal of Climate,* 33**,** 3635-3661.

STEIDLE NETO, A. J., BORGES JÚNIOR, J. C., ANDRADE, C. L., LOPES, D. C. & NASCIMENTO, P. T. 2015. Reference evapotranspiration estimates based on minimum meteorological variable requirements of historical weather data. *Chilean journal of agricultural research,* 75**,** 366-374.

STEVENS, J., VAN HEERDEN, P., REID, P., LIEBENBERG, A., HAGEDOORN, E. & DE KOCK, G. 2012. Training material for extension advisors in irrigation water management.Volume 2: Technical Learner Guide Part 8: Irrigated crop and fodder production.

STROEBEL, A. 2004. *Socio-economic complexities of smallholder resource-poor ruminant livestock production systems in Sub-Saharan Africa (PhD. Thesis, University of the Free State).* University of the Free State.

SUKUMARAN, H. & SAHOO, S. 2020. A Methodological Framework for Identification of Baseline Scenario and Assessing the Impact of DEM Scenarios on SWAT Model Outputs. *Water Resources Management,* 34**,** 1-20.

TABARI, H. & TALAEE, P. H. 2011. Local calibration of the Hargreaves and Priestley-Taylor equations for estimating reference evapotranspiration in arid and cold climates of Iran based on the Penman-Monteith model. *Journal of Hydrologic Engineering,* 16**,** 837.

TAN, M. L., GASSMAN, P. W., SRINIVASAN, R., ARNOLD, J. G. & YANG, X. 2019. A review of swat studies in southeast asia: applications, challenges and future directions. *Water,* 11**,** 914.
TEKLAY, A., DILE, Y. T., ASFAW, D. H., BAYABIL, H. K. & SISAY, K. 2021. Impacts of Climate and Land Use Change on Hydrological Response in Gumara Watershed, Ethiopia. *Ecohydrology & Hydrobiology,* 21**,** 315-332.
TEKLU, S., SOLIMAN, A. H. & EL-ZAWAHRY, A. 2020. Testing the WEAP Hydrologic Model for Awash Basin, Ethiopia "Soil Moisture Module with Watershed Demand Approach". *Civil and Environmental Research,* 12.
TENA, T. M., MWAANGA, P. & NGUVULU, A. 2019. Hydrological modelling and water resources assessment of Chongwe River Catchment using WEAP model. *Water,* 11**,** 839.
THERON, S. N., ARCHER, E., MIDGLEY, S. J. E. & WALKER, S. 2021. Agricultural perspectives on the 2015-2018 Western Cape drought, South Africa: Characteristics and spatial variability in the core wheat growing regions. *Agricultural and Forest Meteorology,* 304-305**,** 108405.
THIESE, M. S., RONNA, B. & OTT, U. 2016. P value interpretations and considerations. *J Thorac Dis,* 8**,** E928-e931.
THOMSON, A. M., CALVIN, K. V., SMITH, S. J., KYLE, G. P., VOLKE, A., PATEL, P., DELGADO-ARIAS, S., BOND-LAMBERTY, B., WISE, M. A. & CLARKE, L. E. 2011. RCP4. 5: a pathway for stabilization of radiative forcing by 2100. *Climatic change,* 109**,** 77.
TIBANGAYUKA, N., MULUNGU, D. M. & IZDORI, F. 2022. Evaluating the performance of HBV, HEC-HMS and ANN models in simulating streamflow for a data scarce high-humid tropical catchment in Tanzania. *Hydrological Sciences Journal*.
TOM–CYPRIAN, N., EDET, J., SAM, E. & AHANEKU, I. 2022. Igbozulike AO Review of Relevant Evapotranspiration Models for Estimating Reference Evapotranspiration. Emerging Trends in Chemical Engineering. 2022; 9 (1): 46–55. *Review of Relevant Evapotranspiration Models for Estimating Cyprian N. et al. STM Journals***,** 15-16.
TRAJKOVIĆ, S. & GOCIĆ, M. 2010. Comparison of some empirical equations for estimating daily reference evapotranspiration. *Facta universitatis-series: Architecture and Civil Engineering,* 8**,** 163-168.
TRAJKOVIC, S., GOCIC, M., PONGRACZ, R., BARTHOLY, J. & MILANOVIC, M. 2020. Assessment of Reference Evapotranspiration by Regionally Calibrated Temperature-Based Equations. *KSCE Journal of Civil Engineering,* 24**,** 1020-1027.
TRIVEDI, A., PYASI, S. K. & GALKATE, R. V. 2018. Estimation of Evapotranspiration using CROPWAT 8.0 Model for Shipra River Basin in Madhya Pradesh. *International Journal of Current Microbiology and Applied Sciences,* 7**,** 1248-1259.
TROIN, M., ARSENAULT, R., MARTEL, J.-L. & BRISSETTE, F. 2018. Uncertainty of hydrological model components in climate change studies over two Nordic Quebec catchments. *Journal of Hydrometeorology,* 19**,** 27-46.
TSHIALA, F., OLWOCH, J. & ENGELBRECHT, F. 2011. Analysis of Temperature Trends over Limpopo Province, South Africa. *Journal of Geography and Geology,* 3.
TSHIALA, M. F. & OLWOCH, J. M. 2010. Impact of climate variability on tomato production in Limpopo Province, South Africa. *African Journal of Agricultural Research,* 5**,** 2945-2951.
UBISI, N., R., MAFONGOYA, P. L., KOLANISI, U. & JIRI, O. 2017. Smallholder farmer's perceived effects of climate change on crop production and household livelihoods in rural Limpopo province, South Africa. *Change Adaptation Socioecol. Syst,* 3**,** 27–38.
URAMA, K. C. & OZOR, N. 2010. Impacts of climate change on water resources in Africa: the role of adaptation. *African Technology Policy Studies Network,* 29**,** 1-29.
VAN DER BANK, M. & KARSTEN, J. 2019. Climate Change and South Africa: A Critical Analysis of the Earthlife Africa Johannesburg and Another v Minister of Energy and Others 65662/16 (2017) Case and the Drive for Concrete Climate Practices. *Air, Soil and Water Research,* 13**,** 1–11.

VAN VUUREN, D. P., EDMONDS, J., KAINUMA, M., RIAHI, K., THOMSON, A., HIBBARD, K., HURTT, G. C., KRAM, T., KREY, V. & LAMARQUE, J.-F. 2011a. The representative concentration pathways: an overview. *Climatic change,* 109**,** 5.

VAN VUUREN, D. P., STEHFEST, E., DEN ELZEN, M. G., KRAM, T., VAN VLIET, J., DEETMAN, S., ISAAC, M., GOLDEWIJK, K. K., HOF, A. & BELTRAN, A. M. 2011b. RCP2. 6: exploring the possibility to keep global mean temperature increase below 2 C. *Climatic Change,* 109**,** 95.

VESTE, M., LITTMANN, T., KUNNEKE, A., DU TOIT, B. & SEIFERT, T. 2020. Windbreaks as part of climate-smart landscapes reduce evapotranspiration in vineyards, Western Cape Province, South Africa. *Plant, Soil and Environment,* 66**,** 119-127.

VETTER, T., REINHARDT, J., FLÖRKE, M., VAN GRIENSVEN, A., HATTERMANN, F., HUANG, S., KOCH, H., PECHLIVANIDIS, I. G., PLÖTNER, S. & SEIDOU, O. 2017. Evaluation of sources of uncertainty in projected hydrological changes under climate change in 12 large-scale river basins. *Climatic Change,* 141**,** 419-433.

VILAYSANE, B., TAKARA, K., LUO, P., AKKHARATH, I. & DUAN, W. 2015. Hydrological stream flow modelling for calibration and uncertainty analysis using SWAT model in the Xedone river basin, Lao PDR. *Procedia Environmental Sciences,* 28**,** 380-390.

WASSERSTEIN, R. & LAZAR, N. 2016. The ASA's Statement on p-Values: Context, Process, and Purpose. *The American Statistician,* 70**,** 00-00.

YAN, X. & MOHAMMADIAN, A. 2020. Forecasting daily reference evapotranspiration for Canada using the Penman–Monteith model and statistically downscaled global climate model projections. *Alexandria Engineering Journal,* 59**,** 883-891.

YE, Q., YANG, X., DAI, S., CHEN, G., LI, Y. & ZHANG, C. 2015. Effects of climate change on suitable rice cropping areas, cropping systems and crop water requirements in southern China. *Agricultural Water Management,* 159**,** 35-44.

ZAREI, A., ZARE, S. & PARSAMEHR, A. 2015. Comparison of several methods to estimate reference evapotranspiration. *West African Journal of Applied Ecology,* 23**,** 17-25.

ZHAN, G. & LIN SHELP, M. 2009. Modified Blaney-Criddle method — an empirical approach to estimate potential evaporation using air temperature. *In:* FOURIE, A. B. & TIBBETT, M. (eds.) *Mine Closure 2009: Proceedings of the Fourth International Conference on Mine Closure.* Perth: Australian Centre for Geomechanics.

ZHANG, X. & CAI, X. 2013. Climate change impacts on global agricultural water deficit. *Geophysical research letters,* 40**,** 1111–1117.

ZHAO, C., LIU, B., PIAO, S., WANG, X., LOBELL, D. B., HUANG, Y., HUANG, M., YAO, Y., BASSU, S., CIAIS, P., DURAND, J.-L., ELLIOTT, J., EWERT, F., JANSSENS, I. A., LI, T., LIN, E., LIU, Q., MARTRES, P., MÜLLER, C., PENG, S., PENUELAS, J., RUANE, A. C., WALLACH, D., WANG, T., WU, D., LIU, Z., ZHU, Y., ZHU, Z. & ASSENG, S. 2017. Temperature increase reduces global yields of major crops in four independent estimates. *Proceedings of the National Academy of Sciences of the United States of America,* 114**,** 9326-9331.

ZHU, T. & RINGLER, C. 2012. Climate change impacts on water availability and use in the Limpopo River Basin. *Water,* 4**,** 63-84.

ZHUANG, X. W., LI, Y. P., NIE, S. & HUANG, G. H. 2019. Modeling Climate Change Impacts on Water Resources. *IOP Conf. Series: Earth and Environmental Science 356*.

ZIERVOGEL, G., NEW, M., ARCHER VAN GARDEREN, E., MIDGLEY, G., TAYLOR, A., HAMANN, R., STUART-HILL, S., MYERS, J. & WARBURTON, M. 2014. Climate change impacts and adaptation in South Africa. *WIREs Climate Change*.

ZWANE, E. M. 2019. Impact of climate change on primary agriculture, water sources and food security in Western Cape, South Africa. *Jàmbá:Journal of Disaster Risk Studies,* 11.